

# **An Investigation into the Development of a Realistic Upper Airway Visualisation System**

**Hassan Mahmoud Raslan**

A thesis submitted to Auckland University of Technology  
in fulfilment of the requirements for the degree of  
**Master of Philosophy (MPhil)**

**2015**

Faculty of Design and Creative Technologies  
School of Engineering  
Institute of Biomedical Technologies  
Auckland, New Zealand

**Primary Supervisor: Professor Ahmed Al-Jumaily**

# ABSTRACT

Obstructive Sleep Apnea (OSA) is a common example of a disease which affects the upper respiratory tract, and occurs when there is an anatomical obstruction or collapse in the upper airways of the respiratory system, leading to a cessation of breathing during sleep and thus resulting in a various number of side effects. Previous research has been undertaken to model the upper respiratory tract in order to entirely understand the factors behind OSA, and thus devise efficient methods and new technologies to treat and prevent it. However, physical visualisation can be one of the best methods of analysis, and no research has been found which enabled the physical visualisation of air flow within a complete and accurate model of the upper airway using a system which simulated realistic respiration.

In order to address this issue, an anatomically accurate model was developed at the Institute of Biomedical Technologies with the three important properties relevant to its purpose: Accuracy, Transparency, and Flexibility. This model included the boundaries of the upper airway, as well as the two main associated organs relevant to OSA: the tongue and the uvula. Furthermore, this model was combined with an external system simulating realistic breathing, thus resulting in a realistic visualisation system of respiration within the upper airway.

This system was then validated by running a series of experiments on the upper airway model and comparing the obtained response to that which was expected.

The final system has potential to be used for future investigation in order to observe the reaction of the upper respiratory tract during respiration, and thus better understand and possibly treat diseases such as OSA.

# TABLE OF CONTENTS

Abstract .....	
Table of Contents .....	I
List of Figures .....	VI
List of Tables .....	X
Attestation of Authorship .....	XI
Acknowledgements .....	XII
Chapter 1 - Introduction .....	1
1.1. Background .....	1
1.2. Division of the Respiratory Tract .....	2
1.3. Diseases and issues associated with the Respiratory Tract .....	3
1.4. Fluid Flow .....	3
1.4.1. Air flow in the Respiratory Tract .....	4
1.5. Motivations, Objectives, and Scope .....	4
1.6. Thesis Structure .....	6
Chapter 2 - Literature Review .....	7
2.1. Introduction .....	7
2.2. The Upper Airway .....	7
2.2.1. Anatomy .....	7
2.2.1.1. Major Parts of the Upper Respiratory Tract .....	8
2.2.1.2. Important Regions Associated with the Upper Airway .....	14
2.2.2. Tissue and Muscles of the Upper Airway .....	15
2.2.2.1. Tissue Composition .....	15
2.2.2.2. Muscle Structure .....	15
2.3. Problems associated with the Upper Airway .....	16
2.3.1. Obstructive Sleep Apnea (OSA) .....	17
2.3.1.1. Diagnosis .....	18
2.3.1.2. Causes and Risk Factors .....	19

2.3.1.3. Consequences .....	22
2.3.1.4. Treatment .....	23
2.3.1.5. Continuous Positive Airway Pressure (CPAP).....	26
2.4. Fluid Flow .....	28
2.4.1. Characterisation and Visual Analysis.....	28
2.4.2. General Properties, Governing Laws, and Equations .....	28
2.4.2.1. Flow Rate .....	29
2.4.2.2. Law of Continuity .....	30
2.4.2.3. Bernoulli's Principle.....	31
2.4.2.4. Turbulence.....	31
2.4.3. Flow of air in the Human Respiratory Tract.....	32
2.4.3.1. General Path of Air Flow during Respiration.....	32
2.4.3.2. Properties of Respired Air in Real Respiratory Systems .....	34
2.4.3.3. Fluid Behaviour in the Airways .....	35
2.5. Previous Research in Upper Airway Modelling.....	37
2.5.1. Mathematical Models .....	38
2.5.2. Virtual Models.....	40
2.5.3. Physical Models .....	42
2.6. Summary .....	43
Chapter 3 - Image Analysis and Model Development .....	45
3.1. Introduction .....	45
3.2. Creating the Virtual Model.....	45
3.3. Physical Modelling of the Upper Airway Boundaries.....	47
3.3.1. Preliminary Investigation and Evolution of ideas .....	48
3.3.1.1. Model 1 – Silicone-Casing Model.....	48
3.3.1.2. Model 2 – Wax-Core Model.....	50
3.3.2. Creating the Final Realistic Boundaries Model.....	57
3.3.2.1. Changes to the Cavity Core.....	57
3.3.2.2. Making the Final Model .....	57



3.4. Physical Modelling of the Upper Airway Organs .....	59
3.4.1. Materials Used.....	59
3.4.2. The Tongue .....	60
3.4.2.1. Model 1 – Gelatine Tongue.....	60
3.4.2.2. Model 2 – Latex Tongue .....	61
3.4.3. The Uvula.....	62
3.5. Completing the Upper Airway: Fitting the Associated Organs.....	63
3.6. Summary .....	64
Chapter 4 - Experimental Simulation .....	65
4.1. Introduction .....	65
4.2. Simulating the lungs: Breathing Simulator .....	65
4.3. Reproducing Breathing Properties .....	67
4.4. Simulating Accurate Human Respiration.....	69
4.5. Experimenting with the Final Model.....	71
4.5.1. Validating Accuracy.....	71
4.5.2. Validating Transparency .....	71
4.5.2.1. “Marking” the Air for Visualisation.....	72
4.5.2.1. Visualising Air Flow within the Upper Airway .....	72
4.5.3. Validating Flexibility .....	73
4.6. Summary .....	75
Chapter 5 - Results .....	76
5.1. Introduction .....	76
5.2. Accuracy: Analysing the Accuracy of the Final Model .....	76
5.2.1. Final Upper Airway Boundary Model.....	76
5.2.1.1. Nasal Cavity .....	79
5.2.1.2. Oral Cavity .....	81
5.2.1.3. Pharynx .....	82
5.2.1.4. Larynx .....	85
5.2.2. Upper Airway Organ Models .....	85

5.2.2.1. Tongue.....	85
5.2.2.2. Uvula .....	87
5.3. Transparency: Visualising Air Flow within the Upper Airway Model .....	89
5.3.1. Standard Closed-Mouth Respiration .....	89
5.3.1.1. Upright Position .....	89
5.3.1.2. Supine Position.....	94
5.3.2. Further Experimentation - Open Mouth .....	97
5.3.2.1. Upright Position .....	98
5.3.2.2. Supine Position.....	102
5.4. Flexibility: Measuring Changes in the Upper Airway model.....	106
5.5. Summary .....	110
Chapter 6 - Discussion .....	111
6.1. Introduction .....	111
6.2. Analysing the Accuracy of the Developed Model.....	111
6.2.1. Nasal Cavity .....	112
6.2.2. Oral Cavity .....	114
6.2.3. Pharynx .....	116
6.2.4. Larynx .....	117
6.2.5. Upper Airway Organs .....	118
6.2.5.1. Accuracy and Suitability of Materials Used.....	119
6.2.5.2. The Tongue .....	119
6.2.5.3. The Uvula.....	120
6.3. Validating Accuracy by Using Transparency.....	121
6.3.1. Observed Behaviour of Air Flow during Closed-Mouth Testing .....	121
6.3.1.1. Inhalation.....	121
6.3.1.2. Exhalation.....	125
6.3.2. Observed Behaviour of Air Flow during Open-Mouth Testing .....	127
6.3.2.1. Inhalation.....	127
6.3.2.2. Exhalation.....	129

6.4. Investigating Effects of Respiration on Upper Airway Response .....	131
6.4.1. Response of Upper Airway Subject to Breath Cycle.....	131
6.4.1.1. During Inhalation .....	131
6.4.1.2. During Exhalation .....	132
6.4.2. Response of Upper Airway Subject to Posture .....	134
6.4.2.1. While Upright.....	134
6.4.2.2. While Supine .....	134
6.5. Limitations .....	135
6.6. Future Research.....	138
6.7. Summary .....	139
Chapter 7 - Conclusion.....	141
References .....	142
Appendices.....	149
Appendix I - Understanding the Technology .....	149
Imaging Modalities and Magnetic Resonance Imaging (MRI) .....	149
Model Reconstruction .....	150
3D printing and Additive Manufacturing .....	150
Appendix II - Anatomical Terms of Location.....	152
Appendix III - Technical Information and Data Sheets.....	153
Solaris.....	153
Dragon Skin .....	154
Special-Effects Gelatine .....	154
Commercial 3D Printer .....	155
PVA Filament.....	155

# LIST OF FIGURES

Figure 2-1 Sagittal and Coronal section diagrams showing the main areas and features of the Nasal Cavity (retrieved from [14]) .....	9
Figure 2-2 Sagittal section and anterior view diagram of the areas and features comprising the oral cavity (retrieved from [16]).....	11
Figure 2-3 Posterior view of entire pharynx opened along the posterior wall (left) with the different regions of the pharynx emphasised (right) (retrieved from [23]).....	12
Figure 2-4 Anterior (left), Sagittal (middle), and Posterior (right) view of the larynx and associated cartilages (retrieved from [15]) .....	13
Figure 2-5 Lateral view of Upper Airway showing the retropalatal and retrolingual regions (Adapted from [30]).....	14
Figure 2-6 Diagram showing lateral view of tongue and associated muscles (a), posterior view of an opened pharynx and position of palatopharyngeal muscle (b), and posterior view of pharynx showing some of the posterolateral pharyngeal wall muscles (c) (retrieved from [44, 45]).....	16
Figure 2-7 Simple diagram showing occurrence of snoring and OSA .....	17
Figure 2-8 Illustration outlining the factors involved in the collapse of the pharynx, which is influenced by an imbalance in collapsing pressures (which drive collapsibility), and dilating pressures (which maintain patency) (retrieved from [74])......	20
Figure 2-9 Use of CPAP on a sleeping subject (top-left) with illustration outlining the concept behind using CPAP devices .....	27
Figure 3-1 Diagram showing process of obtaining virtual model from MRI scan images, done through interactive segmentation and subsequent surface rendering.....	47
Figure 3-2 Process showing the development of a silicone encasing of the upper airway model. The area of the oral cavity shown in panel e) is an example of the final encasing and its opacity.....	49
Figure 3-3 Production of the upper airway mould tool showing the final virtual mould tool (a) and the separate constituents after printing and assembly (b).....	50
Figure 3-4 Example of attempted paraffin wax model of upper respiratory tract .....	51
Figure 3-5 The acquirement of a sugar-wax model of the upper respiratory tract and its similarity in shape to the previously 3D printed physical model.....	52
Figure 3-6 Development of the outer mould in which the final material is to be poured. a) shows the thickened representation of the upper airway which was deducted from the solid block, and b) shows the outer mould and its housing of the core.....	54
Figure 3-7 Final outer moulds coated in thin layer of sugar-wax to allow for easier separation.....	55
Figure 3-8 Development of the final model using the sugar-wax core (b) showing associated transparency (c) and flexibility (d) .....	56

Figure 3-9 3D Printing of PVA-model of air within upper respiratory tract .....	57
Figure 3-10 Preparation of final gelatine-coated 3D-printed PVA model and associated outer mould, and the subsequent addition of degassed Solaris® compound.....	58
Figure 3-11 Procurement of final upper airway model by a) separation of outer mould using warm water, followed by b) dissolving of PVA material once again using warm water, and the consequent c) final transparent model obtained .....	59
Figure 3-12 Process showing the separation of tongue mould parts to yield the final hollow gelatine model of the tongue.....	61
Figure 3-13 Development of latex tongue by obtaining tongue shape using two-part mould, and filling of latex shell with goo material .....	62
Figure 3-14 Use of a two-part mould to yield the final gelatine model of the uvula.....	63
Figure 3-15 A geometrically accurate, transparent, and flexible model of the upper respiratory tract along with associated organs.....	64
Figure 4-1 Diagram of Breathing Simulator with associated components.....	67
Figure 4-2 Diagram showing assembly of components involved in simulating realistic breath characteristics and properties .....	69
Figure 4-3 The suspension of the upper airway model at the output of the human respiration system using a stand and clamp .....	70
Figure 4-4 The Portable Respiration Bench: a complete mobile system simulating regular realistic breathing through an accurate transparent model of the upper respiratory tract .....	71
Figure 4-5 Upper airway model aligned with ruler on the same plane for use in measuring displacements of upper airway walls during respiration simulation. ImageJ software used to first calibrate distance and set usable scale (a) and then measure displacements in the airway walls (b).....	74
Figure 5-1 Diagram showing the core model representing the path of air within the respiratory tract. The model is shown in general (a) with the important features shown in more detail, including the areas which would become the nasal septum (b) and nasal conchae (c), the gap between the path of air and the tongue after (d) and before (e) it is filled, and the holes which would form the piriform recesses (f and g) .....	77
Figure 5-2 Diagram showing the final model in general (a) along with more detailed views of the associated features, including the nasal septum (b and c), nasal conchae (d), pharynx (e), upper half of the oral cavity (f), the piriform recesses (g), and the area where the oral cavity would meet with the pharynx at the larynx end. Note that the core model was kept within the final model to enable the features to become more obvious .....	78
Figure 5-3 Medial view of the nasal cavity of the final model before passing the nasal septum. The entire nasal septum can be seen from this view .....	79
Figure 5-4 Medial view of the nasal cavity of the final model past the nasal septum. The inferior and middle conchae can be vaguely recognised from this view .....	80

Figure 5-5 Coronal cross-sectional view (left) and cut-out (right) of the nasal cavity area in the final model. The different depressions within the outer walls (i.e. the conchae) can clearly be seen from this view .....	80
Figure 5-6 Nasal Cavity of final model outlining the sections used during measurement .....	81
Figure 5-7 Doctor's check-up: a look into the oral cavity through the opening of the mouth to reveal the tongue and the uvula (left) as well as the point at which the uvula is attached (right) .....	82
Figure 5-8 Oral Cavity of final model outlining the sections used during measurement .....	82
Figure 5-9 Posterior view of the pharynx of the final model opened posteriorly. The upper airway organs (tongue and uvula) can be clearly seen from their posterior end.....	83
Figure 5-10 The region of the pharynx in the final model outlining the sections used during measurement .....	84
Figure 5-11 A look at the recesses at the inferior end of the pharynx of the final model.....	85
Figure 5-12 A look at the final latex model of the tongue (left) and its property to stretch (right) .....	86
Figure 5-13 The final tongue model outlining the sections used during measurement .....	87
Figure 5-14 A look at the final gelatine model of the uvula (left) and its property to stretch (right) .....	87
Figure 5-15 The final uvula model outlining the sections used during measurement .....	88
Figure 5-16 A lateral view of the final model with associated organs and their response in the upright (a) and supine (b) positions .....	88
Figure 5-17 Final model ready for nasal breathing visualisation experimentation in the upright position (left) along with snapshot of the experiment taken by high speed camera highlighting the expected path of air (right) .....	89
Figure 5-18 Sequence of images showing flow of air in the final model during nasal-only inhalation in the upright position .....	91
Figure 5-19 Sequence of images showing flow of air in the final model during nasal-only exhalation in the upright position .....	93
Figure 5-20 Final model ready for nasal breathing visualisation experimentation in the supine position (top) along with snapshot of the experiment taken by high speed camera highlighting the expected path of air (bottom) .....	94
Figure 5-21 Sequence of images showing flow of air in the final model during nasal-only inhalation in the supine position .....	95
Figure 5-22 Sequence of images showing flow of air in the final model during nasal-only exhalation in the supine position.....	97
Figure 5-23 Final model ready for nasal and oral breathing visualisation experimentation in the upright position (left) along with snapshot of the experiment taken by high speed camera highlighting the expected path of air (right) .....	98

Figure 5-24 Sequence of images showing flow of air in the final model during nasal and oral inhalation in the upright position .....	100
Figure 5-25 Sequence of images showing flow of air in the final model during nasal and oral exhalation in the upright position .....	101
Figure 5-26 Final model ready for nasal and oral breathing visualisation experimentation in the supine position (top) along with snapshot of the experiment taken by high speed camera highlighting the expected path of air (bottom) .....	102
Figure 5-27 Sequence of images showing flow of air in the final model during nasal and oral inhalation in the supine position.....	104
Figure 5-28 Sequence of images showing flow of air in the final model during nasal and oral exhalation in the supine position.....	105
Figure 5-29 A comparison of the effects of posture on the overall measured displacements of the upper airway boundary width during inhalation (above) and exhalation (below).....	108
Figure 5-30 A comparison of the effects of the breath cycle (inhalation and exhalation) on the overall measured displacements of the upper airway boundary width while upright (above) and supine (below) .....	109
Figure 6-1 Sagittal cross-sectional view of developed models nasal cavity septum alongside diagram from scientific literature [16] for comparison.....	113
Figure 6-2 Sagittal cross-sectional view of outer walls of developed models nasal cavity alongside diagram from scientific literature [16] for comparison .....	114
Figure 6-3 Anterior view of oral cavity of final model alongside diagram from scientific literature [18] for comparison .....	116
Figure 6-4 Posterior view of pharynx in final model alongside scientific diagram for comparison .....	117
Figure 6-5 The laryngeal end of the final model alongside a scientific illustration of the same region for comparison .....	118

LIST OF TABLES

Table 5-1 Overview of the measured boundary width displacements in the final upper airway model during respiration in the Upright position. The table shows the measured distances of the various areas at rest, at maximum displacement during inhalation and exhalation, the total distance displaced at the various areas during inhalation and exhalation, and the percentage change in width of the various areas during inhalation and exhalation ..... 106

Table 5-2 Overview of the measured boundary width displacements in the final upper airway model during respiration in the Supine position. The table shows the measured distances of the various areas at rest, at maximum displacement during inhalation and exhalation, the total distance displaced at the various areas during inhalation and exhalation, and the percentage change in width of the various areas during inhalation and exhalation ..... 107



## ATTESTATION OF AUTHORSHIP

I hereby declare that this submission is my own work and that, to the best of my knowledge and belief, it contains no material previously published or written by another person (except where explicitly defined in the acknowledgements), nor the material which to a substantial extent has been submitted for the award of any other degree or diploma of a university or other institution of higher learning.

Name: Hassan Raslan

Signed: 

## ACKNOWLEDGEMENTS



First and foremost, all my thanks are to Allah the almighty above all else for helping me finish this research. I know that, indeed, without his guidance and mercy I would have never been able to achieve what I had accomplished, nor find the strength to push through it and see it to the end.

Secondly, I would like to sincerely thank my primary supervisor, Professor Ahmed Al-Jumaily, for all his help and for giving me this unique opportunity. I know he always wants help as much as a fatherly figure possibly could, and even though I may not have communicated with him as much as I would have liked to, I hope that this research could be something he is proud of. I would also like to thank my secondary supervisor, Loulin Huang, for his help during the course of my study.

Thirdly, I would like to thank my family for being very supportive of me, and for being patient with the mess I made while completing this research, as well as appreciating and tolerating my time in hermitude away from them. I would particularly like to thank my beloved mother for her unwavering support and encouragement. Even with all the hard and busy times she faced, she was always trying to help, and there was never a time when I felt that she would not sit with me and help me throughout the entire Masters programme if I had only asked.

I would also like to thank Sherif Adel, my other research half and study-buddy, for his valuable help, advice, and support whenever I needed it, Leslie-Anne Jouanno, who's work involved developing the realistic human-exhalation environment used in this research, and Jibril Mussa, who's work involved building the breathing simulator which was also used in this research.

I would like to thank Zeyad Swaid for providing me with both advice on the thesis, as well as the sustenance I needed to finish in the form of giant pretzels, Mohamed Jaballah for his invaluable advice on writing a thesis, and Kareem Ismail for his never-ending offers to help me with my masters, to the degree that at some points I began to forget whose research this really was! I would also like to thank Ali Al-Saudi for pushing me to finish, and a BIG thanks to the people at IC for all their help, services, and for keeping me occupied during all the hard times with fun banter and deep conversations.

Finally, I would like to thank all the rest of my friends for their support during this stressful period, and for keeping me sane by transforming times of tension and pressure into times of relief and enjoyment.

# Chapter 1 - INTRODUCTION

## 1.1. Background

There are few things in life which are inherent in human beings since birth which don't have to be actively learnt. Some functions are so innate that one does not even bother to think about them...until they are lost or affected. One such function, which lasts throughout the entire day, is performed daily by every single individual. Even as one reads into this research, they may not realise how fortunate they are to have been performing this action the entire time! This process is of course: breathing. A well-known Italian poet once quoted that "Breathing is the greatest pleasure in life". To rephrase this in a slightly more scientific context, it is indeed one of the most important autonomous functions of the living body, which consequently makes the respiratory system one of the most vital organ systems of any living organism.

The respiratory system is primarily responsible for the essential delivery of oxygen to the blood stream, which in turn, allows oxygen to be distributed throughout the entire body; a crucial process in maintaining life. While this process seems as easy as, well, breathing, a lot in fact occurs with each breath taken, as the air flows through and alongside a number of different organs and areas, each with various differing characteristics and a range of different functions, and each also adding to the possibility of disease or inhibition of that breath you just took and never considered. People with breathing disorders know that breathing is not so easy when it is somewhat hindered. The nature and naturalness of breathing is such that it is done even during sleep. As the majority of people carry their tired selves to bed at night after a long day of hard postgraduate study, knowing they can look forward to a good night's sleep and start another fresh day in the morning, few ever truly think of how fortunate they are to not have to fight all night just in order to breathe, one of the consequences of a condition known as Sleep Apnea, which further leads to a myriad of problems in the lifestyle of the afflicted individual. It is because of this that ensuring a problem-free flow of air through the respiratory tract can be considered one of the most crucial and vital things one must have in life, and thus analysing the flow of air in the respiratory system and understanding its nature is equally as important.

This first chapter of this research will provide a brief introduction into the respiratory system as well as shed some light on the possible diseases which can be associated with this system and, in particular, with the upper respiratory tract, which will be the main area of focus. The

nature of fluid flow and air flow in the airways will also be highlighted, and finally, the motivations behind this research, as well as its main objectives and the scope within which the research was undertaken, will be outlined.

## 1.2. Division of the Respiratory Tract

In human beings, there are two ways in which the respiratory system can be classified. Each of these ways allows division of the respiratory system into two separate sections. *Functionally*, the respiratory system is divided into a “conducting” portion, which consists of the structures that conduct air into the lungs, and the “respiratory” portion, which consists of the tissues inside the lungs where gaseous exchange occurs between the blood and the air. However, *structurally*, the respiratory system is divided into the “upper” respiratory tract and the “lower” respiratory tract. The lower respiratory tract extends from the larynx to the lungs [1], and includes the organs involved in gaseous exchange between the air and the bloodstream. Meanwhile the upper respiratory tract, also known as the upper airway, constitutes a large portion of the entire respiratory system, and provides the first interface by which the body receives air to be utilised for respiration. Thus the importance of its role in the proper functionality of the entire respiratory system becomes evident: Any defections and problems associated with this portion of the body prevents effective respiration further along the respiratory system, and can thus lead to other debilitating effects on the body and regular bodily function.

The major organs associated with the lower respiratory tract include the larynx, trachea, bronchii, and lungs. Those associated with the upper respiratory tract are the nose and associated nasal cavity, the mouth and associated oral cavity, the pharynx, and the larynx. The Larynx is considered the interface at which the two different sections of the respiratory tract meet, thus some have classified the Larynx as being part of the upper respiratory tract [2], while others see it as part of the lower respiratory tract [3]. This collection of areas and other associated organs, such as the tongue and the uvula, establish a system that is ideal in serving its own purpose of air transfer for respiration, whilst also serving other important functions. Furthermore, the nature of the tissue itself present within the airway also makes for efficient and effective air transfer. These organs, associated tissues, and various areas of the respiratory tract will be observed in more detail in the following chapter.

### 1.3. Diseases and issues associated with the Respiratory Tract

A large number of conditions exist which can affect proper functionality of the respiratory system. The large variation in the possible diseases, disorders, and ailments associated with the respiratory tract indicates just how vulnerable this system really is, and how many different factors can exist which can negatively influence respiration. Some of these diseases include sinusitis, pneumonia, or even the common cold and influenza, which are mainly caused by infection, although they may also be brought about by other factors [4]. Other debilitating issues related to the airways don't have to be diseases caused by infection, and can simply be the cause of irregularities in the structure of the airways, or any other abnormality which disallows proper functionality. For example, a disorder such as snoring may very well be a common (albeit irritating!) occurrence, but it still indicates irregular breathing due to partial occlusion of the airways, which means that the respiratory system, and in particular the upper respiratory tract, isn't working as efficiently as it should be. A more serious condition also affecting the upper respiratory tract, and one which may even be caused by the same factors as those which bring about snoring, is Obstructive Sleep Apnea (OSA), a condition which leads to a cessation of breathing during sleep [5] and results in a wide range of health problems.

The presence of such diseases and disorders reveals just how crucial uninhibited flow of air is for function, and thus why studying air flow within the airways is an important concept.

### 1.4. Fluid Flow

Fluid flow is a general term used to describe the motion and nature of flow associated with "fluids", which includes both liquids and gases. It is an integral part of the field of fluid mechanics; a vast and complicated field of study which looks into the ways in which fluids behave, and why they behave in such a manner. This field can be divided into fluid statics, or the study of fluids at rest, and fluid dynamics, which outlines the study of fluids in motion.

In order to accurately understand and subsequently describe the behaviour of fluids in various systems and under different circumstances and conditions, fluid mechanics is associated with many general laws common to the field of physics in order to analyse why a fluid would behave in a particular way, and consequently predict how a fluid might react under differing conditions [6]. This can in turn be used to reflect upon the system within which fluid flow is

occurring. For example, putting this into a more relevant context: by understanding how fluid *should* flow within the respiratory tract, and then observing its *actual* behaviour, deductions can be made about the functionality of the respiratory tract itself.

### 1.4.1. Air flow in the Respiratory Tract

As mentioned earlier, the detrimental effects of a simple obstruction or occlusion of the respiratory tract can clearly be seen after understanding conditions such as OSA. Whether it be the result of an external influence or a collapse of the airway itself, or even the interference of the internal organs associated with the respiratory tract, the fact that obstruction in the airways is associated with various diseases means that the presence, and thus treatment, of these diseases is directly related to the flow of air, and therein lies the importance of understanding fluid flow within the respiratory tract.

Due to its complexity, fluid flow should be studied in its totality and with all factors considered if understanding it is to be used as a tool to treat airway disorders. This means that fluid flow behaviour within the respiratory tract specifically should be investigated under different conditions, within realistic airway geometry, and in the presence of realistic upper airway organs which may play a role in obstruction.

## 1.5. Motivations, Objectives, and Scope

The ability to accurately analyse fluid flow during respiration in the upper respiratory tract is crucial in order to understand disorders such as OSA and attempt to find efficient treatment. The idea of using a model of the upper respiratory tract, whether it be a virtual, mathematical, or physical model, in order to analyse fluid flow is not a new concept. Previous research has been conducted to not only analyse the changes of air characteristics, such as velocity, pressure, and flow rate, throughout the respiratory tract, but to also measure the changes in these parameters in the presence of obstructions and irregularities. However, little research could be found which allowed for physical visualization of air flow in an accurate, exact model of the respiratory tract which still maintained important properties relevant to the airways, such as flexibility and elasticity of the airway walls. And even more so, *no* such model could be found which also involved the inclusion of other organs associated with the respiratory tract which are very relevant to airway obstruction, such as the tongue and uvula (*more about previous research in Chapter 2*). This means that, short of using a real respiratory tract, which would still need to be transparent in order to visualise the flow of air (not to mention the ethical nightmares associated with such experiments), the most accurate visual analysis one can

have of the flow of fluids in the airway during breathing, akin to that present in a real respiratory system, is by combining the above stated properties: creating an entirely transparent and accurate physical replica of a real respiratory tract with realistic properties, while including the relevant and crucial organs which can influence the flow of air. However, just finding material suitable enough to possess such properties so that the airways may be modelled as desired is a very difficult task, let alone shaping it to accurately resemble the complex geometry of the respiratory tract.

Thus the ultimate aim of this research is to create such a model and provide a complete simulation of respiration in the upper airways which can be physically visualised. This will be achieved with three main objectives in mind:

1. Development of an upper respiratory tract model with the following properties:
  - Accuracy. Achieved by:
    - Acquiring an accurate virtual model of the lumen of the upper respiratory tract and using it to obtain a physical model of the upper airway boundaries
    - Development of accurate models of the upper airway organs: the tongue and the uvula
  - Transparency. Achieved by:
    - Finding suitable material to model the upper airway boundaries
  - Flexibility. Achieved by:
    - Ensuring the material used for the upper airway boundaries is elastic and not rigid
2. Simulation of realistic human respiration, which will be comprised of:
  - Imitation of a continuous breath cycle
  - Recreation of breath properties
3. Validation of the three aforementioned properties of the final model by:
  - Visual investigation of the final developed model for validation of accuracy
  - Observational analysis of fluid flow within the complete final model for validation of transparency
  - The use of realistic breath simulation in evaluating the response of the upper airway walls to regular breathing for validation of flexibility

Although it would be perfect for the sake of research to analyse fluid flow in the entire respiratory system, particularly because certain disorders are associated with specific areas of the airway, unfortunately, due to the complexity of the entire airway and the time limitations associated with this research, only the *upper respiratory tract* will be the subject of this

research. Moreover, because there still exists countless possible diseases and disorders associated with the upper respiratory tract, this research will focus specifically on the causes and conditions of OSA. Also, while common physical laws will be looked at with the aim of explaining the observed behaviour of fluid flow, this research will omit the solving of complex mathematical equations and the measurement of exact values of certain parameters, such as pressure, and validation of the final model will involve mostly visual evaluation and qualitative analysis, rather than the determination of numerical solutions.

## 1.6. Thesis Structure

The thesis is structured as follows:

- The second chapter will provide more details with regards to the topic and the background information behind which this research is based. This will also allow comprehension and familiarization of the relevant anatomical terms which will be used for the remainder of the research. More specifically, this chapter will highlight the anatomy of the upper respiratory tract, provide greater detail of OSA and its modern treatment, explain fluid flow and its important underlying concepts, and discuss previous research undertaken to model the upper airway and analyse fluid flow.
- The third chapter will then highlight the methodology involved in the development of the final airway boundary model, as well as the related models of the tongue and uvula.
- The fourth chapter will outline both the methodology through which human respiration was simulated, and the techniques used in validating the three properties of the complete final model
- The fifth chapter will provide a description of the results obtained with respect to the three desired properties of the complete final model.
- The sixth chapter will discuss and provide more insight into the obtained results, as well as outline the reasoning behind the results and their nature, and compare this with previous research. This chapter will also discuss the limitations of this research and how it could be improved, and what future research of the same topic could include.
- Finally, the sixth chapter will conclude the findings of this research and its relevance to real-world problems and solutions.



# Chapter 2 - LITERATURE REVIEW

## 2.1. Introduction

This chapter will provide further insight into the various topics associated with this research so that the study may be critically understood. It is structured as follows:

- Initially, a more detailed description of the upper airway, along with its various areas and organs, will be provided
- This will allow the following section to look into OSA in more detail, and relate it to upper airway anatomy
- The physics behind fluid flow, and in particular within the upper airway, will then be discussed in order to relate this to the results observed using the model in an attempt to validate it
- The chapter will conclude with a look into previous research in modelling the upper airway, and the use of modelling to analyse fluid flow.

## 2.2. The Upper Airway

### 2.2.1. Anatomy

The condition of the upper respiratory tract directly affects breathing, and thus its proper operation is detrimental to a subject's health and well-being. In order to properly understand disorders such as OSA and how they affect fluid flow in the upper airway, one must first fully understand the upper airway itself and its anatomy. This is important as it then allows comprehension of the possible defects and diseases and, consequently, how they may be treated successfully.

Aside from being the body's first interface with the outside air, the upper respiratory tract is not merely a conduit for outside objects to enter the body, but it serves multiple functions. The most obvious of these functions is that it is a passageway for air. However, the upper airway also plays a crucial role in warming, humidifying, and filtering the air during respiration before it passes into the lungs. It also drives the cough reflex, which ejects secretions from the airways before they enter the lungs, and prevents the entry of foreign material during inhalation. Furthermore, some of the parts associated with the upper respiratory tract are

crucial for their role in speech, taste, olfaction, and gastrointestinal functions, such as deglutition. The upper respiratory tract is able to achieve these functions through the wide arrangement of muscles, soft tissue, cartilage, and bone that it is made up of [7, 8].

The boundaries of the upper respiratory tract extend from the nose at the superior end of the upper airway (*See Appendix II for diagram explaining the anatomical terms of location used*), to the trachea at the inferior end [2], and the structures associated with this section comprise approximately 50% of the resistance found in the entire respiratory system [9].

### **2.2.1.1. Major Parts of the Upper Respiratory Tract**

There are four major parts associated with this section of the respiratory system which makes up the entire upper respiratory tract:

#### **2.2.1.1.1. The Nasal Cavity**

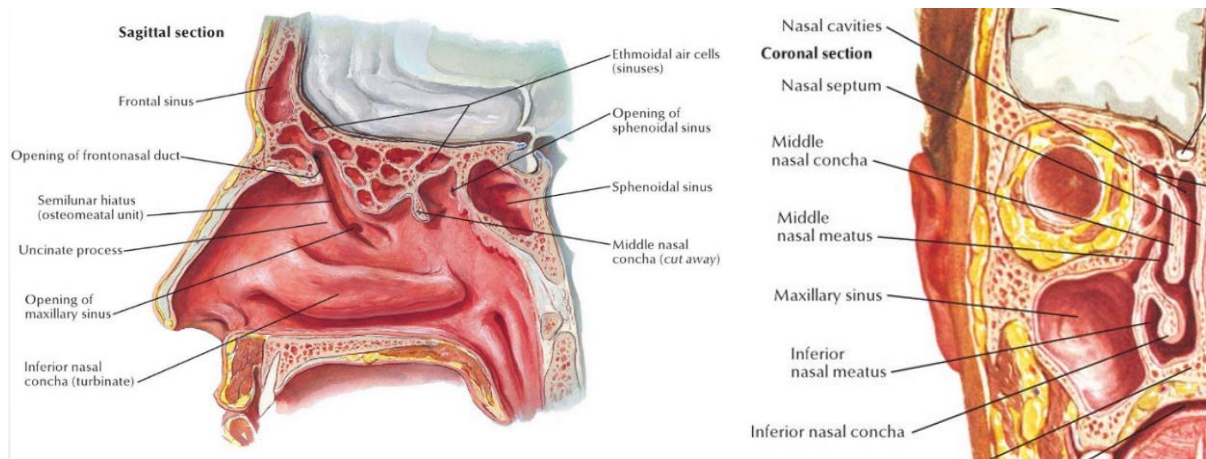
The nasal cavity, as the name suggests, is the area of hollow space behind the nose following the nostrils. It serves several functions, the first of which is to warm as well as humidify the air before the air passes through to the lungs. It also plays a small role in recapturing some of the heat and moisture of exhaled air as it is passed through the nose. Another crucial function of the nose and nasal cavity includes its involvement in olfaction: the sense of smell [10].

The nasal cavity resembles a triangle in shape and is subdivided by the nasal septum into two right-angled triangular halves. The ridge at the posterior border of the nasal septum is known as the Choana. Each half of the nasal cavity contains three “scroll-like” bones called the superior, middle, and inferior conchae (also known as turbinates), which characterise the lateral walls. The superior and middle conchae are extensions of the same bone, while the inferior nasal concha is a separate and independent bone altogether. The floor or base of the nasal cavity, known as the hard palate, is composed of palatine bone, and separates the nasal cavity from the oral cavity [11].

These three conchae which project into the nasal cavity also increase the surface area of the mucous membrane, which is thought to help further filter, moisten, and warm the air before it travels to the lungs [12].

The lining of the nasal cavity consists of a submucosal layer underlying a mucosal epithelial layer, where mucus, produced by the goblet cells of the membrane, traps small foreign particles which enter the nasal cavity. Small hair-like projections called “cilia” on the epithelial cells lining the nasal cavity move the mucus towards the pharynx. Several hairs present on the nostrils also prevent larger particles from being inhaled [8, 10].

Surrounding the nasal cavity are several sinuses, also known as “Paranasal Sinuses”. They decrease the weight of the skull bones, serve as resonating chambers, and are thought to also help in warming and moistening the inhaled air. They too are kept clean through the movement of mucus by the cilia lining the respiratory tract [3, 10, 13]. Altogether, four sinuses are present on each side of the nasal area, and their names correspond to the facial bones with which they are associated. For example, the “sphenoidal” sinuses reside just above the top-most point of the upper ridge on each side of the nasal cavity, as they are contained within the “sphenoid” bone [12].



*Figure 2-1 Sagittal and Coronal section diagrams showing the main areas and features of the Nasal Cavity (retrieved from [14])*

#### 2.2.1.1.2. The Oral Cavity

The oral cavity refers to the space behind the lips where the mouth is situated, and can be divided into 3 main sections: the oral vestibule, defined by the space between the outside boundaries of the teeth and the inside surface of the cheeks or lips. The oral cavity proper, which is the entire cavity of the mouth in the strict sense, bounded at the posterior end by the palatoglossal arch. And the fauces, a region near the throat at the back of the oral cavity.

At the fauces there resides two folds of soft tissue (called the “pillars of the fauces”). These two folds are known as the palatoglossal arch (the anterior fold) and the palatopharyngeal arch (the posterior fold), and in between the pillars of the fauces are the palatine tonsils [15, 16].

Another two important organs of the oral cavity worth studying further are the tongue and the uvula, an extension of the palate.

## o Tongue

The tongue is associated with a number of functions including, amongst other things, mastication, deglutition, taste, and speech. At its base, it is attached to a horseshoe-shaped bone located at the top of the Larynx and just below the mandible called the Hyoid bone. It is also connected by a fold of its own membrane covering, called the frenulum, which extends to the floor of the mouth [17]. It is composed of a mass of muscles lined by a highly differentiated mucus membrane. A large part of the tongue is lined by non-keratinized stratified squamous epithelium, as well as modified epithelial cells for the taste buds, located on the “dorsal surface” (i.e. on the superior surface) of the tongue. One of the most important extrinsic muscles of the tongue is the Genioglossus muscle, a large mass of muscle attached to the inferior side of the tongue which connects the tongue to the mandible [18, 19].

## o Palate

The palate, which acts as the boundary between the nasal and oral cavities (and also separates the regions of the nasopharynx and the oropharynx (*see 2.2.1.1.3*)), is an osteomuscular organ divided into two sections: the hard palate, and the soft palate. At the anterior end of the palate, the hard palate comprises approximately two-thirds of the entire palate and forms the roof of the mouth. It spans across and is continuous with the gums and alveolar arch formed by the upper teeth at its anterior end, while the posterior end of the hard palate is free and acts as the attachment point for the soft palate. It is composed of bone enveloped in periosteum, and is formed by the palatine processes of the maxilla and the horizontal plate of the palatine bones. In contrast to this, the soft palate, located at the posterior end of the palate, is a soft and mobile fold of muscle suspended from the hard palates' posterior border. It is covered in a layer of non-keratinized stratified squamous epithelium. Two important muscles associated with the soft palate are the levator palati muscles, which contract in order to elevate the soft palate, and the tensor palati muscle, whose contraction causes the soft palate to tighten, a process which occurs during eating to allow the food to easily pass through into the oropharynx region [18].

Hanging from the middle of the soft palates inferior surface at the posterior border is a small, conical mass of tissue called the “Uvula” [19, 20].

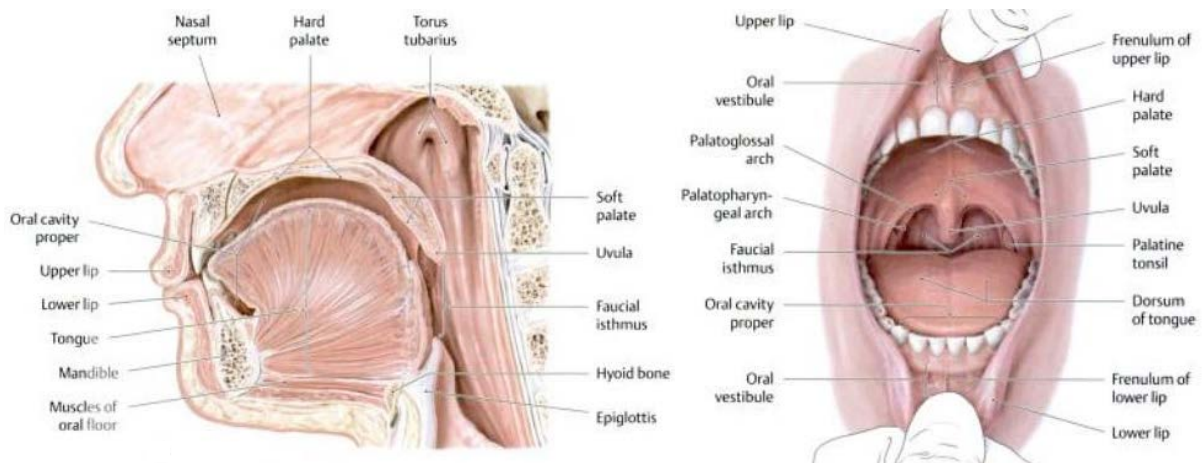


Figure 2-2 Sagittal section and anterior view diagram of the areas and features comprising the oral cavity (retrieved from [16])

### 2.2.1.1.3. The Pharynx

The pharynx is a musculo-membranous tube approximately 12 – 15cm long extending from the base of the skull down to the cricoid cartilage at the bottom of the Larynx. The pharynx is partitioned into three distinct areas.

#### o Nasopharynx

The Nasopharynx (also known as the Epipharynx) is the area of the pharynx associated with the nasal cavity. It lies directly behind the nasal cavity, and above the level of the soft palate. At its superior end, the Nasopharynx is open to the nasal cavity through two openings located at the posterior end of the nasal cavity. These openings are known as the Posterior Nares.

At the other end, the nasopharynx inferiorly joins with the second section of the pharynx, the oropharynx, through a small passageway called the *Pharyngeal Isthmus*, located posterior to the Uvula [18].

#### o Oropharynx

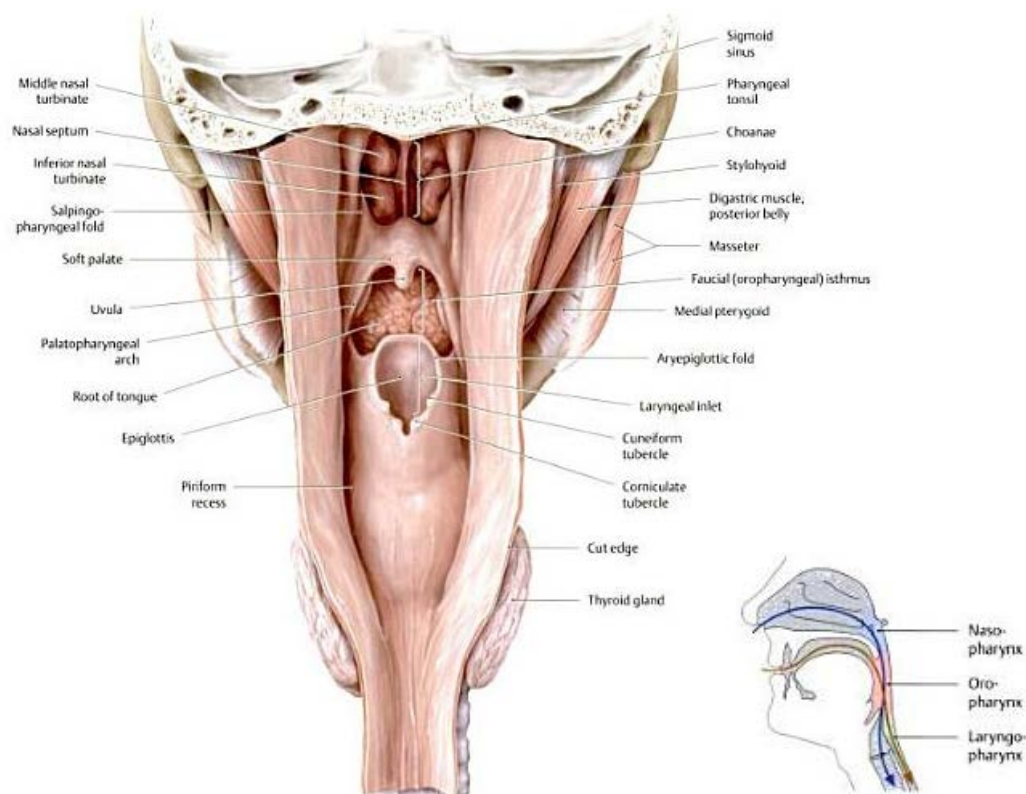
The Oropharynx (also known as the Mesopharynx) is the area of the pharynx located posterior to the oral cavity and tongue, where the separate passageways of food and air intersect. It extends from the soft palate at its superior end down to the upper border of the epiglottis at its inferior end. The oropharynx is open anteriorly to the oral cavity through an opening called the *oropharyngeal isthmus* (also known as the “Isthmus of the Fauces” (see 2.2.1.1.2 for *fauces*)), which is formed by the palatoglossal arches, making the palatoglossal arch the anterior boundary of the Oropharynx (Note that the “oropharyngeal” isthmus (or isthmus of the fauces) is not to be confused with the “pharyngeal” isthmus (or isthmus of the

pharynx), which is the interface between the nasopharynx and oropharynx). The lateral walls of the oropharynx also contain the palatopharyngeal arches, which reach downwards from the soft palates' lower edge and backwards towards the side walls of the pharynx (*figure 2-2 & 2-3*). The pharyngoepiglottic folds, which extend from the lateral pharyngeal walls at the level of the epiglottis to the lateral margins of the epiglottis, define the lateral borders of the oropharynx at the anterior wall. The lateral boundaries outlined by these pharyngoepiglottic folds, along with the epiglottis and the base of the tongue, bound the epiglottic *Valleculae*, a sort of crevice situated at the lower part of the oropharynx between the base of the tongue and the epiglottis [18, 20, 21].

## o Laryngopharynx

The Laryngopharynx (also known as the Hypopharynx) is the area at and around the Larynx. It is continuous with the oropharynx at its superior end, and the oesophagus at its inferior end, also opening into the larynx at the laryngeal inlet to eventually pass into the trachea [20, 21].

Another distinct feature related to the laryngopharynx is the presence of the Piriform recesses (or Piriform Fossa). These recesses are broad at the top and narrower at the bottom, and are located on either side of the section where the pharynx opens into the larynx at the laryngeal inlet (*figure 2-3*) [22].



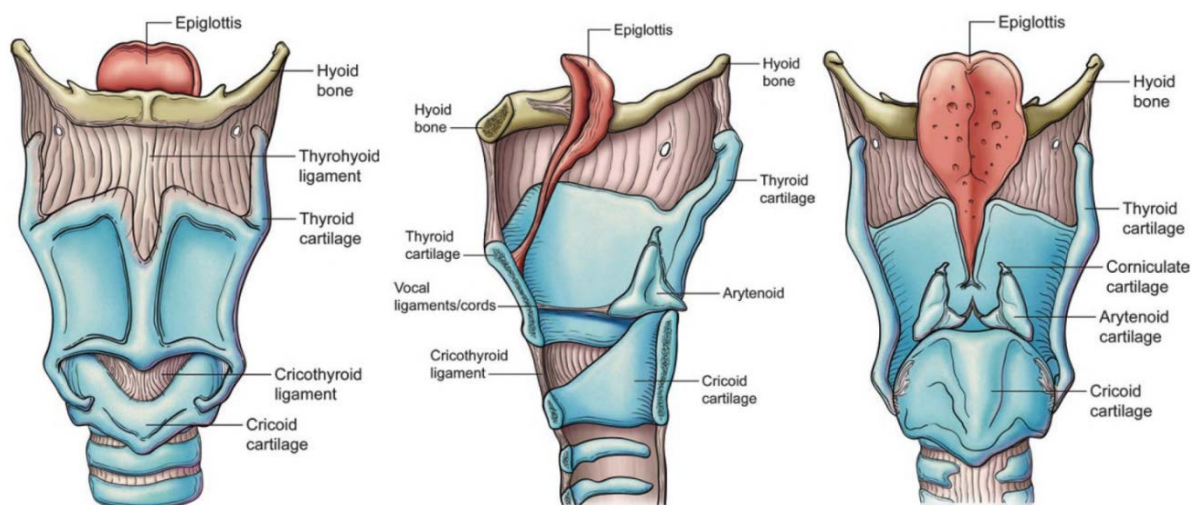
*Figure 2-3 Posterior view of entire pharynx opened along the posterior wall (left) with the different regions of the pharynx emphasised (right) (retrieved from [23])*



#### 2.2.1.1.4. The Larynx

Conventionally, the larynx is the boundary between the upper and lower respiratory tracts, and thus isn't particularly an organ related solely to the upper airway, but plays a role nonetheless, particularly as it is considered the second-most narrow part of the airways. It is a boxlike structure found on the anterior side of the neck [15, 24, 25]. The Larynx at its inferior end leads into both the oesophagus, as the passageway for eating and drinking, and the trachea, or windpipe, as the passageway for air to continue towards the lower respiratory tract. It serves to prevent foreign objects from entering the lower respiratory tract through the trachea, and is the main organ associated with the production of sound as it contains the vocal cords [10]. The Larynx consists of three paired cartilages, and three single, smaller cartilages. These unpaired cartilages ordered from the inferior end upwards to the superior end are the Cricoid cartilage, the Thyroid cartilage, and the Epiglottis, which is leaf-like in shape, and is attached inferiorly to the thyroid cartilage, and anteriorly to the hyoid bone. Its superior end which lies posterior to the tongue is free, and attaches to the base of the tongue by the glossoepiglottic folds. When swallowing occurs the laryngeal muscles contract, allowing the epiglottis to move downwards in effect moving the glottis, the opening in the larynx between the vocal cords which leads into the trachea, upwards and closing it, preventing the food from entering the trachea [15, 18].

Previous research has suggested that the Larynx has a large effect on fluid flow. Functioning as a constriction, the Larynx causes changes in important aspects and characteristics of air flow such as the flow rate, density of the air, and particle flow path. Moreover, it's most obvious effect is its cause of fluctuations, forcing laminar flow into turbulence [26, 27].



*Figure 2-4 Anterior (left), Sagittal (middle), and Posterior (right) view of the larynx and associated cartilages (retrieved from [15])*

### 2.2.1.2. Important Regions Associated with the Upper Airway

There are two main regions associated with the upper respiratory tract which should be recognised due to their dominance in the upper airway and their heavy involvement in upper airway collapse. These sites are common sites of narrowing, making them common sites of obstruction [28].

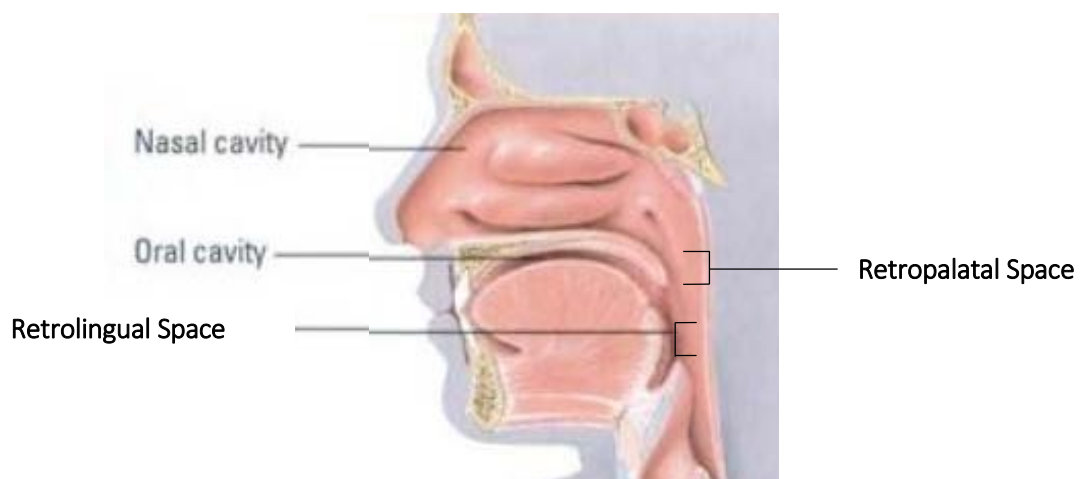
While there seems to be no clear universal definition for the exact boundaries of these regions, the following classifications will maintain for the remainder of this research:

#### o Retropalatal Space

This area is located posterior to the soft palate and is outlined by the Pharynx. It is one of the major sites of collapse, and is the main area associated with medical procedures such as UPPP and UPPGP (see 2.3.1.4) [29]. According to Lee, Kim [28], the retropalatal space is considered the “narrowest posterior airway space at the level of the soft palate”.

#### o Retrolingual Space

This area, also outlined by the Pharynx, is posterior to the vertical portion of the tongue, and can include the area behind the epiglottis. It is the main area associated with procedures such as hyoid myotomy and suspension [29]. This space is situated inferior to the retropalatal space, and is defined as the “narrowest posterior airway space at the level of the tongue base” [28].



*Figure 2-5 Lateral view of Upper Airway showing the retropalatal and retrolingual regions (Adapted from [30])*



## **2.2.2. Tissue and Muscles of the Upper Airway**

### **2.2.2.1. Tissue Composition**

Lining the epithelium of the upper airway is a tissue comprised of pseudo stratified ciliated columnar epithelial cells [31-36]. It is an impermeable barrier formed by tight junctions, which aids in its function of being highly regulated [34, 37, 38]. Surrounding the nasal and Laryngopharyngeal portions of the upper airway are bony and cartilaginous structures which serve to support these areas, providing them with a particular stiffness. The rest of the pharyngeal tissue, however, is not supported by such rigid arrangements, thus making the pharyngeal portion of the upper airway collapsible in structure [39].

### **2.2.2.2. Muscle Structure**

There exists at least twenty muscles associated with the upper airway which surround it and actively constrict and dilate the lumen of the upper airway [40-42]. While many of these muscles overlap between different regions of the pharynx, and in particular at the lateral walls, there are four major groups in which these muscles can be classified: the muscles which determine the position of the soft palate, the tongue muscles, which includes the genioglossus muscle, the hyoid apparatus muscles, and the posterolateral pharyngeal wall muscles, which include the pharyngeal constrictor muscles. The pharyngeal constrictor muscles themselves, which make up the posterolateral walls of the pharynx, can be divided into the superior, middle, and inferior constrictor muscles. These muscles play a major role in both the process of swallowing and the control of airflow, but it is the combined, co-ordinated activity of all of the muscles that determines all the respiratory and non-respiratory functions of the upper airway [9, 40, 43].

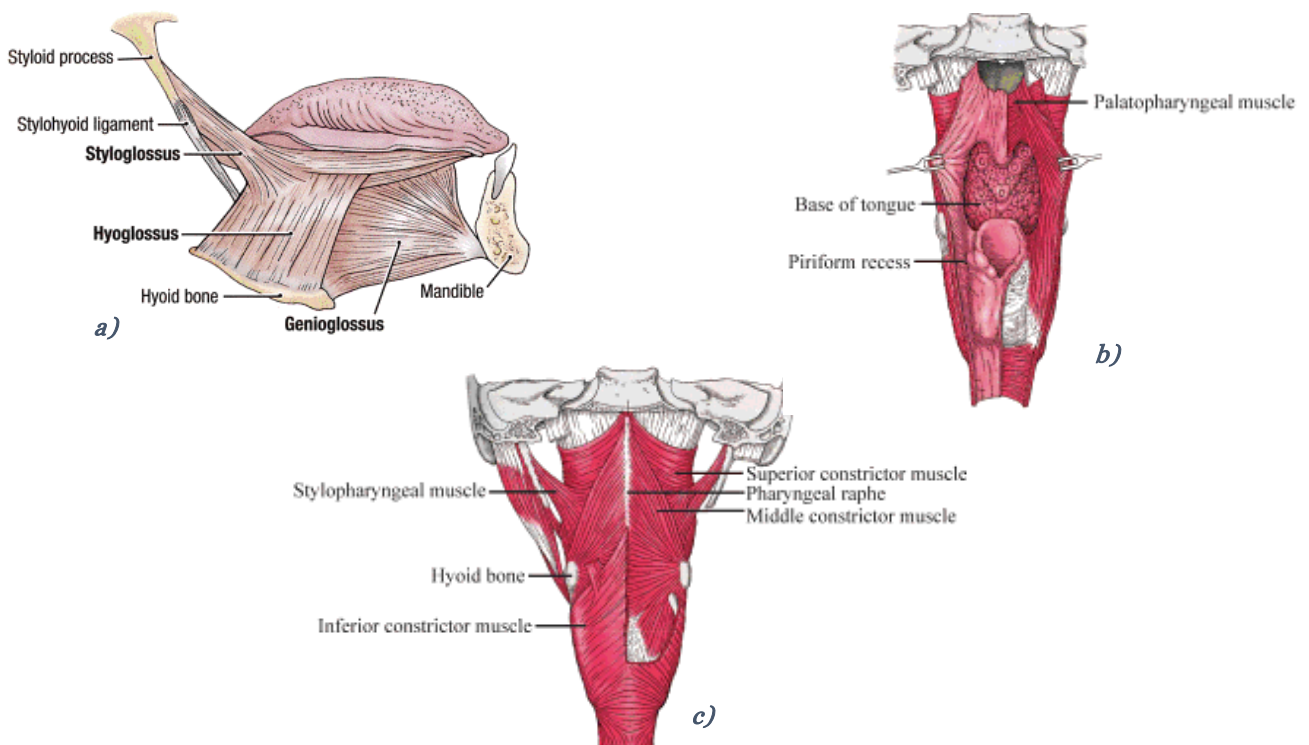


Figure 2-6 Diagram showing lateral view of tongue and associated muscles (a), posterior view of an opened pharynx and position of palatopharyngeal muscle (b), and posterior view of pharynx showing some of the posterolateral pharyngeal wall muscles (c) (retrieved from [44, 45])

### 2.3. Problems associated with the Upper Airway

Just like any organ in the body, the upper respiratory tract is susceptible to health problems and ailments which can severely affect the afflicted individuals' lifestyle. Such problems include infections and a number of various upper airway disorders. However, the most common conditions affecting the upper airway are related to issues of patency.

The nature of the upper airway arrangement and the tissue comprising the respiratory system allows for the possibility of occlusions to be present at any section within the upper respiratory tract. *Apnea* is the term given when complete obstruction of the airway due to occlusion leads to a cessation in breathing for at least 10 seconds despite breathing efforts. A more mild form of apnea is known as *hypopnea*, in which non-occlusive, partial obstruction occurs, leading to an at least 4% desaturation of oxyhaemoglobin and a 30% reduction in airflow for at least 10 seconds when compared to normal breathing. Whether they be partial or total occlusions, these generally give rise to unwanted vibrations and barriers, resulting in conditions such as snoring and the possibility of sleep apnea/hypopnea [46, 47].

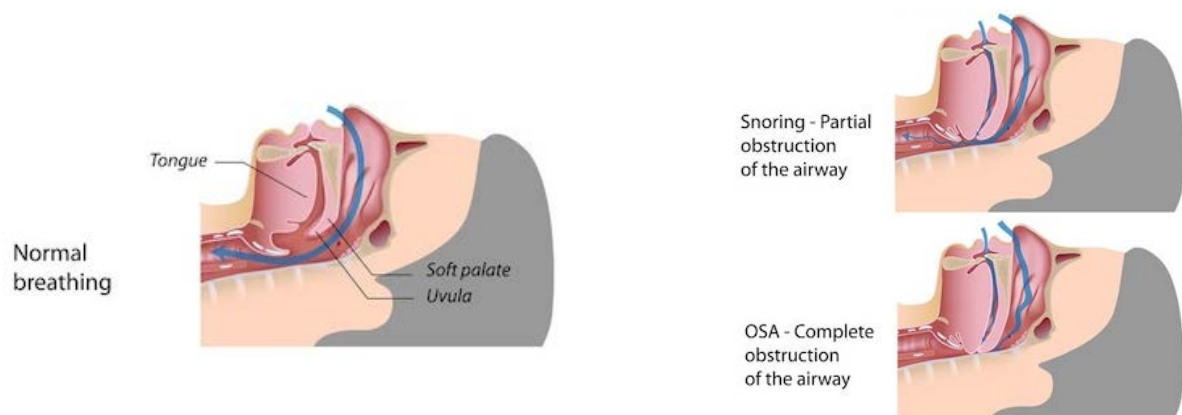
Sleep Apnea is defined by short periods in which breathing stops during sleep [48], giving rise to irregular breathing patterns. It is estimated that approximately 10% of men and 5% of

women are affected by 15 or more apneas and hypoapneas per hour of sleep as of 2012 [49, 50]. The restriction of air flow through such a tight passage, and the nature of the tissue present make one of the most obvious signs, and consequences, of sleep apnea to be snoring, a result of the change in certain upper airway characteristics during sleep. Snoring occurs as a result of the “vibrations of the soft tissues of the pharynx, soft palate, and uvula having specific acoustic characteristics” [40, 51]. These vibrations are a result of several various properties, including more negative pressure during inspiration [40, 52], greater resistance in the respiratory tract during snoring breaths [40, 53], and limitation to flow [40, 53-55], amongst other things. All of which are common instances which occur during sleep. One common form of the sleep apnea condition is better known as Obstructive Sleep Apnea (OSA), and while a condition such as snoring can be a symptom or a tell-tale sign of sleep apnea, it does not quite provide a definite indicator of the presence of OSA [56].

### 2.3.1. Obstructive Sleep Apnea (OSA)

OSA is considered to be one of the most common chronic respiratory disorders. Vries, Ravesloot [57] have indicated that the prevalence of OSA is as similar, and its' presence as common, as that of asthma and possibly Chronic Obstructive Pulmonary Disease (COPD), based on the research conducted and the statistics obtained by Mannino, Homa [58], Lindberg, Jonsson [59], and Von Mutius, Martinez [60].

OSA is generally classified as the cessation of breathing for 10 seconds or more during sleep [5]. Other characteristics of OSA include repetitive pharyngeal collapse, or cessation and reopening of the airflow within the nasal and oral cavities [61] (*figure 2-7*).



*Figure 2-7 Simple diagram showing occurrence of snoring and OSA <sup>1</sup>*

<sup>1</sup> <https://surgicalsleepsolutions.com/obstructive-sleep-apnea/>

### 2.3.1.1. Diagnosis

Several symptoms exist which suggest the presence of OSA, including excessive daytime sleepiness, fatigue, morning headaches, tiredness, depressive moods, insomnia, and neurocognitive dysfunctions [62]. However, because these are rather common symptoms, and thus can be prevalent across a number of various disorders associated with the body, different methods have been adopted in order to diagnose OSA in individuals who display such symptoms.

One common form of diagnosis is the analysis of sound during sleep: because the sound produced during snoring is a cause of the partial collapse of parts of the upper airway, it is an indication that an obstruction is present, and thus OSA can occur due to the inability to breathe regularly as a result of this obstruction. Therefore, by analysing the snore sounds, information can be retrieved on the source of snoring [5], and thus the area in which obstruction is present. However, while this remains a common method used throughout diagnosis, the most commonly tested and currently accepted standard for OSA diagnosis involves the use of polysomnography in a sleep laboratory [63, 64].

By using a Polysomnograph (PSG), respiratory events in the body and the resulting physiological consequences (i.e. hypoxemia, arousals, awakenings, etc) suspected to cause daytime symptoms can be directly monitored and quantified [64]. A PSG involves the simultaneous use of a number of monitoring methods and techniques in order to measure and record certain physiological parameters over the course of several hours, and more commonly, during an entire night. Some of these different techniques include Electroencephalography (EEG), Electromyography (EMG), Electro-oculography (EOG), recordings of air flow, oxygen saturation of the blood, and sometimes even video monitoring and the physical presence of a technician. The combination of these methods allows qualitative and quantitative documentation of abnormalities of sleep, as well as measurement of the physiological functioning of other organ systems which may be influenced by problems during sleep [65].

Portable PSGs have even been developed for efficient diagnosis by the patients themselves without the need for restrictive policies related to sleep laboratories [63]. These were developed so that an accurate diagnosis could be obtained by sufferers of OSA and other similar sleep-disordered breathing syndromes without the need for overly complex procedures, and there exists several studies showing no significant differences in the measured outcomes obtained through the use of either portable or standard PSG [65-68]. In

fact, portable PSG can include the use of all the same leads as those utilised with standard PSG, or can sometimes be as simple as overnight oximetry [65, 69].

This allows for a more readily available form of OSA diagnosis, thus saving efforts on diagnosis and concentrating them on treatment.

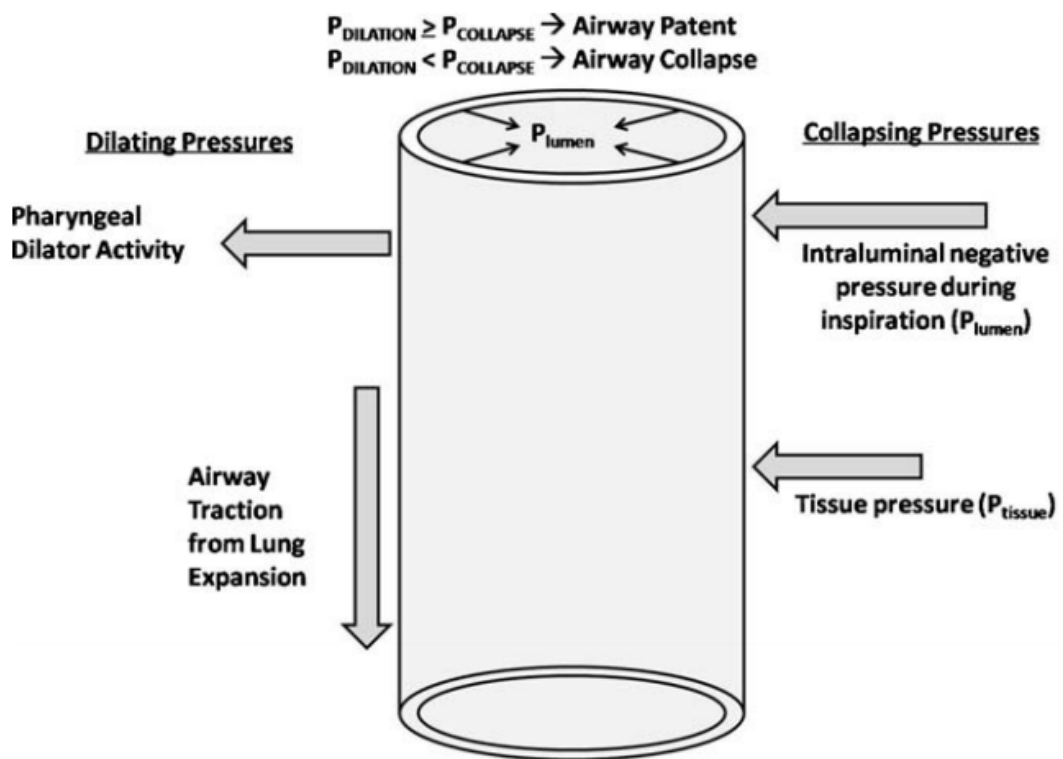
### **2.3.1.2. Causes and Risk Factors**

A wide variety of factors exist which can influence the presence of OSA in an individual. Because the presence of this condition is related to obstruction and decreased latency in the airway, and the resulting improper air transfer through the respiratory tract, any factor affecting this property can play a role in the presence of OSA. Airway obstruction for the most part is the result of a combination of the effects of the mass of the tongue and other tissues, such as the soft palate and associated uvula, and their influence on inspiratory intraluminal pressures, combined with the loss of dilating activity of the pharyngeal muscles during sleep [70, 71].

In general, obstruction due to collapse of the Pharynx can be classified by its belonging to the region of collapse. Collapse can be at the retropalatal region, the retrolingual region, or at both the retropalatal and retrolingual regions [29], and one of the main reasons for airway collapse are changes in muscle activity.

Muscle activity in the upper airway is dependent on a number of factors, such as the pressure in the upper airway [72] and the sleep state of the subject. Research done by Trudo, Geffer [73] suggests that there are significant changes in the volume of the airways and the cross-section of the lumen when the subject is asleep, with as much as a 19% reduction in volume at the retropalatal region during sleep, due to the thickening of the lateral pharyngeal walls. The reason for the decreased patency in the pharynx is an imbalance between collapsing forces and dilating forces affecting the pharyngeal walls [71, 74] (*figure 2-8*). The collapsing forces include intra-luminal upper airway pressure during inspiration, and are also attributed to by the structure and composition of the walls of the pharynx themselves, while the dilating forces are mostly related to dilator-muscle tone [74-76]. The imbalance between these two forces can be caused by several factors, with one such crucial factor being a decrease in the activation of the reflex contractions of the dilator muscles. Several studies [77, 78] have indicated that activation of particular dilator muscles is sufficient during wakefulness, and sometimes may even be heightened. However, during sleep, there is a significant decrease in this negative pressure reflex, causing an imbalance in the forces keeping the upper airway open and thus leading to upper airway collapse [79, 80]. Furthermore, research done by Kuna, Smickley [81] suggests a large variation in the activity of the superior, middle, and

inferior pharyngeal constrictor muscles, with bursts of activity during REM sleep, and a lack of activity during non-REM sleep, indicating a reduction in muscle tone, which could be the cause of the thickening of the lateral walls during sleep, resulting in the narrowing of the airways as a product of their relaxation [73]. Indeed, the increase in the neuromuscular tone of the muscles of the airway in general allows dilation and stiffening of the airway walls, and this muscle tone may be determined by the different levels of consciousness (degree of wakefulness or sleep). However, several other factors also affects this property, such as posture, voluntary activity, response of mechanoreceptors in the upper airway, ventilation, and changes in the lung volume [71].



*Figure 2-8 Illustration outlining the factors involved in the collapse of the pharynx, which is influenced by an imbalance in collapsing pressures (which drive collapsibility), and dilating pressures (which maintain patency) (retrieved from [74]).*

One such very important dilator muscle which plays a big role in the patency of the upper airway is the genioglossus, an extrinsic muscle of the tongue. Susarla, Thomas [74] state that, along with various other pharyngeal muscles which act to dilate the airway, the genioglossus muscle is the largest airway dilator, as well as the most extensively studied. Contraction of this muscle causes the tongue to move anteriorly, widening the airway at the oropharynx, which occurs during inspiration preventing collapse of the airway due to the negative airway pressures generated at inspiration [82, 83], this makes the tongue one of the major organs

which plays a role in inhibited breathing and sleep apnea, since it acts alongside major dilator muscles. In OSA patients, signals associated with activation of genioglossal muscle activity is highly reduced when compared to that of normal subjects [80, 84].

Another set of muscles which play an important role in the narrowing of airways during sleep are those associated with the soft palate, and the presence of the associated uvula. Once more, signals associated with, and thus activation of, the muscles involved in stiffening the soft palate were greatly reduced during sleep, suggesting a general relaxation of the soft palate, which may in turn result in the thickening or the posterior movement of the soft palate, reducing the openness of the airways and thus limiting the flow of air [73, 85]. Changes in the tone of the palatal muscles also affect the shape of the Uvula, which in turn can also affect patency of the upper airway, given that airway closure during OSA is most often at the airway section surrounding the soft palate and uvula, between the soft palate and the pharyngeal walls [82]. Thus it can be seen how, even when a patient is healthy, being born with an abnormally large tongue, tonsil, uvula, or any other organ associated with the upper airway, or abnormal activity of the muscles of the upper airway, can lead to varying degrees of OSA [86].

While all these are natural causes which can lead to the possibility of OSA depending on the degree of their presence, certain other factors can increase the risk of obstructions. These include obesity, the effects of smoking, nasal congestion/obstruction, menopause, and even the ethnicity of the individual [87]. Smoking plays a role in OSA as it produces upper airway mucosal edema, which is a build-up of tissue fluid within the layer of tissue lining the interior walls of the airway, leading to increased resistance in the upper airway [88], while the increased risk of OSA in obese subjects is a result of increased adipose tissue in the tongue, soft palate, and lateral pharyngeal fat pads, which is suspected to increase the pressure of the tissues on the pharyngeal wall, making it more susceptible to collapse [74, 89-92]. This fat deposition in the pharyngeal walls also increases the mass of the tissues associated with the area, meaning increased tissue pressure and, once again, decreased airway volume and an increased susceptibility to collapse [74, 93-95]. Even the presence of other syndromes and diseases, such as asthma, leads to a greater risk of suffering from OSA. Research conducted by Teodorescu, Barnet [96] suggests that there is a direct association between the presence of asthma and the increased risk of new-onset OSA.

Having mentioned only factors related to organ structure and composition, and their influence on upper airway patency, it is important to note that not all the factors associated with OSA are merely limited to such causes, but can be the result of abnormal activity on the part of the afflicted individual. One common example of this are the effects of body posture during sleep. Studies performed by Oksenbergs, Khamaysi [97] indicate that apnea is more severe when the

body is in the supine position than when compared to in the lateral position, leading to an increase in arousal length and frequency, as well as an increase in minimum oxygen desaturation. Other research performed by Cartwright [98] even suggests that by avoiding the supine posture during sleep, some individuals can resolve problems related to sleep apnea altogether [99].

Another unnatural factor which could attribute to the cause of OSA is the result of a related incident which leads to the formation of an abscess or haemorrhage as a result of trauma or tumour growth. This would lead to swelling and, subsequently, airway obstruction [15].

### **2.3.1.3. Consequences**

The consequences which result from OSA can depend on the severity of this syndrome. Being a sleep disorder, the most obvious negative effect of OSA is sleep deprivation or daytime fatigue and sleepiness. When a subject sleeps, the body enters several different sleep “states”, each one of which benefits the body and the mind. Particular deeper sleep states are directly related to the regeneration and rest of muscles and the mind, encouraging processes such as protein synthesis, for example. Parallel to this, the property of the upper airways’ smooth muscle tissue to relax and harden during sleep also depends on sleep state. When an individual enters a deeper sleep state, one which allows the body to recover, the smooth muscle tissues associated with the respiratory tract relax, decreasing the muscle tone in the upper airway, leading to obstruction and sleep apnea, and causing the individual to stop breathing. This cessation of breathing leads to abnormally high levels of CO<sub>2</sub> in the blood, and an increase in blood acidity, which stimulates specific sites in the central nervous system to bring about increased respiratory efforts and force the body to wake up or return to a lighter sleep state, provoking the smooth muscle tissue to harden and overcome the obstruction, and allowing the individual to continue breathing once again. Once the subject is comfortable, he begins to enter a deeper state of sleep once more, and the cycle continues to repeat. This means that someone who is affected by sleep apnea can spend all night asleep, but never really enter a deep sleep state for any prolonged period of time, preventing the body and the mind from getting the rest and recovery it requires, and leaving the individual very tired even after a long night of sleep [86, 100, 101].

While sleep deprivation may not seem too severe or fatal, research can directly relate lack of sleep due to OSA with certain reduced neurocognitive functionality. This includes a reduction in memory, learning, and the attention of the individual [102]. This isn’t merely the case for adults, but even children with OSA are more “prone to irritability, impaired attention and vigilance, emotional instability, and decreased intelligence” [102, 103], this means that



untreated OSA can have a large impact on both a subjects present life, and his development for the future. Furthermore, sleepiness is a large contributor to human error due to reduced levels of alertness and attentiveness, and in particular in a vehicle or on the road, leading to an increased risk of being involved in things such as motor accidents [104, 105]. Studies even suggest that the presence of OSA in children can possibly lead to injury and even death due to lack of focus and impulsivity. Research undertaken by Avis, Gamble [106], in which a virtual environment was setup to measure and relate the effects of OSA in children with the likelihood of getting hit by a car, suggests that while the presence of OSA in children did not affect their ability to look at oncoming traffic or their latency when they started crossing the street, children with OSA still waited for less time to initially start to cross the street, a behaviour which can be related to impulsivity. This led to approximately 63% of children with OSA to be hit or at least have a close call, compared to the 43% of the controls that were hit. These factors are a clear indication of the potential OSA has to be an indirect cause of fatality.

Moreover, OSA can even have more direct consequences relating to debilitation and sometimes fatality. Without proper treatment, some physical conditions which can be caused by OSA include hypertension, Coronary Artery Disease, Congestive Heart Failure, Arrhythmias, and diabetes [87]. Furthermore, there is also a correlation between the presence of OSA and conditions such as nocturia, erectile dysfunction, and impotence [107].

OSA can even have detrimental effects on mental wellbeing, leading to depression [108]. While this correlation remains difficult to validate entirely and definitively, research at least suggests an indirect correlation between apnea severity and depressive symptoms as a result of poor sleep quality [109]. This could be due to neural injuries caused by hypoxia and other conditions, which would lead to disturbances in the person's mood [109-111].

#### **2.3.1.4. Treatment**

Depending on the degree and severity of apnea present, treatment of OSA can vary quite considerably. With some causes of sleep apnea, OSA can be avoided simply by taking better care of one's health. For example, if the cause of OSA is obesity or smoking, these are controllable factors which the individual themselves can rectify in order to avoid sleep apnea. Such treatment is known as a behavioural modification, in which the afflicted individual changes a controllable aspect of their lifestyle in order to mitigate the effects of OSA and its presence without the use of external devices or invasive surgical procedures. Other forms of treatment in this manner can include avoidance of sedative substances or heavy meals before sleep, and, as mentioned previously, sleep position therapy, in which the subject can minimise the presence of OSA by changing the position in which they sleep [112]. This form of

treatment is effective in minimising the risk of OSA, however, for more severe causes of OSA, such treatment is not likely to be effective on its own, and other more direct methods of treatment are required.

Treatment of OSA can be classified into three different categories: behavioural modification, surgical therapy, and the use of devices which can be worn to assist in regular breathing [112]. Behavioural modification, as mentioned above, is the change in ones behaviour and habits in order to prevent or minimise the presence of OSA depending on its severity. For more severe cases of OSA, surgical therapy may be required, which is also present in different forms.

In a general sense, surgical modification of the upper airway can be classified as skeletal modification (or soft tissue repositioning), soft tissue modification or ablation, and upper airway by-pass procedures. Naturally, a lot of ethical consideration is taken into account before surgical treatment can be applied, and treatment in this way is highly dependent on a number of factors, such as the severity of OSA, the individual anatomy of the patient, their personal desires, and any other disorders or diseases that the patient may have. Furthermore, a lot of the reconstructive surgery associated with the skeletal structure or tissues relevant to OSA are in fact done to rectify the presence of already abnormal anatomy and irregular anatomical and tissue structure, rather than being applied to normal anatomy [29, 112].

Skeletal Modification or repositioning of the soft tissue is done with the purpose of placing the soft tissue responsible for OSA under tension and changing their interaction in the space of the airway in such a way so as to prevent them from blocking the airway [29]. One such form of this process includes Maxillo-Mandibular advancement, in which the maxilla, mandible, and hyoid bone are advanced, allowing advancement of the associated anterior pharyngeal tissues, such as the soft palate and the base of the tongue, in effect enlarging the airway at an area of common obstruction without altering the pharyngeal tissues themselves [113]. Other processes related to modification of the skeletal structure include hyoid myotomy and suspension, which involves suspension of the hyoid in effect enlarging the retrolingual airway [29, 114, 115], and Transpalatal Advancement Pharyngoplasty (TPAP), which involves enlarging the airway through removal of part of the posterior end of the hard palate, and thus advancing the soft palate in the anterior direction [29, 116].

Soft tissue modification or ablation is the second form of treatment done by surgical procedure, and is performed with the purpose of reducing the overall size of soft tissue structures heavily involved in obstruction of the airway. A lot of discussion however needs to be established first with the patient due to the irreversibility of these procedures. Some

examples of these procedures include Uvulopalatopharyngoplasty (UPPP), which mainly involves removing the tonsils, parts of the uvula, and the posterior end of the soft palate, as well as closure of the tonsillar pillars, to enlarge the airway at the retropalatal region, Laser Assisted Uvulopalatoplasty (LAUP), which is done to shorten the uvula and alter and tighten the tissue of the soft palate through the use of laser incisions and vaporisations, Radiofrequency tongue base ablation, where radiofrequency energy is employed and focused at the tongue base with a needle electrode to enlarge the retrolingual airway, and Uvulopalatopharyngo-glossoplasty (UPPGP), which is performed by combining UPPP with limited resectioning of the tongue-base, allowing for an enlargement of both the retropalatal and retrolingual sections of the airway [29, 88, 113].

Finally, the third form of surgery which can be performed to rectify the causes of OSA is Tracheotomy, a procedure which by-passes the pharynx all-together, allowing transfer of air with the external environment without the need to travel through areas of obstruction and collapse. This is done by creating an opening directly into the trachea, which is maintained by insertion of a hollow tube into the airway proximal to the pharynx, by-passing the areas which lead to obstruction. The tube can then be sealed when the patient is awake, allowing air transfer to occur naturally through the upper airway and associated organs, and then unsealed before sleeping [29, 117]. While this process is very effective in preventing sleep apnea, since a clear and unobstructed path is provided for the transfer of air during sleep, it, however, should only be considered as an urgent medical procedure, or in a situation where no other existing options are available. Moreover, tracheotomy is also commonly used only on a temporary basis during the period preceding operation for patients who are scheduled to undergo other forms of surgery in the upper airway for treatment of OSA [88, 112].

The invasive nature and hygienic considerations associated with such procedures as a method of treatment for OSA entail that surgical treatment is a final option for those unable to non-invasively rectify the problems associated with this condition. Some patients undergo surgery because they can't adhere to other forms of treatment, such as Positive Airway Pressure (PAP) therapy which requires the use of sometimes large and cumbersome devices. However, the use of external devices which assist in normal breathing as a method of treatment for OSA is usually first line of treatment [112, 113].

Some of the devices which can be worn involve, once again, the repositioning or modification of the skeletal structure or tissue position for the same purpose as that associated with repositioning surgery as described above. Mandibular advancing devices work by modifying the posture of the mandible, in effect controlling the position of the associated organs which are widely responsible for obstruction and collapse of the upper airway. It does so by

imposing a slight downward rotation of the mandible, and can sometimes also advance it. Such devices most often have to be custom developed to suit the individual due to the highly variable individual anatomy of the upper airway and associated structures. Tongue retainers are another example of devices which control the positions of relevant tissue. They are designed to hold the tongue in an anterior position during sleep, preventing it from falling towards the back of the throat when relaxed and blocking the airway. It does so by using negative pressure to secure the tongue into a soft, plastic bulb, which sits on the surface of the teeth or lips, keeping the tongue from retracting posteriorly. While they only act directly on the tongue, they also slightly alter mandibular posture, also by a downward rotation [118]. It was also found that the use of tongue retaining devices reduced genioglossus electromyogram activity, and muscle tone in the upper airway was increased with the use of mandible repositioning devices, indicating that the effectiveness of these devices is not only found in physically increasing the size of the upper airway at specific sites, but also improving upper airway muscle tone, thus minimising the collapse of the airway due to relaxation of the muscle and the loss of muscle tone which occurs during sleep [119-122].

While these devices are somewhat effective as external devices used to treat OSA, the “gold standard for treatment of all categories of OSA” is considered to be nasal Positive Airway Pressure (PAP) [88]. PAP is still recognised as the most adequate and efficient method of treatment for OSA, and for moderate to severe OSA in particular. It involves the application of positive air pressure into the airway, acting in effect as a “pneumatic splint”, thus preventing the collapse of the upper airway which leads to OSA. Although this method of treatment is very effective and available, and yields no major side effects while also being reversible, it assumes that the patient is willing to tolerate wearing a device on their face during sleep. Furthermore, in comparison to surgical treatment, patients view the use of PAP devices as being more inconvenient as it may require constant monitoring and subsequent following-up [112, 123].

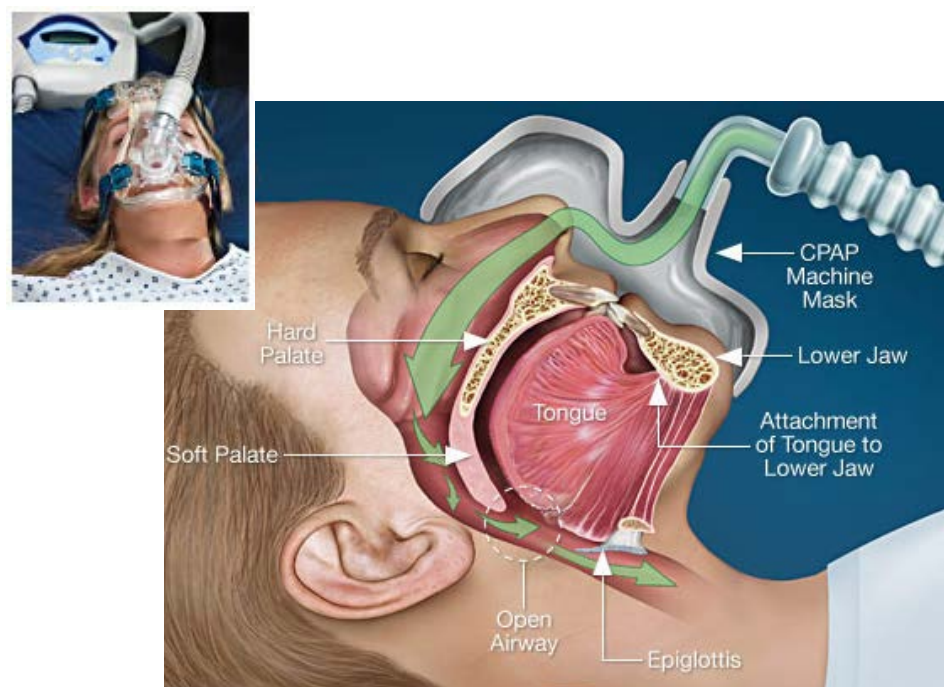
While they all operate under the same principal and method of treatment, there exists several various forms of PAP, such as Continuous Positive Airway Pressure (CPAP), Bi-level PAP, which can be used by patients with obesity, restrictive lung diseases, and congestive heart failure, Autotitrating PAP, which is mainly used for patients who cannot tolerate fixed CPAP pressures, and Demand PAP [88, 112].

#### **2.3.1.5. Continuous Positive Airway Pressure (CPAP)**

CPAP is the most commonly used form of PAP, and remains the treatment of choice when it comes to preventing OSA. Its operation is quite standard, in that it maintains a continuous

constant pressure in the upper airway, physiologically acting as a pneumatic splint, forcing the airway to remain open during inhalation and exhalation [86, 124-126] (*figure 2-9*). This pressure is delivered by a special fan in the CPAP machine that is the source of the air pressure, which generally ranges from 20 to 60 litres per minute, that is passed into the airway through the nasal or oro-nasal interface [86, 127, 128].

CPAP is a safe and simple method of treatment for preventing OSA when compared to the other forms of treatment highlighted previously, as well as being a more effective practice in the presence of moderate to severe sleep apnea, although other research [129] suggests that the majority of studies conducted were “homogeneous for OSA severity”, and somewhat inconclusive of the efficacy and efficiency of CPAP across the range of disease severity. It can be said, however, that the general evidence indicates an overall improvement in breathing during sleep, alertness, concentration, neurocognitive function, and mood. The use of CPAP has sometimes even indicated an improvement in cardiovascular function; reducing blood pressure and thus minimising the risk of heart disease and congestive heart failure, one of the many possible consequences of OSA which were mentioned earlier [86, 107, 126, 129].



*Figure 2-9 Use of CPAP on a sleeping subject (top-left) with illustration outlining the concept behind using CPAP devices <sup>2</sup>*

---

<sup>2</sup> <http://carlossantosmdpa.com/cpap.html>

## 2.4. Fluid Flow

### 2.4.1. Characterisation and Visual Analysis

Fluid in the general sense is a term given to matter which flows and can conform to the outline of the container housing the fluid. This includes gases, liquids, and plasmas. Looking at the physics of fluids means looking at the study of why fluids act the way they do, and the forces which bring about these actions [130, 131]. One important field related to fluid physics is the analysis of the natural motion of the fluid, otherwise known as fluid flow. LaNasa and Upp [130] have defined fluid flow as “...smoothly moving particles that fill and conform to the piping in an uninterrupted stream...”.

The motion of fluid can be extremely complex in real-life situations; as it flows over a surface, there exists a velocity gradient due to the interaction of the fluid with the boundaries, which gives rise to shear stresses in the fluid, altering its behaviour. Furthermore, gases in particular are easily compressible; yet another factor which may affect fluid flow [132].

Depending on the properties of the fluid, a fluid can be identified within two different categories: If the magnitude and direction of the velocity of the fluid does not change from one point to another, the fluid is considered to be *uniform*, while other fluids are considered *non-uniform*. Similarly, if the velocity, pressure, or cross-section of the stream of fluid remains constant over time at a single given point, the fluid is considered to be *steady*. Variations in these properties will lead to *non-steady* fluid flow [132].

Another important concept which forms a basis of fluid flow is the principle of *mass conservation*, which in the context of fluid flow means that a moving fluid flows through a specific region in such a way that its mass is conserved. This entails that, when fluid flow is steady, the flow rate of the fluid at the entrance of a control volume, such as a fixed tube, is equal to the flow rate of the fluid at the end of the control volume [133].

### 2.4.2. General Properties, Governing Laws, and Equations

Fluids are driven by certain physics which allows for the understanding of their motion and behaviour. Therefore, understanding these physics and applying them is very important when it comes to something as dynamic as flow analysis. By understanding the general concepts behind these physics, the observed reaction of fluids to different conditions can be understood, and subsequently, flow can be manipulated.

Two highly influential factors which bring about or control fluid flow are the viscosity of the fluid and the pressure gradient. The viscosity of the fluid is essentially how thick and dense it is in comparison to other fluids. The presence of fluid viscosity leads to shear stresses which develop in a moving fluid, and act as forces acting on the fluid, thus affecting fluid flow. When looking at an ideal fluid, viscosity is so small that the shearing stresses are assumed to be negligible, and thus such fluids, known as inviscid or frictionless fluids, are considered to have no viscosity. With regards to the pressure gradient, which is the difference in pressure from one area to another, this induces a driving pressure, which is the term used when pressure drives fluid to flow in a particular direction with a particular force, from an area of high pressure to an area of low pressure. This gives pressure gradient, as well as driving pressure, both a quantity and a vector component [6, 131].

### 2.4.2.1. Flow Rate

#### 2.4.2.1.1. Volumetric Flow Rate

In measuring fluid flow rate (i.e. the amount of fluid passing a particular point per unit of time), one of the most common solutions to the description of motion of viscous fluids can be derived by assuming steady, incompressible, laminar flow through a straight, circular tube with a constant cross-section. Such flow is known as the *Hagen-Poiseuille flow*. The volume rate of this flow can be described using the mathematical formula commonly known as Poiseuille's law, which describes the effects of different factors on fluid flow through tubes:

$$Q = \frac{\pi r^4 \Delta P}{8\mu L} \quad (2.1)$$

where  $Q$  is the volumetric flow rate,  $r$  is the radius of the tube,  $\Delta P$  is the driving pressure,  $\mu$  is the viscosity of the fluid, and  $L$  is the length of the tube [6]. The volumetric flow rate is an indication of the *volume* of fluid passing through a specific point per unit time, and thus is widely used in the field of fluid dynamics for fluid flow analysis. From the above equation, it can be seen that the rate of volume flow of fluid is directly proportional to the difference in driving pressure and the tube radius, and inversely proportional to the length of the tube and the viscosity of the fluid. This is an important concept to understand as it will later be applied to fluid flow within the respiratory tract.

#### 2.4.2.1.2. Mass Flow Rate

While the volumetric flow rate may be more specific to fluids, another common equation worth studying is that of the mass flow rate. The mass flow rate,  $\dot{m}$ , is an indication of the *mass* of a

substance passing a particular point per unit time. It is directly related to the volumetric flow rate through the equation:

$$\dot{m} = \rho Q \quad (2.2)$$

where  $\rho$  is the density of the fluid, and  $Q$  is the volumetric flow rate.

For a fluid flowing through a tube of cross-sectional area (normal to the direction of flow)  $A$  at an average velocity  $V$ , then the rate of volume flow at a specific point is equal to the product of the cross-sectional area at that point and the average velocity of fluid flow. I.e.:

$$Q = AV \quad (2.3)$$

This yields the following equation which provides a way of measuring mass flow rate:

$$\dot{m} = \rho AV \quad (2.4)$$

This is of course assuming one-dimensional, uniformly distributed flow [6].

#### 2.4.2.2. Law of Continuity

Given that mass is conserved as described earlier, it stands to reason that the mass of fluid remains constant even when flowing through a pipe of varying diameter. The law of continuity states that when flow is constant, the product of flow and the cross-sectional area of the tube remains constant. Thus for any given flow rate,  $Q$ , a change in the cross-sectional area,  $A$ , forces a change in the velocity,  $V$ , of the fluid at that point. With this in mind, and the fact that  $\sum_{in} \dot{m} = \sum_{out} \dot{m}$ , it can be deduced that:

$$\rho_1 A_1 V_1 = \rho_2 A_2 V_2 \quad (2.5)$$

where  $\rho_1 A_1 V_1$  represents the fluid properties at a particular section in the pipe, and  $\rho_2 A_2 V_2$  are the fluid properties at a different point in the pipe with a different cross-section.

Furthermore, because gases are compressible, their density  $\rho$  is largely dependent on factors such as pressure and temperature. However, in assuming incompressible flow,  $\rho$  stays constant, meaning  $\rho_1 = \rho_2$ . Therefore the previous equation can be simplified to:

$$A_1 V_1 = A_2 V_2 = Q \quad (2.6)$$

This is known as the continuity, or *continuity of flow*, equation for incompressible flow.

From this equation it can then be seen that if, for instance, the size of the tube increases, meaning the cross-sectional area increases, then the velocity must decrease in order for the flow rate to remain constant, and vice versa.



Likewise, following the same principle of continuity of flow, if a tube bifurcates at a point, the total flow rate before the junction must equal the sum of flow rates after the junction. I.e.  $\dot{m}_1 = \dot{m}_2 + \dot{m}_3$ . Therefore:

$$\rho_1 Q_1 = \rho_2 Q_2 + \rho_3 Q_3 \quad (2.7)$$

Which can once again be simplified to:

$$A_1 V_1 = A_2 V_2 + A_3 V_3 \quad (2.8)$$

for incompressible fluids, since  $\rho$  is constant and thus  $\rho_1 = \rho_2 = \rho_3$  [131, 132].

### 2.4.2.3. Bernoulli's Principle

Bernoulli's principle only applies to inviscid (i.e. viscous friction is assumed to be negligible and the fluid to have no viscosity), incompressible, steady flow of constant density (i.e. the density changes in the flow field are assumed to be very small) along the same streamline (i.e. any rotational flow is neglected) [132, 134]. It is useful in that it provides a relationship between the height of a fluid particle, the velocity of flow, and the pressure exerted by the flow of a fluid at any given point.

Bernoulli's principle can be represented by the equation known as *Bernoulli's equation*:

$$\frac{p}{\rho} + \frac{v^2}{2} + gz = K \quad (2.9)$$

Where  $p$  is the pressure the fluid exerts,  $\rho$  is the fluid density,  $v$  is the fluid velocity,  $g$  is the value of acceleration due to gravity,  $z$  is the particle height above ground level, and  $K$  is a constant representing the product of the total energy per unit weight and the gravity.

More importantly, when considering air in particular (which is relatively light), the effects of height on the fluid particle may not be as important, and thus the relationship between velocity and pressure specifically is very valuable when fluid flow in the airways is studied later in this chapter.

### 2.4.2.4. Turbulence

Fluids can be found in one of three different states depending on the nature of their flow. The first type, *laminar* flow, is the terms given when the fluid flows parallel to the walls of the enclosing vessel. Fluid particles during laminar flow move in parallel lines.

If, for example, the fluid velocity is increased, the flow can be seen to start oscillating from these parallel lines after some distance, with intermittent bursts of irregular behaviour. This is when flow begins to be classified as *transitional*.

Finally, if flow velocity was increased even further, the flow would not remain laminar for long before it would start to break up and diffuse into different areas, where the particles would travel in different directions. This type of flow is known as *turbulent* flow, and is represented by small changes in the magnitude and direction of the velocity of the fluid particles, which would also result in small changes in pressure. Turbulent flow is much more likely to occur in practical situations [6, 132].

These changes in type of flow occur as the viscous shear stresses, which conform the velocity of fluid particles in laminar flow to one direction and a constant magnitude, are no longer strong enough to overcome the inertia driving the fluid particles to move in a different direction. Thus it can be deduced that turbulence is dependent on the ratio of the inertial force to the viscous force. The final derived relationship between the relevant fluid properties which can be used to measure the type of flow at any given point is given by the following equation:

$$\frac{\text{Inertial Force}}{\text{Viscous Force}} = K \frac{\rho v d}{\mu} \quad (2.10)$$

where  $K$  is some constant,  $\rho$  is the mass density of the fluid,  $v$  is the velocity of the fluid,  $d$  is the distance from the leading edge at which flow transitions to turbulent for plate flow or the diameter of the pipe for pipe flow, and  $\mu$  is the viscosity coefficient. Being a ratio, the resulting number, known as *Reynolds Number*, is dimensionless, and is simply an indication of the type of flow depending on the given values. As a general rule for fluid flow in pipes, if the value of the Reynolds number is below 2,000 – 2,100, the fluid is found to be laminar. If the Reynolds number exceeds 4000, flow is found to become turbulent. With a Reynolds number anywhere in between these two values, flow is transitional between laminar and turbulent [132, 133].

### **2.4.3. Flow of air in the Human Respiratory Tract**

#### **2.4.3.1. General Path of Air Flow during Respiration**

The general flow of air during respiration is different depending on which one of the two actions associated with respiration is taking place: inhalation, or exhalation.

#### 2.4.3.1.1. Path of Air: Inspiration

In order to allow a person to breathe in (known as inhalation or inspiration), the muscles at and around the lungs in the lower respiratory tract contract, allowing the thoracic cavity, which houses the lungs, to expand. The resultant negative pressure induced from this action creates a pressure gradient, drawing air from the atmosphere into the lungs through one or both of the external entrances of the respiratory system: the nose and the mouth [12].

When the mouth is closed, air first enters the body through the right and left external nares (also known as the nostrils). The air entering the nose is divided into the right and left cavities by the nasal septum. The air then passes between the conchae on either side and meet once again at the posterior end of the nasal cavity, where it travels from the nose into the pharynx. The first part of the pharynx the air passes through is the nasopharynx, which remains a passageway for air only, and where some air can also enter into the Eustachian (auditory) tubes to the middle ear cavities, allowing proper functioning of the eardrums. The air then travels inferiorly into the oropharynx, which is a passageway for both air and food. The air then travels further down into the laryngopharynx, where a division exists to separate the different passageways of air and food. Finally, only air is allowed to pass into the larynx from the pharynx. Being comprised of cartilage and acting as the boundary between the upper and lower respiratory tracts, the larynx keeps the airways open at all times, allowing air to travel freely from the upper respiratory tract into the lower respiratory tract, while preventing food from entering the airways through the actions of the lid-like epiglottis (see 2.2.1.1.4) [12].

When the mouth is open, inhalation causes air to enter through both the nose and the mouth. Air entering through the nose follows the same path as that described above, while air entering through the mouth first flows through the oral cavity, along the dorsal surface of the tongue, and passes through the oropharyngeal isthmus into the oropharynx (see 2.2.1.1.3), where it combines with the air at the oropharynx and follows the same path towards the laryngopharynx as that described previously.

#### 2.4.3.1.2. Path of Air: Expiration

In contrast to breathing in, when breathing out (also known as exhalation or expiration), the elastic properties of the respiratory muscles and the lungs allow the thoracic cavity to passively contract when the muscles relax, expelling air out of the lungs and back up into the upper respiratory tract (although this process can also be actively induced for more forced breathing, called *forced exhalation*), making non-forced exhalation more of a passive process [133]. The air then follows the exact same path in reverse as that which was described during

inspiration, exiting through the nose if the mouth is closed, or through both the nose and the mouth in the case where the mouth is open.

#### 2.4.3.2. Properties of Respired Air in Real Respiratory Systems

During respiration, the properties of breath can differ depending on the condition of the subject. Someone who is asleep, for example, will naturally not breathe as hard as someone who is exercising, and thus it is important to understand and control these properties if accurate measurements of air flow under certain desired conditions are to be maintained. One of the most important properties of breathing is the *Tidal Volume*. This is essentially the volume of air inhaled with each breath during normal rested, quiet breathing, which should approximately also equal the volume of breath exhaled. A typical value for tidal volume is around 500 mL. Another important property of breathing is the *breathing frequency* (or breathing rate), which defines how many breaths a subject takes per minute during rested, quiet breathing. This is usually around 12 breaths per minute. The product of these two properties gives the total volume of air entering (or leaving) the lungs each minute, otherwise known as *minute ventilation* [135].

Air also has specific characteristics during respiration. Three particularly important characteristics which, as we will see, vary depending on their location in the airways, and can even slightly vary between each breath, are temperature, pressure, and flow rate. For example, during inspiration, the inhaled air has a particular flow rate, temperature, and pressure at the interface with the outside air (at the nostrils or the lips), which change in value at the interface between the upper and lower respiratory tract (at the Larynx).

In order to preserve function at the lungs, the inspired air needs to be heated to body core temperature (37 °C), and needs to contain as much water vapour as possible. As a result, during inhalation, by the time the air reaches the lungs it is 100% saturated with water vapour, and is heated to 37 °C. The majority of the conditioning of air is in fact done in the nasal cavity, which saturates the air with water vapour and raises the temperature of air to approximately 26 °C, given that the temperature at the mucosal surface of the nasal cavity is approximately 32-33 °C [135-137].

Flow rate and pressure in the respiratory system are directly related. As described earlier, flow rate is highly dependent on, and directly proportional to, the gradient in pressure when it comes to fluid flow (see 2.4.2.1.1). According to polysomnograph results obtained in previous research, the average flow rate during steady respiration at rest in the pharynx is seen to be approximately 0.3 to 0.4 L/s during inspiration, and -0.4 L/s during expiration. In terms of pressure, one recording measured pressures in the pharynx ranging from -5 to -8 cmH<sub>2</sub>O

during inspiration, while another measured pressure at -8 cmH<sub>2</sub>O. Both measurements were close in their location of measurement: at the area of the epiglottis or the entrance of the oesophagus. Likewise a pressure value of approximately 8 cmH<sub>2</sub>O was measured during expiration [138-140].

### 2.4.3.3. Fluid Behaviour in the Airways

In the airways, the “fluid” in question is, of course, the air which is inhaled and exhaled, and thus, properties and characteristics related to air specifically can be applied when looking at behaviour of fluid flow in the airways. In assessing the two important factors described earlier which control fluid flow (i.e. viscosity of the fluid and the pressure gradient) (see 2.4.2), air is driven through the respiratory system by the pressure differences generated by the lungs and surrounding muscle, allowing air to flow from one end to other [133] . As for viscosity, we can assume the viscosity of air plays a minor role in flow rate.

Looking once again at the equation for volumetric flow rate, this time in the context of respiration and the flow of air in the upper airway, for clinical purposes, we can remove the viscosity and the  $\frac{\pi}{8}$  constant from the equation related to Poiseuille’s law (*equation 2.1*) in order to simplify it into the following equation [131]:

$$Q = \frac{r^4 \Delta P}{L} \quad (2.11)$$

From this equation two things can be directly deduced:

1. Fluid flow rate is directly proportional to the driving pressure and the tubes’ radius
2. Fluid flow rate is inversely proportional to the length of the tube

These relations are important when analysing fluid flow so that the logic behind flow behaviour within the airways can be deduced.

It is obvious, given the irregularity of the shape of the upper respiratory tract, that the area of the lumen through which air travels varies greatly. If flow of air through a particular section of the pharynx,  $S_1$ , with a specific cross-sectional area is considered, and then the air flow was to be followed through to a different section,  $S_2$ , with half the cross-sectional area as that at  $S_1$ , then, given the equation for continuity of flow as previously derived (*equation 2.6*), following the concept of mass conservation, it can be deduced that the flow would *accelerate* from  $S_1$  to  $S_2$  in order to maintain the flow rate at the two different sections [133]. This is how air would

be expected to behave during steady respiration as it flows through the various differing shapes and sizes of the lumen at the different parts of the upper respiratory tract, and in particular as it flows through an area of obstruction.

Of course, flow cannot be expected to remain steady throughout respiration, since fluid flow accelerates during the beginning of inhalation and exhalation, and decelerates at the end of inhalation and exhalation. Therefore, the momentum of flow needs to be considered.

A series of assumptions can be applied given that it is air in the airways which is being considered.

1. It can be assumed that the viscosity of air is so small that air can be considered inviscid, making the shearing stresses negligible, and thus allowing the disregard of any viscous forces.
2. Only 2-dimensional motion will be considered as the fluid flows through the airway channels.
3. Since the fluid being dealt with is very light (given that it is air), the effects of gravity on the fluid can be disregarded.

If the momentum is studied in a single direction only, say the flow travelling through the pharynx vertically in the  $y$ -direction, this would mean that no velocity in the  $x$ -direction is measured, and thus the rate of change of velocity in the  $x$ -direction would equal zero. This would yield a simplified version of the well-known *Euler's equation of motion* which, in the  $y$ -direction, would be represented as:

$$\frac{\partial v}{\partial t} + v \frac{\partial v}{\partial y} = -\frac{1}{\rho} \frac{\partial p}{\partial y} \quad (2.12)$$

This final equation presents a simple formula for mapping the velocity and pressure in the airways both spatially and temporally, and thus can be used to represent air flow in the respiratory tract during respiration. The first component of the inertial force (the local acceleration term,  $\frac{\partial v}{\partial t}$ ) represents the change in flow velocity in a particular direction at a specific point over time, thus describing the motion of the air in the airways over time locally. The second component of the inertial force (the convection term,  $v \frac{\partial v}{\partial y}$ ) represents the change in velocity along a particular direction as air flows through the respiratory tract, thus describing the acceleration of fluid spatially. Finally, the pressure force (appearing through the pressure gradient,  $-\frac{\partial p}{\partial y}$ ) represents the differences in pressure induced by the flow. Note that if Euler's

equation of motion was integrated, what would remain would be the previously encountered Bernoulli's Equation (*equation 2.9*), which relates velocity to pressure (see 2.4.2.3) [6, 133]. To put this into context, if the previous example is to be considered of air flowing through a section of the pharynx of a particular cross-sectional area into a separate section with half the cross-sectional area, it was deduced earlier that the velocity would need to increase in order to maintain the same flow rate, following the continuity of flow equation (*equation 2.6*) (see 2.4.2.2). If the pressure was to be measured at this section as velocity increases and the air accelerates into the narrower section of the pharynx, the pressure gradient, according to previous research [27, 133, 141, 142], would show as negative (i.e.  $\frac{\partial p}{\partial y} < 0$ ). In the above equation, this can be seen to correlate with an increase in the velocity of the fluid, given that a more negative value of pressure in the term  $\frac{\partial p}{\partial y}$  would lead to an increase in acceleration,  $\frac{\partial v}{\partial t}$ . Likewise, when the opposite happens and flow decelerates into a different section, the resulting pressure would be measured as positive (i.e.  $\frac{\partial p}{\partial x} > 0$ ), corresponding to a decrease in fluid velocity. In relating this to the derived equation above (*equation 2.12*), a positive pressure value would mean a decrease in acceleration. This agrees precisely with what would be expected by looking at Bernoulli's equation (*equation 2.9*), where an increase in fluid velocity would lead the pressure to be more negative, and vice versa.

## 2.5. Previous Research in Upper Airway Modelling

When it comes to experimentation in the field of medicine and biology, problems are always prevalent, depending on the goals and desired results, due to the obvious ethical boundaries and practical difficulties present in biological settings. Modelling is such a useful tool as it enables the ability to test and experiment with concepts as they are required without the need for unattainable resources, providing the freedom to utilise the model as desired. It also presents the ability to maintain control over external parameters in order to achieve and manipulate the desired results. Different forms of modelling have been done in the past with regards to respiration, and used for the purpose of analysis of air flow within the respiratory tract during breathing.

### 2.5.1. Mathematical Models

Mathematical modelling, which involves the numerical representation of entire systems, provides a very easy way of measuring the reaction of a system to changes in the variables which constitute the modelled structure. Modelling using this process is usually done through a series of simplifications, assumptions, utilisation of known physical laws, and mathematical equations. As described by Aittokallio, Virkki [143], it provides a quantitative means of understanding the behaviour of complex systems and predicting events related to their functions, and in the case of biological organ systems in particular, mathematical modelling can be used to test the efficiency of different available treatments. On the other hand, while mathematical modelling can be very accurate when representing an arrangement or physical phenomenon, the disadvantage of using mathematical modelling, aside from the fact that it negates the inclusion of random, unexpected events or situations, is that it is largely based on a set of assumptions which simplify sometimes highly complex systems into general equations. This can often result in failing to achieve the level of accuracy needed to properly represent real systems and processes, which can lead to unexpected results. Furthermore, when a mathematical model is produced, validation is usually required in order to ensure that the mathematical model accurately represents the behaviour of the modelled system under the set conditions, although validation in any case, regardless of the method of modelling, is beneficial.

In their research, Aittokallio, Virkki [143] test the validity of using mathematical models in order to study how the human respiratory system operates in health and in disease, and place a large focus on the behaviour of the airways during the transition from wakefulness to sleep. Through the solution and alteration of a partial differential equation model of a collapsible upper airway, they are able to show how this model can be used in order to explain distinct flow characteristics between healthy individuals, and individuals with sleep-disordered breathing. Aittokallio, Virkki [143] conclude, however, by stating that these simplified models cannot be used to reflect the entire range of various factors involved in sleep-disordered breathing, even though they can likely be used to accurately estimate individual parameters of the respiratory system such as the critical pressure of pharyngeal collapsibility.

Mathematical modelling is generally more successful when applied to a single area of similar structure and function throughout, so that the set of derived equations used can somewhat be applied to the entire system. Previous experiments have had airflow in specific organs, such as the nasal cavity [144, 145], pharynx [146, 147], and parts of the lower respiratory tract [148] individually numerically modelled. Keyhani, Scherer [144] constructed a finite element



mesh of an adult human nose using 42 coronal CAT scans of the nose. Velocity profiles within the nasal cavity were then computed using equations relevant to the conservation of mass and momentum laws for incompressible steady fluid flow. This was enabled by using a series of calculated assumptions, such as considering only laminar flow, and assuming rigid walls to represent the boundaries of the nasal cavity (*see section 2.4 for more information on fluid flow*).

Likewise, the mathematical model of the pharynx developed by Shome, Wang [147] involved the establishment of similar governing equations achieved through a series of assumptions related to the conservation of mass and momentum laws. Some of these assumptions included considering flow to be incompressible and steady, and regarded the pharynx walls as passive and rigid.

It is worth noting these assumptions underlying mathematical models of the upper airway in order to gain an understanding into its behaviour and so that this may be accurately carried forward when building a physical model. Several research has had the upper airway modelled using the same concept as a Starling resistor [149, 150], in which the area of collapse is represented by a flexible, collapsible, cylindrical tube fixed within a sealed chamber. Aittokallio, Gyllenberg [149] did so by utilising a model comprised of a set of partial differential equations along with associated boundary conditions in order to analyse and predict regular behaviour of the upper airway, as well as include partial collapse and flow oscillation. In this model, the respiratory parameters most significant to the operation of the upper airway were the respiratory pump drive, the stiffness of the pharyngeal soft tissues, and the support of the muscles surrounding the upper airway. By taking a brief look at the important factors used to mathematically represent air flow in the upper airway, this can provide an indication of the important factors to consider during other methods of modelling.

As it can be seen, mathematical models on their own can provide very important information about a system and the way in which it operates. However, given that this method of modelling is largely based on general assumptions, this can sometimes not be the most accurate method of modelling. Furthermore, because modelling biological and physical factors can lead to highly complex equations and relations, most mathematical models are translated into virtual models so that calculations can be computed virtually and so that, in the case of fluid flow in the airways, air flow can be modelled in a structure which accurately resembles that of the complicated respiratory system and its organs.

### 2.5.2. Virtual Models

Almost any form of modelling is likely to involve the use of a virtual model at some stage, or at least the creation of one. This is due to the level of accuracy which can be maintained by modern computers when reproducing the expected activity of the modelled organs and the flow of fluids. Moreover, creating a virtual model means that simulations and calculations can be performed at a high speed and with high efficiency. Even most of the mathematical representations of models completed using mathematical modelling are carried over to be included in computer simulations and evaluations. Such is the case when using Computational Fluid Dynamics to look at fluid flow. Computational Fluid Dynamics is the study of fluid flow and fluid behaviour through the numerical solution and manipulation of mathematical equations representative of the fluid flow [133]. While the specifics of this very diverse and widely used field unfortunately lie outside the scope of this research, the results achieved in previous research using this method can provide great insight into expected fluid flow behaviour within the upper airway.

In their research, Nithiarasu, Hassan [151] use Computational Fluid Dynamics to analyse fluid flow in the upper airway. Their results indicate large pressure forces, as well as high values of shear stress on the airway walls, particularly at the area of the pharynx where the laryngopharynx and the oropharynx intersect. This area is equivalent to the space posterior to the base of the tongue. Likewise, Wang, Liu [152] observed a spike in the pressure and shear stresses at the pharyngeal walls in the area of the pharynx behind the base of the tongue. Interestingly enough, this increase in pressure and shear stress was less evident at the area behind the uvula in the retropalatal space, where it would be expected. Furthermore, at the highest flow rate during inspiration, some of the highest velocity magnitudes of air flow are seen at the nasal cavity, after which the velocity of air decreases entering the pharynx and increases once again as it passes behind the epiglottis in the retrolingual space. The increase in velocity in this area is once again seen as the highest flow rate during expiration, no doubt a result of the constriction of the upper airway lumen at this area. This constriction becomes more evident when looking at the deposition of micro- and nano-particles in the upper airway where, in their article, Kleinstreuer and Zhang [153] indicate heavy depositions of these particles at the retrolingual space and at the interface with the larynx. The aforementioned velocity profiles are also the same as those found by Zhang and Kleinstreuer [154] in the upper airway in a different article when the transport of nano-particles were simulated, and their flow analysed using numerical methods. Although, once again, even though there was a slight increase in velocity compared to that which was observed in the nasal cavity, there was no notable major and sudden increase in velocity at the retropalatal region.

Another virtual experiment involving Computational Fluid Dynamics worth reviewing is that of Yu, Zhang [155], due to the combination of airflow paths tested. In their research, air flow was not only analysed during both inhalation and exhalation, but it also involved air flow analysis during nasal only, nasal and oral, and oral only breathing. The results show the difference in airflow in the presence of another entry. In the situation of nasal-only breathing, the highest flow rate can be seen at the retropalatal and retrolingual spaces as expected, particularly during inhalation. During exhalation, a large flow rate profile can be seen in almost the entire pharynx in general, extending from the larynx up through the nasopharynx. In the presence of both nasal and oral respiration, a similar velocity profile can be seen during inhalation, however it is obvious that the measured flow rate is largely decreased at the retropalatal region, and slightly decreased at the retrolingual region. During exhalation, a similar flow rate profile is seen as that which was measured during nasal-only breathing, but flow rate is seen to have largely decreased at the nasopharynx close to the retropalatal region. These changes in measured flow rate are expected given that the results also show that the largest magnitudes of fluid velocity, and thus the majority of air transfer, occurring through the mouth rather than the nose during both inhalation and exhalation. Finally, in oral-only respiration, there is an increased flow rate at the retrolingual region during inhalation, with the most evident increase at the anterior edge of the pharyngeal boundary.

It is clear to see how virtual models provide a means through which already derived mathematical models could be applied to realistic geometry, since complicated shapes can be modelled virtually and processed to allow for simulation. In the case of the upper respiratory tract, some research [155, 156] based the virtual model on an already made physical impression of a model used for teaching at a medical school. The airways were made out of silicone rubber using a negative impression of an existing physical model. The silicone model was then thinly sliced into several cross-sections, and these cross-sections were scanned and their outlines digitized, allowing for virtual reconstruction of the physical silicone model. Further to this, the 3D reconstruction by Martonen, Zhang [156] was combined with other methods for grid generation, enabling the future use of computational flow calculations on the virtual model, therein presenting the virtual model with its purpose. This research is one example which highlights the importance behind the use of virtual models, and the possibilities which ensue in experimentation and analysis.

While this method may have been efficient in obtaining a virtual model, it was based on the use of an already existing physical model. Some other research, however, focuses on the opposite: building a physical model through the use of a virtual one, with the purpose of carrying that level of accuracy produced by the virtual model over to a physical model. When

this is the case, another method would be required to obtain a virtual model without the need to use an already existing physical one.

Most other research involving virtually creating an upper respiratory tract was based on obtaining the geometry from medical imaging technologies, such as MRI machines and CT scanners [145, 151, 157, 158], with the notion being that the resultant images used would provide the most accurate geometry possible given that it would be based on detailed images of actual organs. These models can then be represented by a surface mesh, before being converted to volume models [151, 158]. By obtaining a mesh framework of an accurate geometry of the upper airway, tests can then be successfully adapted to that geometry in order to measure the desired behaviour of specific characteristics of the upper airway in a realistic environment.

### **2.5.3. Physical Models**

Because modelling is often done in order to represent physical systems, it stands to reason that the best way to model these systems is physically, provided it is done accurately and the underlying factors behind which the system is based on are maintained.

By building an accurate physical model of the respiratory tract, tests can be conducted using these models to provide a somewhat accurate indication of what would be likely to occur, and the results which would be expected, in a real respiratory tract given the same conditions. In fact, as mentioned before, models developed through numerical procedures are often validated by subjecting some form of a physical representation model to the same conditions as those being tested, indicating the accuracy and confidence of results of physical systems [151, 158].

Depending on that which is being measured, and the desired outcome of the experiments, physical models can be simplistic representations, consisting of only the parts necessary to provide the desired conditions. One such example is the validation of numerical simulations of the human pharynx by Chouly, Van Hirtum [146]. In this research, the aim of the experiment was reproducing a fluid-structure interaction in the upper airway in order to predict the effects of flow-induced collapse within the pharyngeal airway. Given that the area near the base of the tongue is a common site of collapse (see 2.3.1.2), this area was modelled using a latex tube filled with water to represent the tongue, which lied orthogonal to a rigid metallic pipe which represented the pharynx. While this may not be the most accurate model in terms of

replicating this area of the upper airway, it serves the purpose of the aim of this research, and the obtained results are representative of what would occur realistically.

On the other hand, other research, such as that performed by Mylavarapu, Murugappan [158] has had relevant organs modelled more accurately. In constructing their model airway, a surface mesh representing the outer boundaries of the upper airway was constructed using a series of grayscale image slices obtained through MRI scans. This surface mesh was then reconstructed as a 3D model, and then physically created using stereolithography. While this model was an accurate representation of the upper airway, certain areas associated with the upper airway were omitted altogether, such as the oral cavity, due to its irrelevance in this research. Meanwhile other investigations more relevant to the entire airway have been carried out to model all upper airway cavities, which was done by obtaining wax negatives of the airway, and building a resin mould through a lost wax process [159]. However, all the described research either omitted important properties associated with the upper airway (such as flexibility of the airway walls), important organs associated with the airway (such as the tongue and uvula), or entire sections of the upper airway altogether (such as the oral cavity).

## 2.6. Summary

This chapter has highlighted just how complex the different divisions of the upper respiratory tract really are. Understanding their complexity, overall structure, and basic composition also provided a better understanding of the common yet critical disease known as Obstructive Sleep Apnea, and how its presence is based upon the flow of air within the upper airway. Thus in order to better understand OSA, fluid flow in general was studied and its concepts applied specifically to the upper airway. Upon understanding OSA and its dependency on fluid flow, the importance of understanding and analysing fluid flow within the upper respiratory tract became evident, indicating why modelling of the upper respiratory tract and the subsequent use of the models for fluid flow analysis, a process which is very difficult to achieve in living beings, is crucial. Therefore, previous research in modelling and analysis of the upper airway was outlined. From this it could be seen that, while somewhat effective, a lot of unrealistic assumptions were made in order to obtain the desired results, such as regarding the airway walls as rigid, which is in fact not the case. Furthermore, given the wide range of different models created for fluid flow analysis, no physical models were developed which had all three properties of accuracy, transparency, and flexibility. As a result, ***none of the above models presented an entirely realistic physical simulation model for the upper airway, even though physical analysis through observation is crucial for completely***

***understanding the nature of fluid flow.*** This is the reason the development of a realistic upper airway visualisation model was attempted.

The next chapter will outline the methodology by which a complete virtual model of the upper respiratory tract was obtained, and used to develop a complete and accurate physical model of the upper respiratory tract.

# Chapter 3 - IMAGE ANALYSIS AND MODEL DEVELOPMENT

## 3.1. Introduction

During the development of the upper respiratory tract model, it was especially important to take care in maintaining the intricate details of the respiratory tract, both with respect to the geometry and properties of the inner boundaries and the associated organs, so that fluid flow in this section of the airways would realistically represent real airflow during respiration when viewed in real-time.

Thus this chapter will outline the methodology behind the creation of the complete upper respiratory tract model by dividing the entire process into three stages:

- The first stage involves the obtainment of a virtual model representing both the airway boundaries and the associated organs of the upper respiratory tract
- The second stage involves the development of the physical model of the upper airway boundaries, and will highlight the preliminary investigations and evolution of thought process involved with achieving the final airway boundary model
- The third stage highlights the methodology behind which the organs associated with the upper airway were developed

## 3.2. Creating the Virtual Model

In order to maintain the highest level of accuracy for modelling the upper airway, an MRI scan was the method by which real images of a respiratory tract were obtained, and subsequently used in order to provide the basis upon which the final model was built (*See Appendix I for more information on MRI technology*).

The following steps outline the process used to obtain a virtual model of the complete upper airway:

1. MRI images were collected of a healthy male subject. The subject was 21 years of age, weighed 65 kg, was 165cm tall, had a BMI of 23.9, and was of Indian ethnicity. The upper respiratory tract of this subject was used to represent the general shape of

the respiratory tract in the average healthy male. The MRI scan was performed along the sagittal plane of the male subjects head, and resulted in a total of 176 grayscale images. However, because the airway lies along the centre of the body and does not span the entire width of the body, of the 176 images, only 61 images were selected which were closer to the midline, and thus more relevant to the upper airway (*figure 3-1 a*).

2. These grayscale images were then loaded using 3D modelling and imaging software 3D doctor™ (*figure 3-1 b*).
3. Further to selecting only the frames relevant to the upper airway, a specific boundary was highlighted around the upper airway region, establishing this as the region of interest and ensuring that further processes only concerned this area, and as a result would only be applied to the upper airway (*figure 3-1 c*).
4. After the upper airway region was emphasised, interactive segmentation was performed within the region of interest, establishing all the object boundary lines for the selected relevant planes (*figure 3-1 d*).
5. This resulted in a series of boundaries which were constructed by highlighting the borders where there were sudden changes in shade, these borders of course being the interface between tissue and air (*figure 3-1 e*).
6. Because this process involved the automatic formation of boundaries within the entire region of interest, some manual alterations were required: deleting all irrelevant boundaries not related to the upper airway, splitting the boundaries where required, and closing the boundaries at specific undesired openings, such as at the nostrils. After ensuring all the present boundaries were specific to the upper airway only, the boundaries were then smoothed so as to produce a more realistic outline of the inside of the airway, and this entire process was repeated for each frame. The resulting boundary lines were a representation of the empty air spaces within the upper airway, and thus in each frame the boundaries represented a cross-sectional outline of the inner linings of the upper respiratory tract, which would be the confines within which air flow would be observed (*figure 3-1 f*).
7. Using the software's 3D rendering function, the series of outlines were then "merged" through a surface rendering process in order to provide an accurate, realistic, virtual, 3D representation model of the entire space within the upper respiratory tract, extending from the tip of the nasal cavity down to the Larynx (*figure 3-1 g*).
8. Finally, the developed virtual model of the airway boundaries was then combined with models of the tongue and uvula (obtained using the same procedure as that outlined above), and the final model was exported in STL format so that it may be read by 3D



printers as well as external CAD software (figure 3-1 h). This process resulted in the obtainment of an accurate virtual model of the airways combined with the associated organs of the upper respiratory tract.

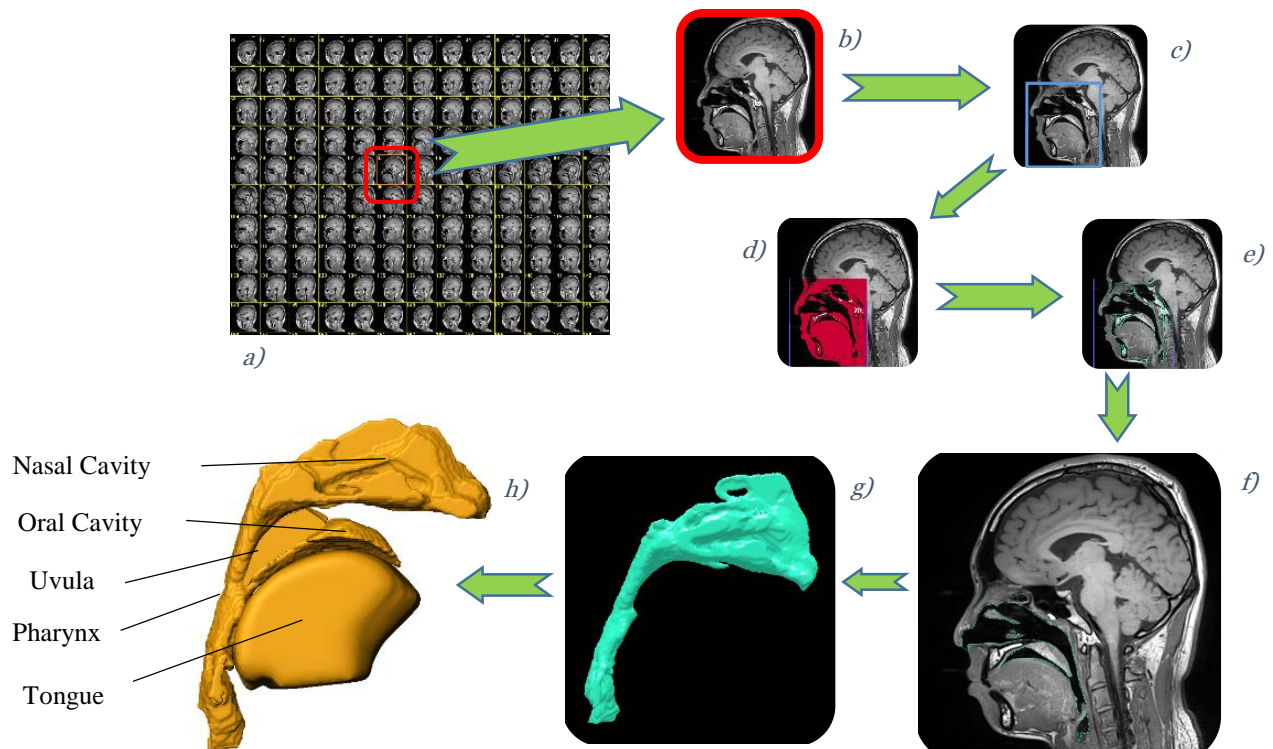


Figure 3-1 Diagram showing process of obtaining virtual model from MRI scan images, done through interactive segmentation and subsequent surface rendering

### 3.3. Physical Modelling of the Upper Airway Boundaries

Given that, during respiration, the only interface with which inhaled and exhaled air interacts with is the inner lining of the upper respiratory tract, during the physical airway modelling process the main objective was to develop a thickened representation of this boundary while maintaining the necessary characteristics of transparency, flexibility, and accuracy, as stated previously. The most challenging and time-consuming task for this research was by far the recreation of a usable model which accurately represented the complex geometry of the upper airway boundaries, but it was realised that this could be done by making a physical model of the air within the airways and, using it as a core, encasing it and coating it with the material which would make up the final upper airway boundary model. This would allow the final material to assume the models' boundaries, in effect forming the inner lining of the upper respiratory tract. In addition to this, because the final material would need to be in liquid form

in order to effectively and accurately coat the entire model of the upper airway, a casing was required within which the material could be poured into in order to take its shape around the model of air in the airways.

### **3.3.1. Preliminary Investigation and Evolution of ideas**

In the early stages of investigation during the modelling process, a few models were attempted and adapted in order to achieve the final model. These preliminary models are summarised below:

#### **3.3.1.1. Model 1 – Silicone-Casing Model**

Probably the most generic material which would be considered when modelling an organ or part of the body is silicone rubber, given that it shares a lot of the same properties found in skin and soft tissue, and is thus used extensively in the special effects industry. This material has been used in the past to physically model even the upper airways themselves [155, 156].

Creating the first physical upper airway boundaries model was done through the following steps:

1. A physical model of the upper airway boundaries and associated organs was 3D printed using the virtual model obtained by the process outlined in the previous sub-chapter (*figure 3-2 a*)
2. The printed upper airway model was attached onto a metal cylinder, and suspended within an empty carton (*figure 3-2 b*)
3. Liquid silicone rubber was poured into the empty carton to take the shape around the printed airway model, and the solution left for 24 hours (*figure 3-2 c*). The silicone rubber used was the Dragon Skin® 20 silicone rubber from Smooth-On, Inc. (See *Appendix III for Technical Information and Data Sheets of materials used*)
4. After the silicone rubber had dried, the carton was cut around the now solid model and removed, leaving behind a silicone rubber encasing of the shape of the upper airway (*figure 3-2 d*).

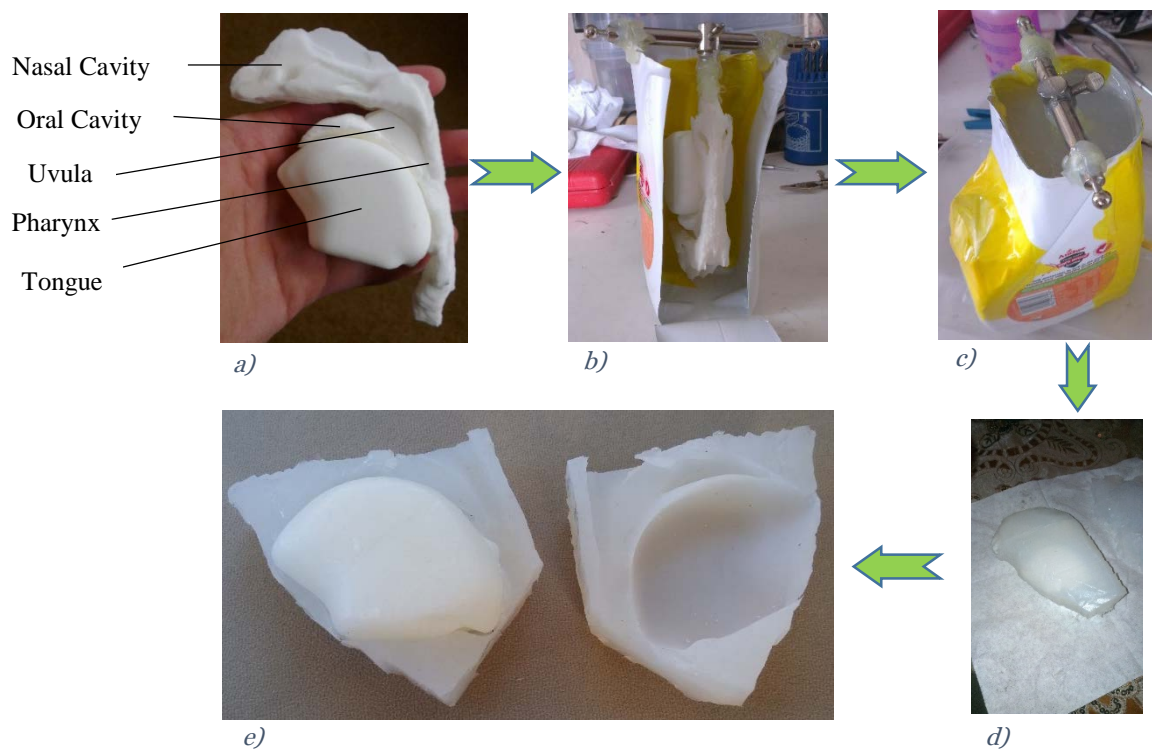
This technique, however, was ineffective for the purpose of this research due to two main problems:

- The first problem being that while the model exhibited the property of flexibility, it was still far too opaque to be able to view the flow of air as well as the deflections of the

inner organs within the empty spaces (*figure 3-2 e*). This meant that standard silicone rubber was not an ideal material to be used for modelling.

- The second problem found was that, due to the complexity of the upper respiratory tracts' geometry as well as the lack of flexibility of the solid model making up the core, it was far too difficult to cleanly and accurately cut around the silicone and remove the solid upper airway model from within the silicone encasing without altering the overall required shape and destroying the integrity of the material. Also, certain areas which contained holes, such as at the laryngopharynx, could not be maintained in the model without cutting through the silicone.

Thus two main points became evident from this process: that another material would need to be found which would be more suited to use in order to build the model, and that the initially solid physical model making up the core would need to be melted or dissolved once the final outer material had hardened in order to effectively remove it and obtain the final desired shape while still maintaining the intricate details which are a part of the upper respiratory tract.

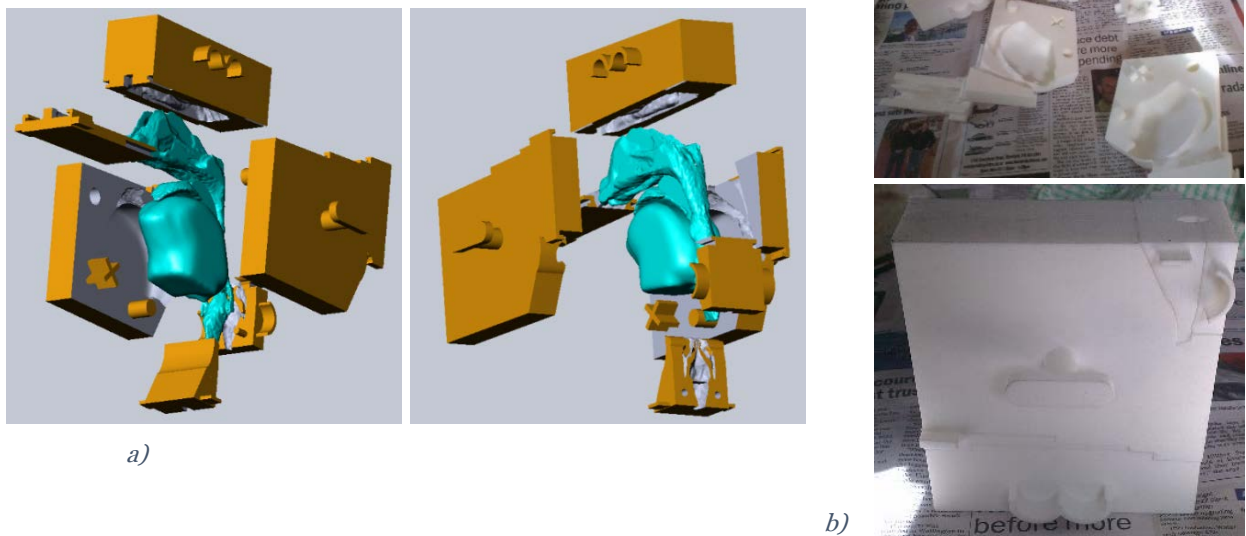


*Figure 3-2 Process showing the development of a silicone encasing of the upper airway model. The area of the oral cavity shown in panel e) is an example of the final encasing and its opacity*

### 3.3.1.2. Model 2 – Wax-Core Model

#### 3.3.1.2.1. Making a Mould Tool of the Upper Airway

Given that the material comprising the core needed to be melted, it was deduced that if a core was to be made which maintained the accurate shape of the upper respiratory tract, it would need to be hardened into that shape from an initial liquid form. Therefore, using CAD software, the virtual model developed of the upper airway was subtracted out of a solid cuboid block, effectively making a mould tool of the upper airway. This block was then altered slightly and segmented into 6 different parts in order to allow for the parts to be separated whilst still preserving the shape of the inside model (*figure 3-3 a*). Once again this was necessary due to the complexity of the geometry of the upper respiratory tract, which prevented a simple two-piece separation. The parts were then sent to be 3D printed out of Nylon material using SLS, thus providing a complete mould tool of the upper respiratory tract resistant to high temperatures (*figure 3-3 b*).



*Figure 3-3 Production of the upper airway mould tool showing the final virtual mould tool (a) and the separate constituents after printing and assembly (b)*

#### 3.3.1.2.2. Making the Core

Initially, paraffin wax, obtained by melting regular candles in a pot within a water bath, was poured into the developed mould tool to be used as the core. A number of candles were melted and kept at a high temperature, providing a liquid which would harden into solid wax once left to set at normal temperatures. The final model could then be heated once more, or placed in hot water, in order to remove the wax core, leaving behind an empty model of the

upper airway. However, once the liquid wax was poured into the mould tool and left to set, the wax was too brittle and the final shape too complex to allow for easy separation of the mould tool parts without compromising the structure of the airway model. Particularly at the area of the nasal cavity, where the wax would break each time the parts were separated (*figure 3-4*). Furthermore, the difficulty in removing the hardened wax stuck within the mould tools meant that further repetitions required an unnecessary amount of time and effort. Given these reasons, it was obvious that another, slightly more malleable material would be required.



*Figure 3-4 Example of attempted paraffin wax model of upper respiratory tract*

Consequently, a new material, sugar-wax, was tested. Sugar-wax was made by dissolving a large amount of sugar in water, and cooking it over the stove while adding small amounts of lemon. This resulted in a very hot and sticky liquid which cooled down to form a hard (and delicious!) solid. Furthermore, given that it was made exclusively from sugar and water, the solid sugar-wax was entirely, easily dissolvable.

The inside of the mould tools were then coated in a layer of cooking oil and flour in order to prevent the sugar-wax from later sticking to the surface, and after being prepared, the sugar-wax was instantly poured into the closed mould tool (*figure 3-5 a*) and left to cool for approximately 45 – 60 minutes, allowing the liquid to solidify to the point where it would hold a shape while still being somewhat flexible. Upon reaching this point, the mould tool was removed from around the now solid model of the upper airway (*figure 3-5 b*) which led to the



successful production of a solid, accurate, dissolvable core model, representative of the upper airway (*figure 3-5 c*). This core was then kept refrigerated in order to prevent degradation at normal room temperatures.



a)



b)



Nasal Cavity  
Oral Cavity  
Uvula  
Pharynx  
Tongue

c)

*Figure 3-5 The acquirement of a sugar-wax model of the upper respiratory tract and its similarity in shape to the previously 3D printed physical model*

#### 3.3.1.2.3. Altering the Core

Before coating the core in the final material, the core was slightly altered to better represent the upper airway boundaries. This involved adding additional wax at the top of the nasal cavity to compensate for the lost material which the shape of the mould could not capture, and filling the gaps between the tongue and the modelled air above the tongue to more realistically represent the cavity within which air flows.

#### 3.3.1.2.4. Creating an Outer Mould for Physical Modelling

A more accurate outer casing within which the final model would be poured was developed using the following steps:

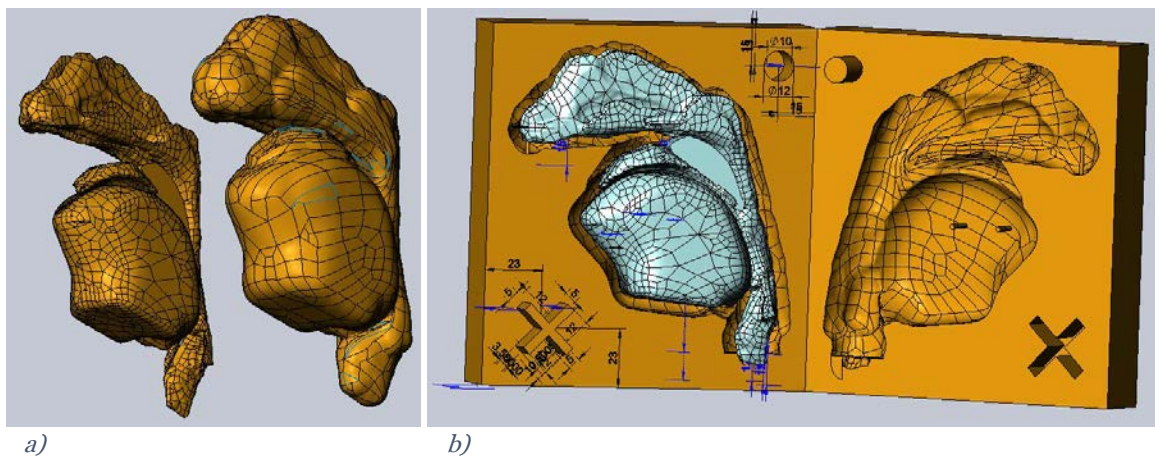
1. The virtual model created of the upper airway was copied and, using 3D CAD software SolidWorks®, converted from STL format into a usable format by using the in-built ScanTo3D function in order to open the STL format file as a mesh file. The original mesh file contained 1,873,832 faces.
2. This mesh file was then converted into a complete surface by first removing facets with topology errors, and then using the software's surface generating tool in order to completely transform the mesh into a surface.
3. The resulting surfaces with errors were then deleted and recreated manually, allowing the final closed surface of the upper respiratory tract to be saved as a solid file.
4. The final modifiable format of the model was then thickened outwards by a distance of 5mm (*figure 3-6 a*), and the resultant shape centred within a solid cuboid, and hollowed out of the solid block.

This produced an empty cavity within the solid block which shaped the outer contours of the upper airway model, and within which the core could be suspended. The purpose of this outer mould was for the 5mm gap between the inside surface of this outer mould and the outer surface of the core centred within this cavity to be filled with the desired end material in order to physically recreate an exact thickened representation of the complete upper airway boundaries. This would allow for more accurate representation of the upper respiratory tract, and more precise manipulation of the model in order to simulate different circumstances, such as obstruction and collapse.

In order to suspend the core within the outer mould, two cylindrical extrusions were added on either side of the mould within the space of the oral cavity (*figure 3-6 b*). The cylindrical extrusions were carefully positioned at the sides of the oral cavity so that the holes produced in the final model as a consequence of these extrusions would not affect the final function of

the model, given that this area would later be cut in order to simulate the opening of the mouth.

The mould was then split into two halves, and handles were included on either side to allow for easy opening of the mould once the material inside had set. The final copy of the mould was then once again sent to a 3D Printing Lab in order to be printed by SLS, and the final mould was produced once more out of Nylon material.



*Figure 3-6 Development of the outer mould in which the final material is to be poured. a) shows the thickened representation of the upper airway which was deducted from the solid block, and b) shows the outer mould and it's housing of the core*

Finally, the inside of the printed mould was coated with a thin layer of sugar-wax (figure 3-7), which served 2 purposes: one, it produced a smooth surface which allowed the final material to be entirely transparent and not subject to the opacity caused by small irregularities on the surface, and two, it prevented the end material being poured into the empty spaces from sticking to the outer moulds' inner surface as it set, allowing for easy separation of the two halves of the mould after the wax had been dissolved in water.





*Figure 3-7 Final outer moulds coated in thin layer of sugar-wax to allow for easier separation*

#### 3.3.1.2.5. Making the Model

The sugar-wax core created earlier was suspended within the outer moulds' cavity by drilling holes on either side of the tongue area and aligning them with the extruded cylinders on either side of the outer mould, and then closing the two parts of the outer mould. A larger hole was also drilled into the top-most point of the outer mould wherein the final material could be poured. Finally, the material Solaris® by Smooth-On, Inc., a clear liquid platinum cure silicone rubber compound, was mixed and poured into the outer mould from the top (*figure 3-8 a*), then left to dry for approximately 24 hours.

When the Solaris® material had set the entire block was submerged in hot water, allowing the sugar-wax core model of the upper airway, as well as the thin layer lining the inside surface of the outer mould, to dissolve. The two halves of the outer mould were then separated, leaving behind a 5mm-thick representation of the inner lining of the upper respiratory tract. Finally, small holes were created at the end of the nasal cavity space to act as an opening for the nostrils, and a gap was incised across the front of the oral cavity in order to represent the opening of the mouth. This meant the successful procurement of a transparent and flexible, rubber-like representation of the upper airway (*figure 3-8 b*) which permitted the clear viewing of the flow of air during respiration (*figure 3-8 c*), as well as the response of related organs within the upper respiratory tract, while still maintaining the same flexible nature (*figure 3-8 d*) as that found in a real respiratory tract to enable convenient and easy manipulation of the shape as desired.

However, while this methodology described above resulted in the successful production of a model with the desired specifications, there remained some concerns due to the unstable nature of the wax core. Given that it began to melt at room temperature, it was possible that its' overall shape began to degrade while the silicone rubber material was in the process of curing, thus affecting the accuracy of the upper respiratory tract shape in the final model. The accuracy of the airway geometry may also have been compromised when there was a need to alter the shape due to the limitations of the core-making process (see 3.3.1.2.3). Furthermore, while the final model was still transparent, there was a large amount of air bubbles on the inner surface caused by degradation of the core during the curing of the silicone rubber. As a result an alternative to the sugar-wax was used, both as the model core and to line the inner surface of the outer mould, which would remain stable at room temperature.



a)



Nasal Cavity

Oral Cavity



b)



c)



d)

*Figure 3-8 Development of the final model using the sugar-wax core (b) showing associated transparency (c) and flexibility (d)*

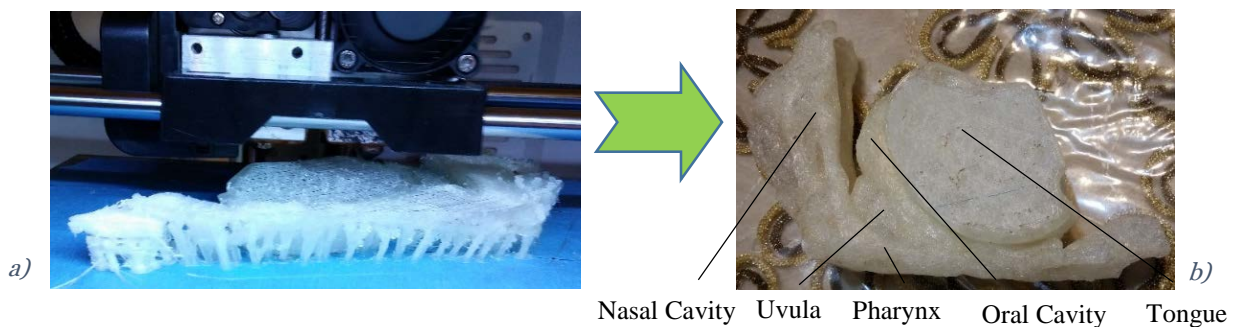
### 3.3.2. Creating the Final Realistic Boundaries Model

Given that the model developed previously was still somewhat inaccurate or unsuitable due to the reasons stated above, some changes were made to the methodology of the development of the final model.

#### 3.3.2.1. Changes to the Cavity Core

The original virtual model obtained of the upper respiratory tract was adapted to include two holes on either side of the tongue area so that it may be later suspended within the outer mould cavity, and the final model was printed by a commercial FLASHFORGE Dreamer Dual-Extrusion 3D Printer, using 1.75mm diameter PVA-based water-soluble filament (*figure 3-9 a*). Printing was done with an extruder temperature of 230° C at a speed of 60 mms<sup>-1</sup> with a 20% fill density.

This meant that not only could the physical model of the upper airway be accurately produced without the need for further alterations (*figure 3-9 b*), but this model would also remain unchanged until dissolved in water, and the finer details could be preserved to better represent the upper respiratory tract in the final model.



*Figure 3-9 3D Printing of PVA-model of air within upper respiratory tract*

#### 3.3.2.2. Making the Final Model

Making the final model was done much the same way as described earlier with a few changes:

1. The developed PVA model was coated in a soft water-soluble special-effects gelatine material (see 3.4.1) in order to create a smooth boundary which would once again prevent opacity as a result of irregularities on the surface of the 3D printed model (*figure 3-10*).

2. The inner surface of the outer mould was also lined with this gelatine material for the same reason and to also allow for easier separation of the two halves of the mould after the final material had cured (*figure 3-10*).
3. After mixing, the Solaris® two-part compound was left in a home-made vacuum chamber for approximately 15 minutes in order to remove any air bubbles which might affect the integrity and visibility of the final model (*figure 3-10*).

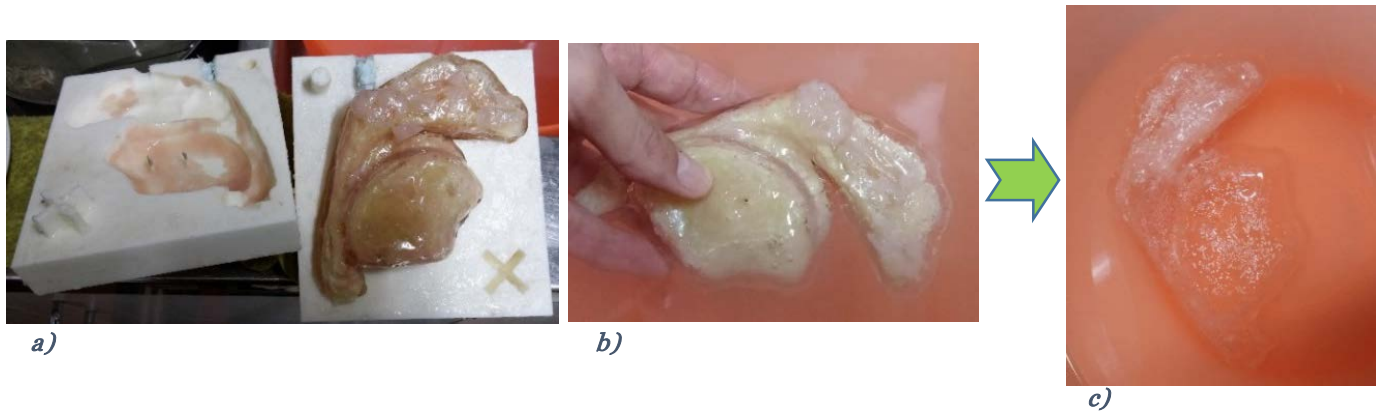
The core was then once again suspended within the cavity of the outer mould, and the final Solaris® mixture was poured in through the top in order to assume the shape around the core.



*Figure 3-10 Preparation of final gelatine-coated 3D-printed PVA model and associated outer mould, and the subsequent addition of degassed Solaris® compound*

After the Solaris® compound had dried, the outer mould was then submerged into hot water once again to be separated (*figure 3-11 a*), and the final model was left in the water for approximately 12 hours (*figure 3-11 b*). When the core had dissolved along with the gelatine coating, the desired final model of the upper airway boundaries was left behind (*figure 3-11 c*).





*Figure 3-11 Procurement of final upper airway model by a) separation of outer mould using warm water, followed by b) dissolving of PVA material once again using warm water, and the consequent c) final transparent model obtained*

### 3.4. Physical Modelling of the Upper Airway Organs

Two key organs associated with the upper respiratory tract play a crucial role in fluid flow in the upper airway, and thus are largely involved, for example, in the presence (or lack thereof) of OSA in a subject. These two organs of course being the tongue and the uvula.

Therefore, if the upper respiratory tract is to be physically modelled accurately, these organs need to also be replicated accurately and included with our previously developed model of the upper airway, thus completing the upper respiratory tract.

#### 3.4.1. Materials Used

The three main materials used to make the tongue and uvula were gelatine, latex, and silly-putty.

- *Gelatine*: The gelatine used was a special-effects gelatine commonly used in the special-effects industry for movies and costumes, and it is the same material used to coat the PVA model of the upper respiratory tract (see 3.3.2.2). The properties of the gelatine were tested, and it exhibited a density of  $1150\text{kgm}^{-3}$  and a Young's modulus of approximately 47,000 Pa for strains below 60% (See Appendix III for results of tests performed on Gelatine material).
- *Latex*: The latex used in this research was liquid latex, made of a mixture of latex, water, and ammonia. When exposed to the air, the liquid latex dries up and after

approximately 1 hour begins to adopt rubber-like properties. After approximately 24 hours the latex dries to a strong, tense rubbery film. While the average properties of some forms of natural rubber can be up to 20,000,000 Pa, with a density of  $910 \text{ kgm}^{-3}$  [160], only a thin film of latex was used, allowing for easier deformation and a more elastic response.

- *Silly-Putty*: The silly-putty used is essentially the slime commonly found as a children's toy. It was included in the model given that it was liquid enough to not maintain any particular shape, yet viscous enough to carry some weight and give the model some density. The presence of this thick goo within a layer of latex was ideal to replicate the feel of relaxed muscle tissue such as that associated with the tongue during rest, and to allow the shape to deform as it would when the muscles are relaxed.

### 3.4.2. The Tongue

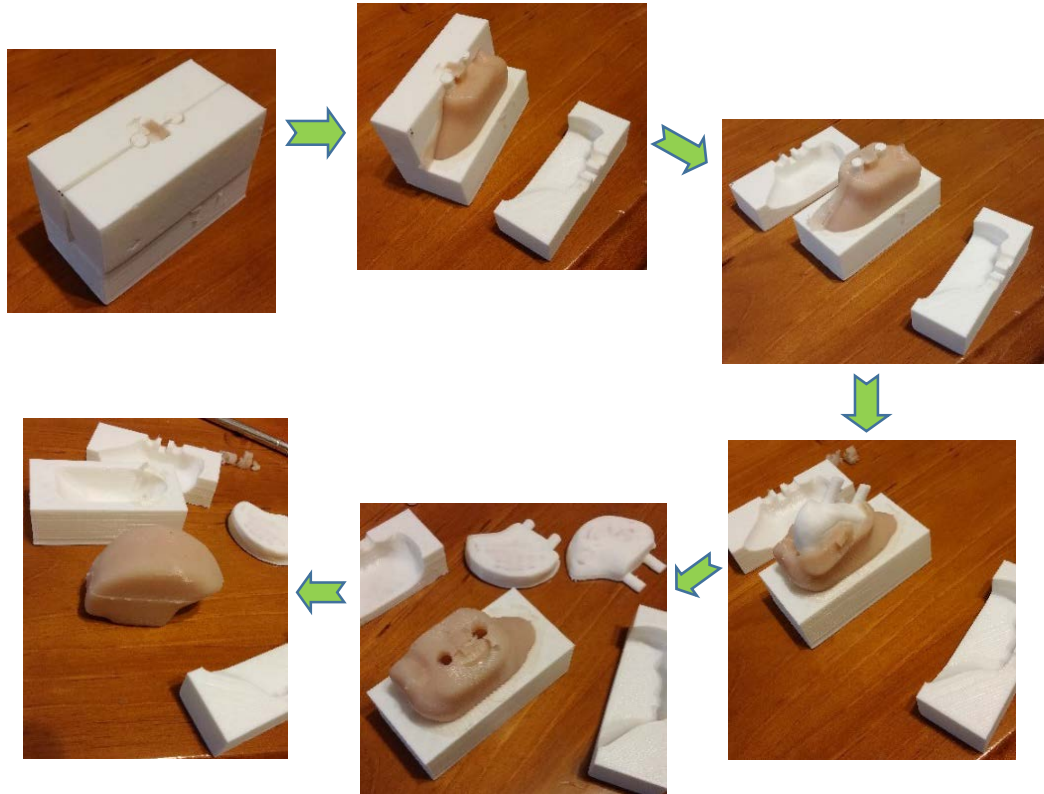
A virtual model of the tongue was obtained through the same process which was described earlier (see 3.2) using the same male subject whom the virtual model of the upper airway was based on. The virtual model of the tongue was then scaled down to 0.9x of its original size, allowing it the freedom for subsequent movement and deformation during breathing when placed in the oral cavity. This is because the MRI scan of the subject was performed at rest during which the tongue almost takes the shape of the entire oral cavity, which would prevent it from moving freely in the model.

#### 3.4.2.1. Model 1 – Gelatine Tongue

Using the new scaled down model of the tongue, a three-part mould was printed using a commercial 3D printer, and developed to encapsulate the shape of the tongue. The gelatine material was then melted and poured into the cavity of this three-part mould, resulting in a soft, rubbery replica of the tongue.

Although, in terms of the texture of the material used and the shape of the tongue (and fortunately even the colour!), the replicated tongue was very successful, it was still too rigid to move as freely as a real tongue. Therefore, in order to rectify this, another virtual copy of the tongue was scaled down to act as the core within the three-part mould, allowing the final tongue, which was made out of the same material, to be hollow. When the mould was later separated after the gelatine had solidified, the core, which was a combination of two parts,

was removed through the base of the tongue where the tongue would be attached when inserted into the airway boundaries model. This provided a hollow model with the precise geometry of the tongue, allowing it to be both soft and flexible in order to resemble a real tongue (figure 3-12).



*Figure 3-12 Process showing the separation of tongue mould parts to yield the final hollow gelatine model of the tongue*

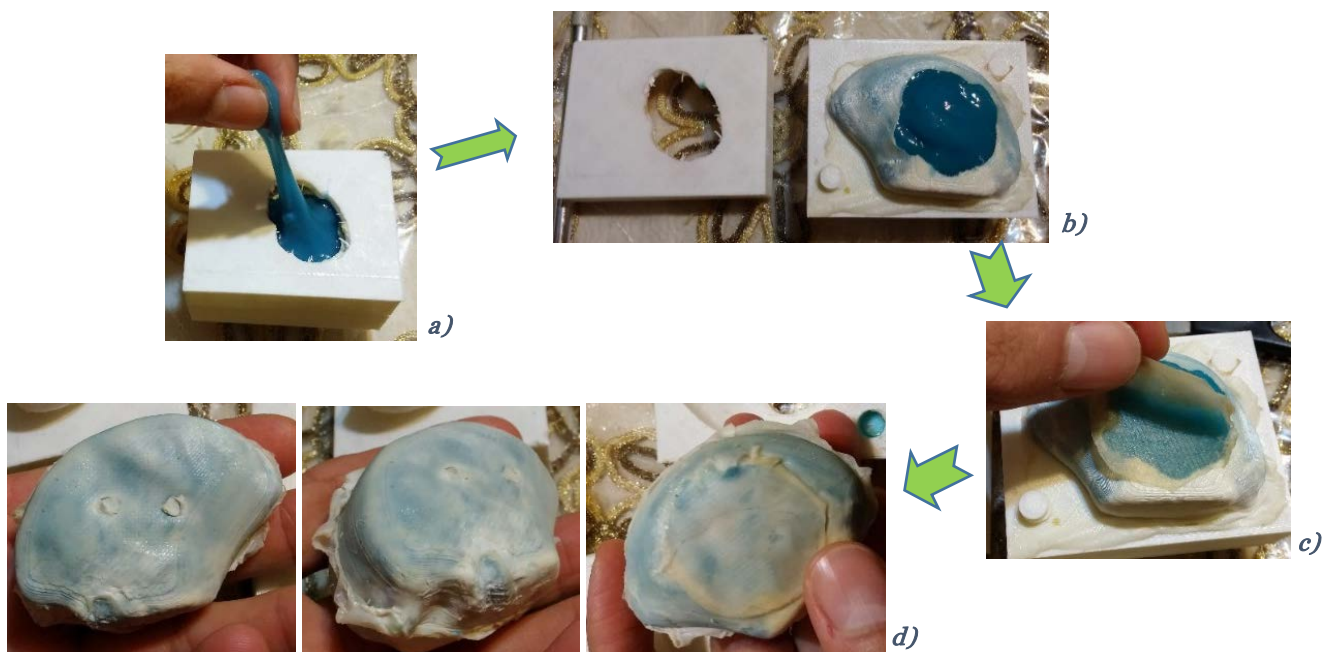
#### **3.4.2.2. Model 2 – Latex Tongue**

The tongue was remade using different materials which would allow the model tongue to better simulate the effects of relaxed muscle tone within the airway boundary model. This was developed using the following process:

1. Using the new scaled down model of the tongue, a two-part mould was printed using a commercial 3D printer, and developed to encapsulate the shape of the tongue.
2. A large hole was cut into one of the sides, and liquid latex was poured into the combined two-part mould, and then instantly poured out
3. The thin layer of liquid latex lining the insides of the two part mould was left to dry. And the two-part mould was once again filled and emptied to coat the insides in a new layer of liquid latex. This process was repeated four times, creating a tough and solid film of rubber latex.

4. The hollow two-part mould was then filled with silly putty until it occupied the entire cavity (*figure 3-13 a*).
5. The one section of the two-part mould was then removed, exposing half the dried, filled tongue model (*figure 3-13 b*).
6. A thin layer of rubber latex was then placed upon the exposed hole to the latex shell, and secured onto the shell using more liquid latex (*figure 3-13 c*).

This resulted in a soft and flexible tongue which maintained a strict shape (*figure 3-13 d*) but deformed over time due to the effects of gravity, just as desired.



*Figure 3-13 Development of latex tongue by obtaining tongue shape using two-part mould, and filling of latex shell with goo material*

### 3.4.3. The Uvula

The uvula model was developed using the following process:

1. A virtual model of the uvula was obtained using the same male subject, and a two-part mould was printed using a commercial 3D printer.
2. A hole was then drilled into one of the sides, allowing an entrance within which material could be poured.
3. A section of tough dental floss was then cut into strings, and the cavity within the two-part mould was filled with these sections of floss material. This was used to hold the final uvula model together, so that the uvula model would not rip when subjected to the pressures of respiration (*figure 3-14 a*).



4. The gelatine material was then melted and poured into the cavity of this two-part mould as a liquid and then left to solidify (*figure 3-14 b*).

Once the two-part mould was separated, a soft, rubbery replica of the uvula was left behind. The uvula was sprinkled with Talcum powder in order to complete its texture and allow handling of the model organ, resulting in a very successful, highly pliable, smooth model of the Uvula (*figure 3-14 c*).



*Figure 3-14 Use of a two-part mould to yield the final gelatine model of the uvula*

### 3.5. Completing the Upper Airway: Fitting the Associated Organs

The final step in completing the final model of the upper airway was attaching the models of the tongue and the uvula to the transparent upper airway boundaries model. Given that the developed models of these two organs were based on the organs of the same subject whom the upper airway boundaries model was based on, no extra modifications except those already mentioned previously were required to either the tongue, the uvula, or the upper airway boundary model in order to combine all the parts.

The walls surrounding the oral cavity were removed on one side of the model in order to insert the tongue and uvula models, and then attached once again using the same Solaris® material with which the upper airway boundaries model was made of.

The tongue was secured using a two-part epoxy glue, given that this adhesive could be peeled off the silicone material without damaging or affecting it, and thus providing the freedom to interchange the tongue as required in order to test the different materials and their response. The uvula was attached at the area of the soft palate using regular super-glue, given that it did not need to be later removed or modified any further, and this acted as a more permanent fix.



*Figure 3-15 A geometrically accurate, transparent, and flexible model of the upper respiratory tract along with associated organs*

### 3.6. Summary

This chapter outlined the methodology used in developing both the realistic, transparent, flexible upper respiratory tract boundaries model, as well as the models of the associated organs, and described the way in which it was all combined in order to provide the final complete upper airway model.

The following chapter will highlight the way in which complete and accurate respiration was simulated, and the integration of the final complete model with this system in order to provide a visualisation of accurate breathing in the upper respiratory tract. It will also describe the experiments performed using the final model in order to validate its three main properties of accuracy, transparency, and flexibility.

## Chapter 4 - EXPERIMENTAL SIMULATION

### 4.1. Introduction

In order to accurately observe and analyse realistic fluid flow in an airway, there is a need to establish a reasonable environment in which not only is the model of the upper airway as close as possible to that of a real upper airway, but the characteristics and properties of the respired air itself (e.g. temperature and pressure) need to be adapted to resemble the air which circulates throughout the airway due to the action of the lungs. Moreover, there needs to be a consistent simulation of the lungs' breath cycle. This would allow for greater accuracy when studying the efficiency of the final developed model in representing a realistic airway during respiration.

A variety of equipment was prepared and were combined in order to establish a single complete system which would in effect simulate the presence of human lungs. This chapter will outline the following:

- The set-up used to simulate breathing and the standard breath cycle
- The process used to monitor and alter the properties of the air before entry into the upper airway model
- A summary of the process by which the models' accuracy, flexibility, and transparency were tested in order to validate the final developed model

### 4.2. Simulating the lungs: Breathing Simulator

The first step in creating respiration, and thus airflow, was through the reproduction of a consistent breathing pattern. Thus a "lung simulator" was used as the first piece of equipment through which airflow and a simulation of breath was produced. The lung/breathing simulator (*figure 4-1 f*) was previously designed at the Institute of Biomedical Technologies at the Auckland University of Technology. It contains 5 main components which work to serve its function of simulation of the breath cycle:

1. A servo motor (Model GYS751DC2-T2A) is connected to a linear motor screw (*figure 4-1 d*).

2. The controlled rotation of this screw guides the movement of the second main component in the lung set-up: a piston housed within a pneumatic cylinder (*figure 4-1 b*).
3. The piston position is detected by the use of a Festo MLO-POT analogue type displacement encoder (*figure 4-1 c*). This allows the position of the piston to be measured, providing feedback of the pistons' movements and thus presenting a pattern for the simulated breathing cycle and allowing subsequent control.
4. The piston housed within the cylinder opens up to a chamber where air can escape from and be drawn into (*figure 4-1 a*). This meant that the movement of the piston and resulting expansion and contraction of air within the cylinder altered the pressure within the chamber, pumping air in and out through a connected tube.
5. Finally, this pneumatic drive was controlled through the control panel of a FALDIC-w series servo amplifier (Model RYC751D3-VVT2) (*figure 4-1 e*), wherein the amplifier was configured into test running mode and a pattern operation was used in order to simulate the breath cycle. The servo amplifier was also connected to an external computer so that, through the use of LabVIEW™ software, the user would be able to adapt the speed and range of the servo motors' rotation, in effect providing the freedom to control the parameters associated with the breath cycle, such as the tidal volume and the rate of breathing. However, for the purpose of this research, this pattern was set manually to allow experimentation with the control of movement.

The resulting effect was the intake and expulsion of air through a tube in a repetitive pattern and at a constant rate, simulating the inhalation and exhalation which make up the breathing cycle produced by a human lung.

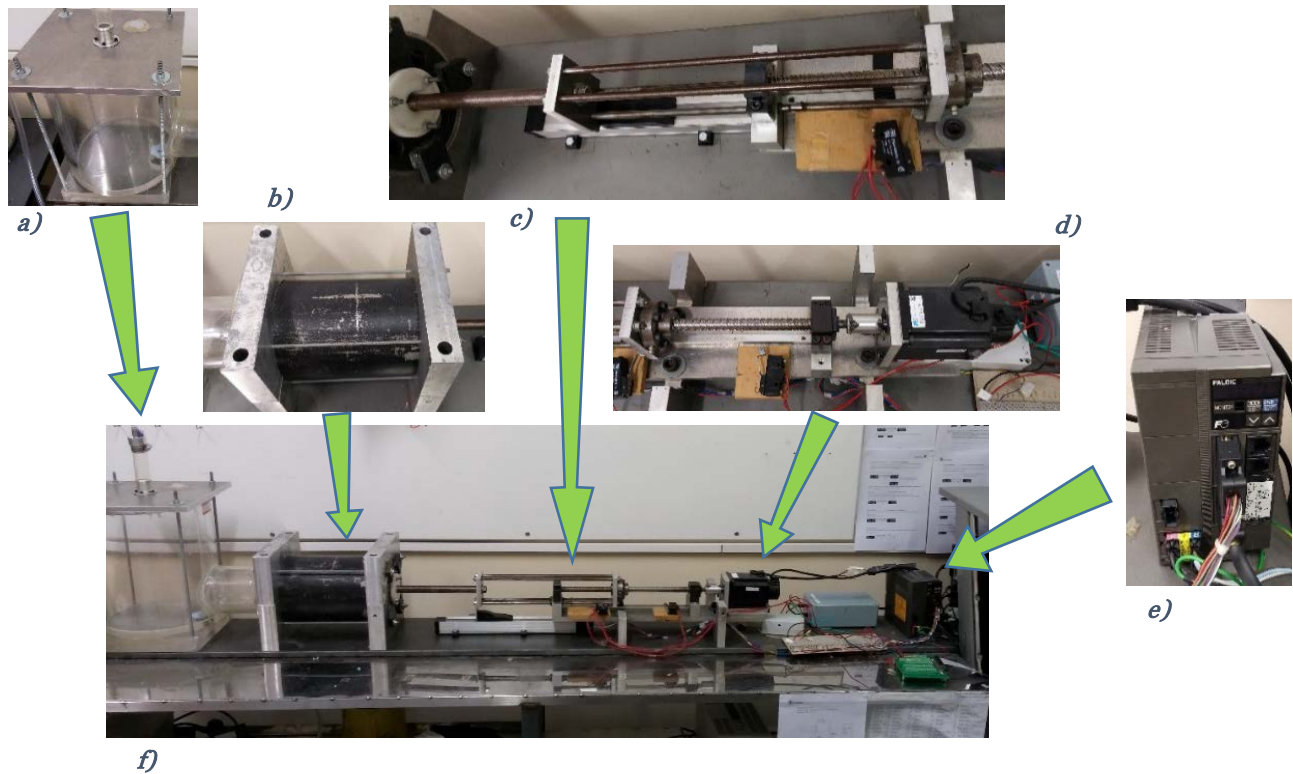


Figure 4-1 Diagram of Breathing Simulator with associated components

### 4.3. Reproducing Breathing Properties

As discovered earlier, air properties during respiration are specific and can vary throughout the respiratory system (see 2.4.3.2). Accordingly, it is important to understand these characteristics and maintain accurate values if accurate fluid flow is to be reproduced, since fluid flow can be affected by the properties of the fluid.

In the process of simulating the air being expelled from the lungs, the properties of breath were simulated through a system (figure 4-2 e) which was used to maintain accurate and realistic breath characteristics. This involved the control of flow, pressure, temperature, and nature of air flow. Once more, this set-up was previously developed at the Institute of Biomedical Technologies at the Auckland University of Technology, and is comprised of the following parts:

1. The input tube to this system is connected directly to an Impress pressure transducer (Model IMP-G0300-5A4-AAV-00-000) and its' associated pressure sensor (figure 4-2 a). This pressure transducer enabled the measurement of pressures between 0 and 0.3 bar above atmospheric pressure (i.e. 0 – 30 kPa), and served to monitor the pressure of air as it entered and exited the system.

2. Connected directly to the pressure transducer was an OMEGA® flow controller (Model FMA5540) (*figure 4-2 b*). This digital flow regulator provided a means by which the rate of air flow could be monitored. Given that the flow would mostly be directly controlled at the level of the breathing simulator itself, the flow regulator wasn't required to control the flow of air, but rather used to simply measure air flow in order to ensure and confirm the required flow rate travelling through the final model relative to the desired characteristics.
3. The output from the flow regulator extended as an input to an air-heater and temperature-sensor feedback system. The heating box (*figure 4-2 c*) through which air flowed served to increase the temperature of the air as it entered, and the output was fitted with a temperature sensor in order to survey the temperature of the air exiting the system. The resulting signal was then fed back to a data acquisition board in order to maintain temperature regulation at the desired user-selected temperature.
4. Finally, the air was fed through a diffuser/nozzle assembly (*figure 4-2 d*), which acted as a laminarisation chamber ensuring that the final expelled air was laminar and not turbulent.

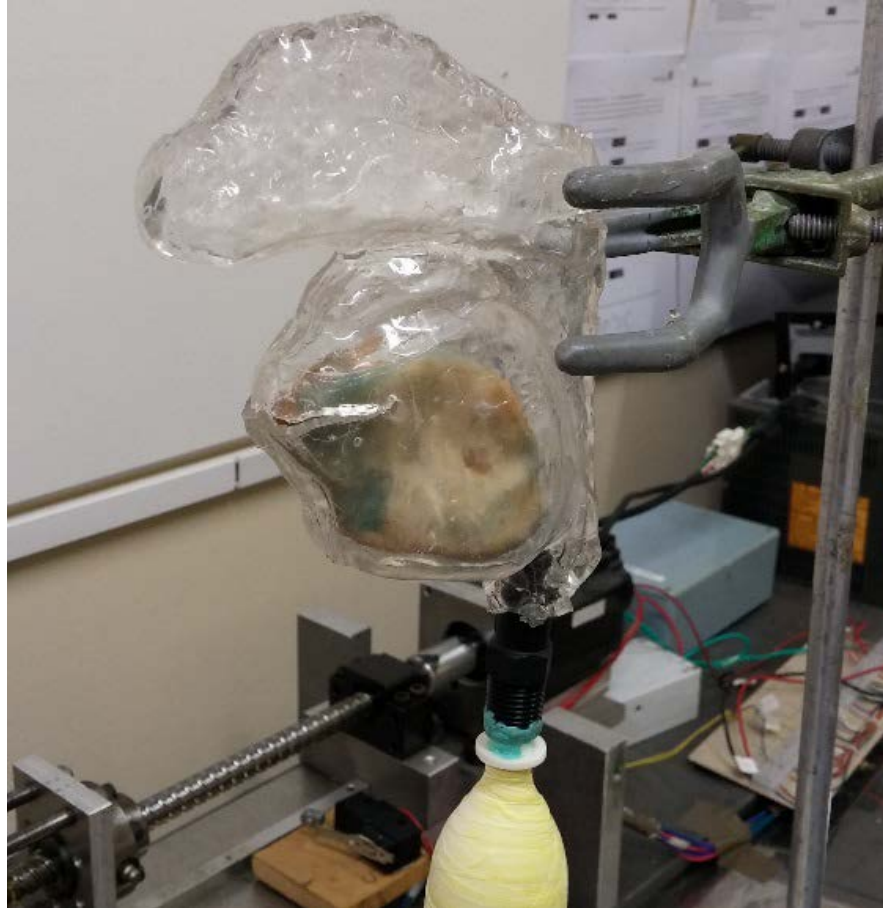
The final result was an output of laminar air maintained at a flow rate and a pressure, and heated to a temperature, similar to that associated with natural air expelled by the lungs.

This entire process was monitored and controlled through an externally connected computer and associated LabVIEW™ software.





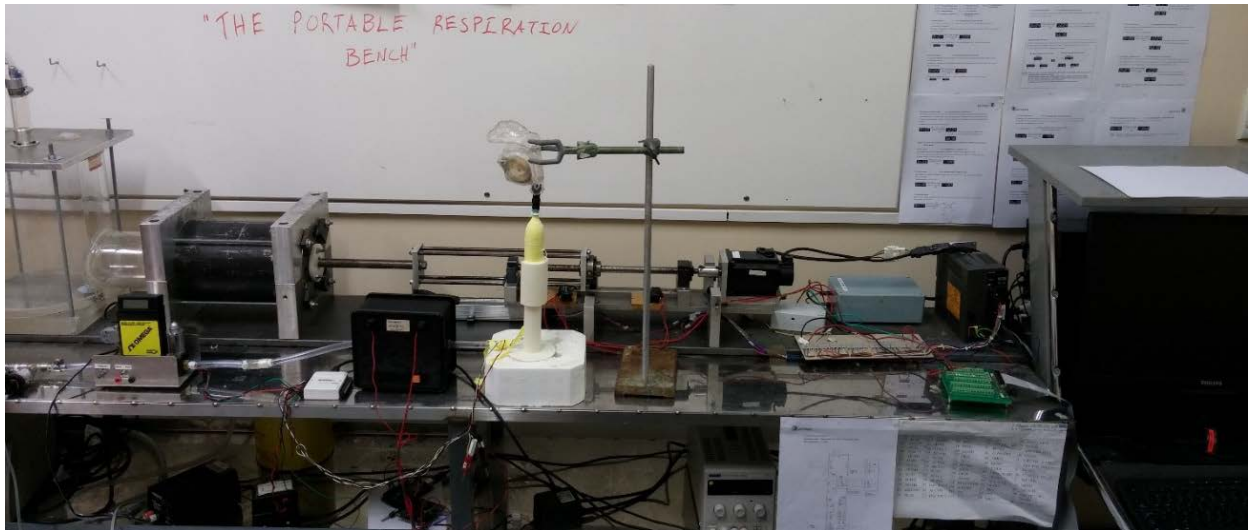
obstruct the flow of air within. It also held the nasal cavity and prevented it from expansion during exhalation given that, realistically, the nasal cavity in living beings is surrounded by tough, solid bone.



*Figure 4-3 The suspension of the upper airway model at the output of the human respiration system using a stand and clamp*

In this way, air generated at the breathing simulator travelled through the human-exhalation setup to simulate real breath, which finally flowed through the accurate physical model of the upper airway, in effect resembling a complete respiratory system related to the upper airway, and providing a realistic observation of air flow and organ response in the upper respiratory tract. The entire system was set-up on a mobile bench, forming the final “Portable Respiration Bench” (figure 4-4).





*Figure 4-4 The Portable Respiration Bench: a complete mobile system simulating regular realistic breathing through an accurate transparent model of the upper respiratory tract*

## **4.5. Experimenting with the Final Model**

Upon completing the modelling, and setting up the environment through which respiration would be produced, the final system was ready to be tested in order to ensure that it maintained the three specific properties desired of the final complete model.

### **4.5.1. Validating Accuracy**

In order to gauge the accuracy of the final developed model, it was dissected at the various regions so that the inner boundaries and their interface with the attached organs could be clearly viewed and compared to that which would be expected.

The behaviour of the separate organs was also examined and described independently to test their accuracy in simulating real organs.

### **4.5.2. Validating Transparency**

Given that the purpose of the property of transparency in the final model was to observe real-time fluid flow within an accurate respiratory tract, the final model was tested in order to confirm its feasibility in being used for accurate visualisation of fluid flow as it would occur in the human upper respiratory tract.

However, in this an obvious and major problem is presented: how could the motion of air within the upper airway be distinguished in order to be viewed?

Two main steps were taken in order to address the aforementioned issue and analyse fluid flow as required. Firstly, the air was “marked” by smoke, giving it the property of being visible. Secondly, fluid flow was captured using a high speed camera in order to observe the detailed flow of air.

#### **4.5.2.1. “Marking” the Air for Visualisation**

In making the air visible for visualisation during inhalation, long tubes were attached to the openings of the final model at the nostrils (and later at the anterior end of the oral cavity for further research in open-mouth testing) and filled with thick smoke produced from an electronic cigarette (smoking is certainly not encouraged! (see 2.3.1.2: causes and risk factors of OSA)). Air was then manually drawn through the bottom end of the laminarisation chamber in order to observe the behaviour of fluid flow within the model during inhalation. This process was repeated in both the upright and the supine positions, and allowed streams of smoke to be seen within the upper respiratory tract model

During exhalation, the smoke was forced through the bottom end of the laminarisation chamber and through the final accurate model to permit the smoke to travel through the upper airway model, allowing the behaviour of the air to be observed. Once again, this process was repeated in both the upright and supine positions.

#### **4.5.2.1. Visualising Air Flow within the Upper Airway**

Even though the air was now visible with smoke, and the ways in which the tongue and uvula were situated within the upper airway was obvious for the upright and supine positions, fluid flow is quite a fast process, and a lot can occur which can't be analysed by the naked eye, thus creating difficulties in accurately describing fluid flow behaviour in real-time. Therefore, in order to capture the intricate details occurring within the airway model during the respiration process, a Photron FASTCAM 1024 PCI high speed camera was used to record the flow of air against a black background. Unfortunately, the high speed camera only provided black and white images and recordings. Recording was done at 125 frames per second with a shutter exposure time of 1/frame second at a resolution of 1024 x 1024. An F0.95 CCTV lens with a format size of 1 inch and a focal length of 50mm (Model COYAL M-5095C) was used with the camera to capture the flow of air. This allowed a clear recording of fluid flow within the upper airway model, whose behaviour was assessed to validate the use of the model as a representation of the upper respiratory tract.

### 4.5.3. Validating Flexibility

In order to measure the models flexibility and thus verify its suitability in representing the walls of the upper respiratory tract, the complete model was examined subject to the different positions with which testing occurred (upright and supine), and complete respiration was established through the model using the final assembly (see 4.4). The deflections and changes in the dimensions of the final model were then measured in order to provide a numerical description of the changes in the airway walls during respiration.

The first step was to configure the entire respiration assembly in order to represent realistic breathing in humans during rest, which would be achieved by maintaining the individual values identified earlier (see 2.4.3.2) for the average human breath cycle. More specifically, these values were:

- Breathing Rate – 12 breaths per minute
- Air Temperature – 37° C
- Flow rate –  $-0.4 \text{ Ls}^{-1}$  to  $0.4 \text{ Ls}^{-1}$  (or  $-24 \text{ Lmin}^{-1}$  to  $24 \text{ Lmin}^{-1}$ )
- Pressure –  $-8 \text{ cmH}_2\text{O}$  to  $8 \text{ cmH}_2\text{O}$  ( $-785 \text{ Pa}$  to  $785 \text{ Pa}$ )

By maintaining values as close to these as possible, a practical respiration environment can be established. In order to achieve this experimentally, the alternating piston movement of the breathing simulator was regulated by controlling the rotation of the servo motor, and the following were the parameters used for the servo motor and for the LabVIEW™ application in order to configure the breathing simulator and the breath-characteristics simulation system, respectively:

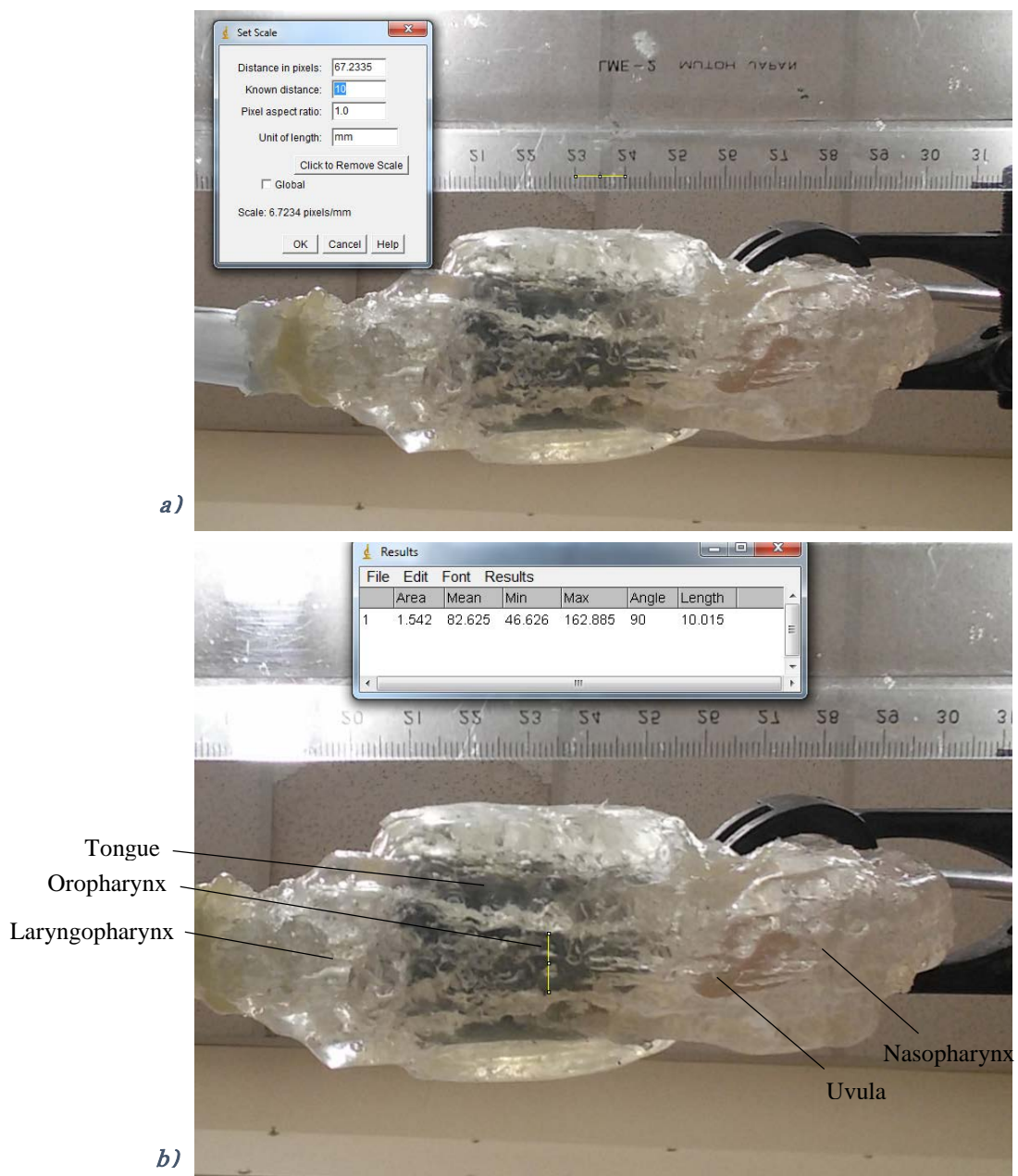
- Travel setting (for the distance of piston movement): 8 revolutions
- Speed setting: 600 revolutions per minute
- Timer setting: 1.1 seconds
- Acceleration time: 0.1 seconds
- Deceleration time: 0.1 seconds
- Temperature: set at 37° C

The use of these parameters yielded the following properties in air flow through the system:

- Breathing Rate – 13 breaths per minute
- Air Temperature – 37° C
- Flow rate ~  $-15 \text{ Lmin}^{-1}$  to  $24 \text{ Lmin}^{-1}$
- Pressure ~  $-10.2 \text{ cmH}_2\text{O}$  to  $10.2 \text{ cmH}_2\text{O}$  ( $-1000 \text{ Pa}$  to  $1000 \text{ Pa}$ )

After establishing realistic breathing simulation, the breath cycle was initiated and a camera was used to capture the changes in width at the various areas of the upper airway model. The frames were then used to measure these changes in dimension, giving an indication of the distribution of pressure within the final model.

Measurement of the deflections of the upper airway walls was done using image processing software ImageJ. A virtual scale was initially calibrated by setting the number of pixels which corresponded to a centimetre (*figure 4-5 a*), and then the set scale was used to measure deflections in the walls of the upper respiratory tract (*figure 4-5 b*).



*Figure 4-5 Upper airway model aligned with ruler on the same plane for use in measuring displacements of upper airway walls during respiration simulation. ImageJ software used to first calibrate distance and set usable scale (a) and then measure displacements in the airway walls (b)*

## 4.6. Summary

Establishing a system of respiration and combining it with an accurate and transparent model of the upper respiratory tract enables the ability to view realistic respiration with the upper airway, as well as observe the upper airways ensuing response to the process of breathing. This chapter highlighted the methodology through which this was established, and outlined the experiments performed using the final upper airway model for the purpose of validating its properties of accuracy, transparency, and flexibility, and how these properties may be used to serve the models purpose of airflow visualization within the upper airway.

The following chapter will provide details with regards to the results obtained in developing the upper airway model with the desired properties, and the outcomes achieved by the experiments described in this chapter.

# Chapter 5 - RESULTS

## 5.1. Introduction

As outlined previously (see 2.5), although many studies have been carried out to model the upper airway and use it to analyse fluid flow, none have resulted in the creation of realistic models within which air flow could be realistically observed, giving rise to the main purpose of this research to develop such a model which could be used for further investigation. The results presented in this chapter will present the following with regards to the final model:

- A *qualitative* outline of the accuracy of the final developed model, showing all the individual different sections which make up the upper respiratory tract as outlined in *Chapter 2*. This will provide a measure of the models accuracy.
- A *qualitative* description of air flow within the model respiratory tract and fluid flow behaviour subject to the effects of organ interaction in different positions of the model. These results will provide a measure of the models transparency and accuracy, and thus suitability for use in visual air flow analysis.
- A *quantitative* demonstration of the response of the developed model to realistic respiration by measuring changes in lumen width subject to respiration. This will provide a measure of the models flexibility and thus suitability in representing a real airway

## 5.2. Accuracy: Analysing the Accuracy of the Final Model

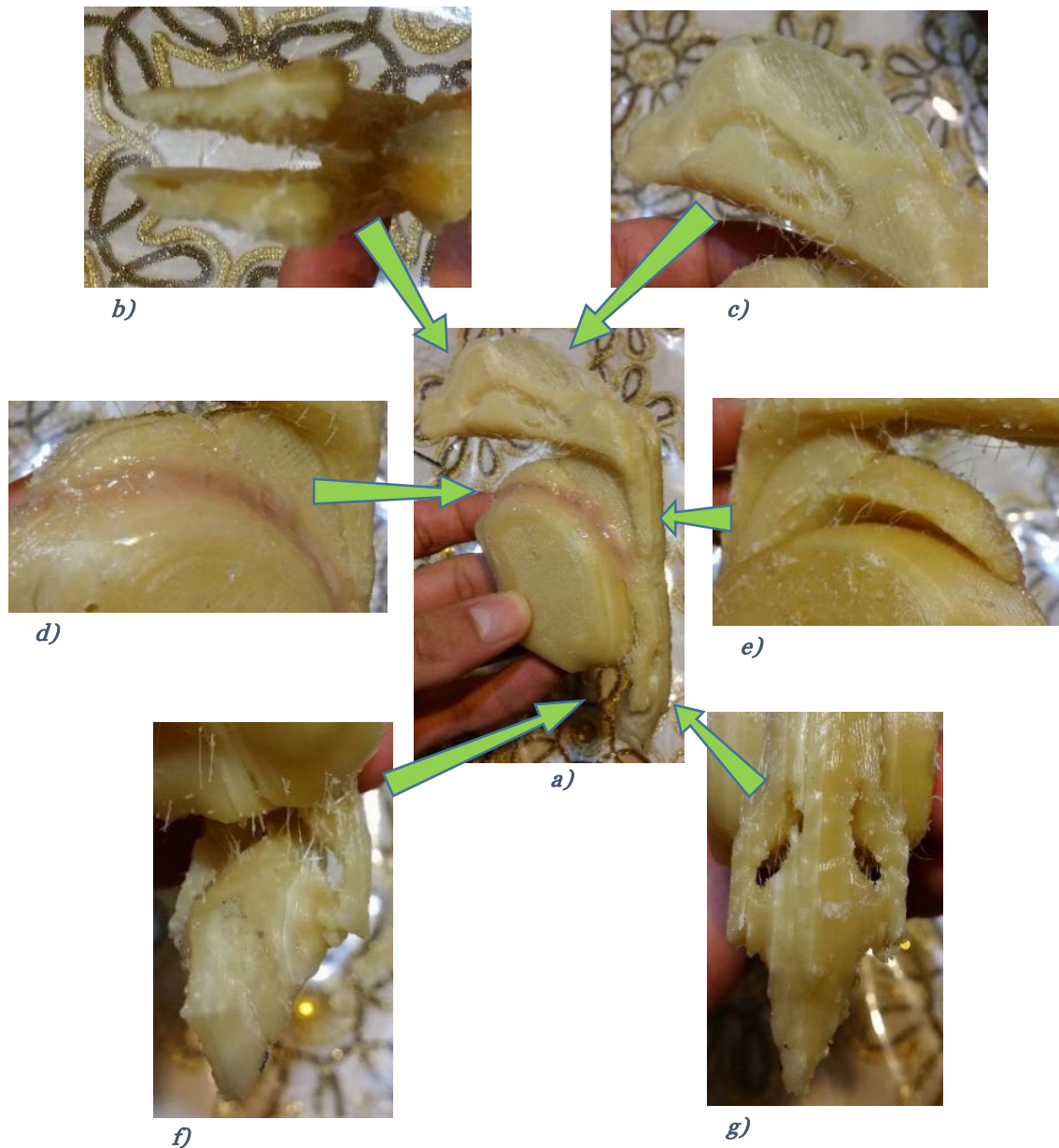
The final model was dissected and each individual section making up the entire upper airway is described.

### 5.2.1. Final Upper Airway Boundary Model

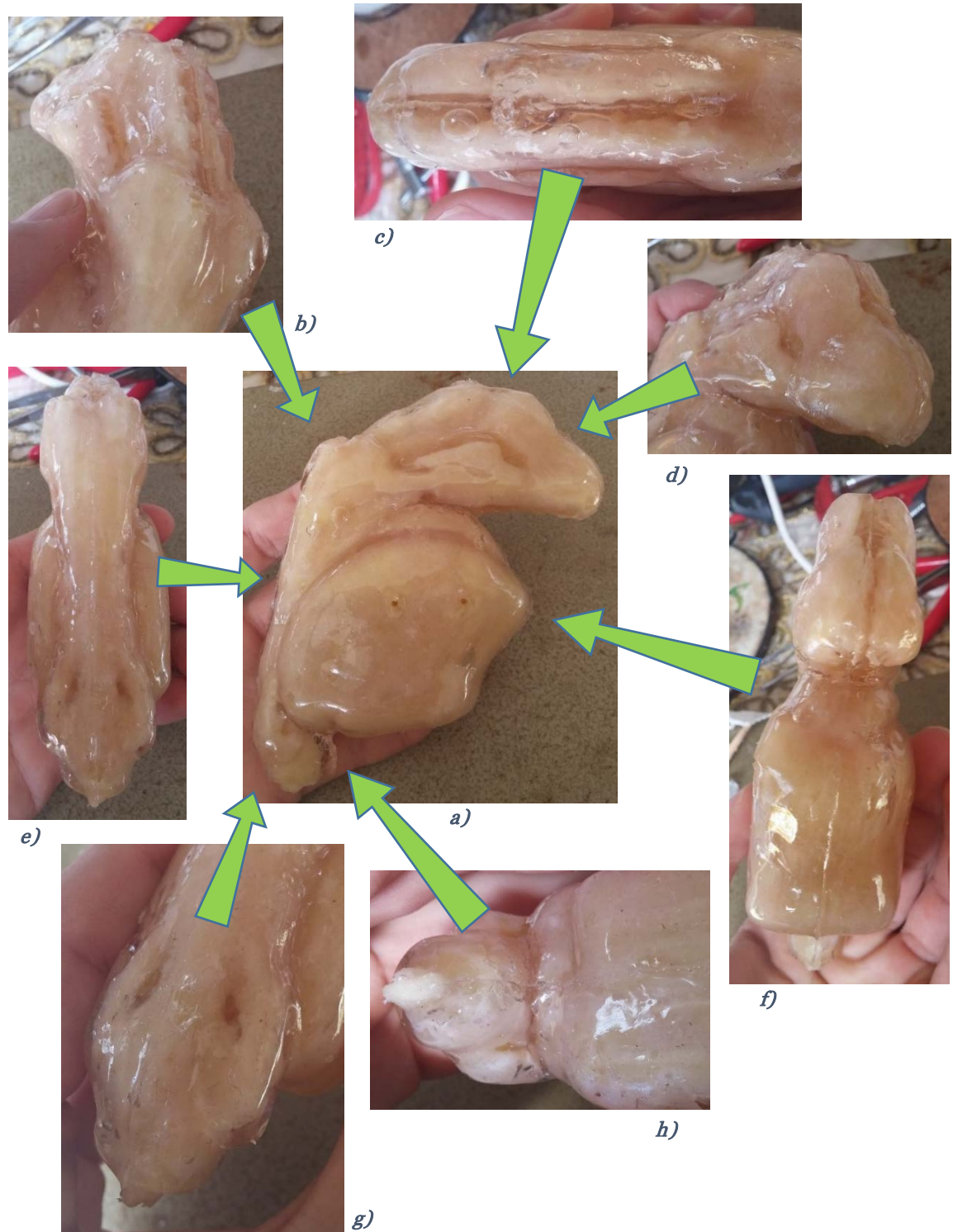
The upper airway model made was highly accurate with regards to its geometry being a replica of the overall shape of the upper respiratory tract, and it exhibited similar properties (flexibility and motility in particular) to those found in a real airway, as well as provided the necessary characteristics (most importantly, transparency) for testing and fluid flow analysis.



The fleshy tongue and uvula models demonstrated characteristics analogous to those expressed by their real organ counterparts in terms of softness, flexibility, and pliability, and thus were able to be utilised in order to measure their effects on air flow during respiration, and the part they play in snoring and sleep apnea. Note that when presenting the following results associated with the different areas of the airway, given that the purpose was to analyse the accuracy of the model in its shape and resemblance to the upper airway, the gelatine model for the tongue was used as this provided the most accurate *visual* representation since its colour and surface texture most resembled that of the real organ.



*Figure 5-1 Diagram showing the core model representing the path of air within the respiratory tract. The model is shown in general (a) with the important features shown in more detail, including the areas which would become the nasal septum (b) and nasal conchae (c), the gap between the path of air and the tongue after (d) and before (e) it is filled, and the holes which would form the piriform recesses (f and g)*



*Figure 5-2 Diagram showing the final model in general (a) along with more detailed views of the associated features, including the nasal septum (b and c), nasal conchae (d), pharynx (e), upper half of the oral cavity (f), the piriform recesses (g), and the area where the oral cavity would meet with the pharynx at the larynx end. Note that the core model was kept within the final model to enable the features to become more obvious*



### 5.2.1.1. Nasal Cavity

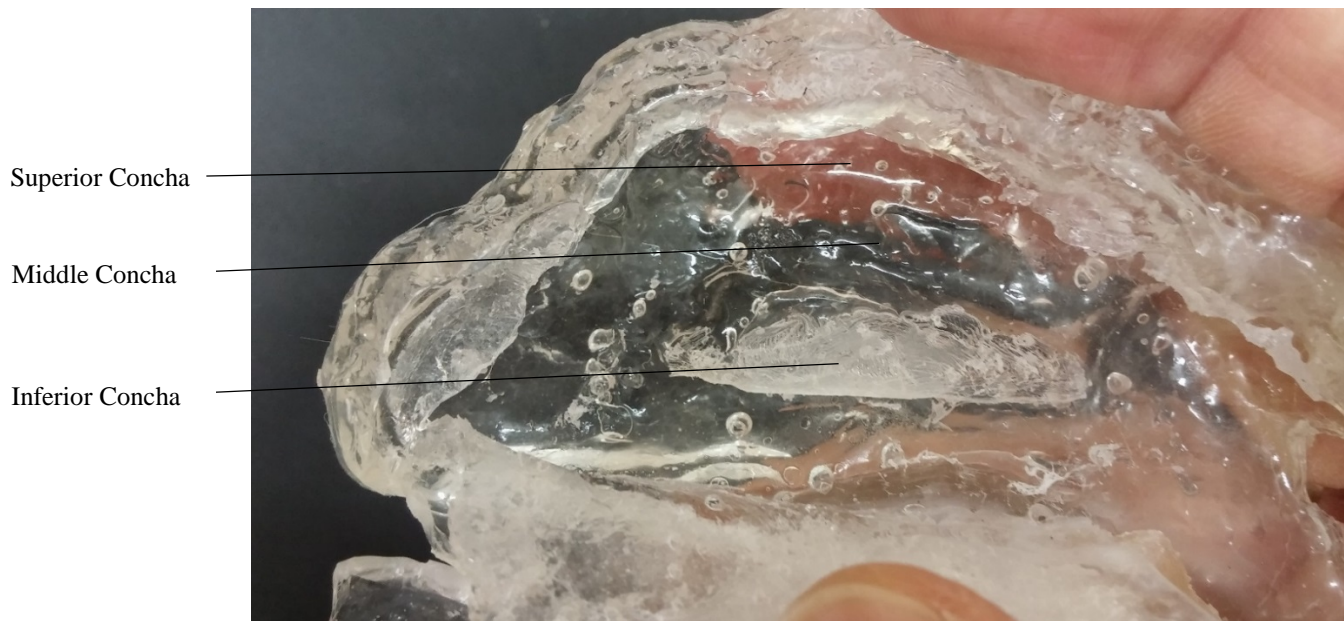
*Figure 5-1 a* shows the physical model of the path of air in the upper respiratory tract which was used as the core when making the final upper airway model (see 3.3). By looking at the nasal cavity area of this model, the two separate areas of the nose represent the two individual cavities of the nasal cavity divided by the nasal septum. On the outer surface of those separate areas of the nose, the different depressions in the outer walls of this air model reflect the presence of the nasal conchae (*figure 5-1 c*), which would be present in the insides of the outer walls of the final model. The negative impression of the inferior concha is the most obvious, extending outwards and upwards in the core model. Above this, the negative impression of the middle concha is a little less obvious, but it can be seen here as a ridge running along the outer surface (*figure 5-1 c*). Even less obvious is the presence of a superior concha, which is simply shown as a slight depression in the surface of the core model. The gap in between the two different extensions at the nose in the core model would become the nasal septum in the final model (*figure 5-1 b*).

These features of the nasal cavity are better represented in the final model. *Figure 5-3* shows a medial view of the nasal cavity before passing the nasal septum. The entire nasal septum and the shape of its surface can be seen through this section. Its bottom edge is seen to extend from the anterior tip of the nasal cavity to the posterior boundary of the hard palate.



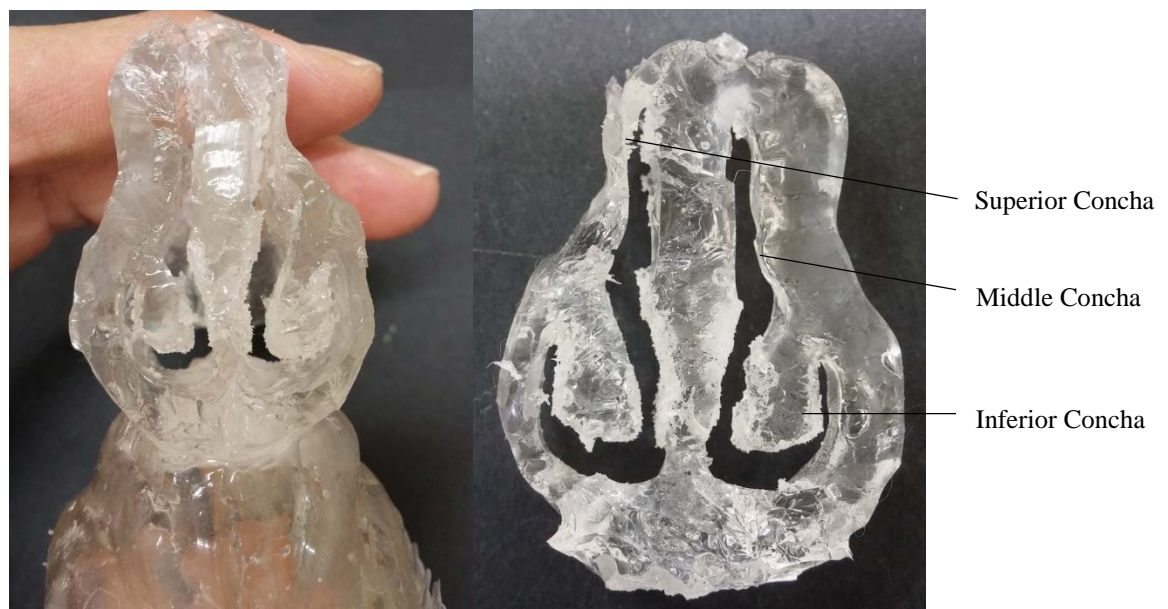
*Figure 5-3 Medial view of the nasal cavity of the final model before passing the nasal septum. The entire nasal septum can be seen from this view*

The same medial view of the nasal cavity past the septum (*figure 5-4*) shows a lateral view of the inner surface of the outer walls of the nasal cavity area. The presence of the 3 conchae on the inner surface of the lateral walls are emphasised in this view.



*Figure 5-4 Medial view of the nasal cavity of the final model past the nasal septum. The inferior and middle conchae can be vaguely recognised from this view*

While these features can be vaguely seen by laterally viewing the outer walls, they are much more prominent in the coronal cross-sections shown in *figure 5-5*, where the changes in thickness of the nasal septum are obvious along the anteroposterior axis, and the middle and inferior conchae are clearly identified and can be seen to protrude inwards out of the lateral walls.

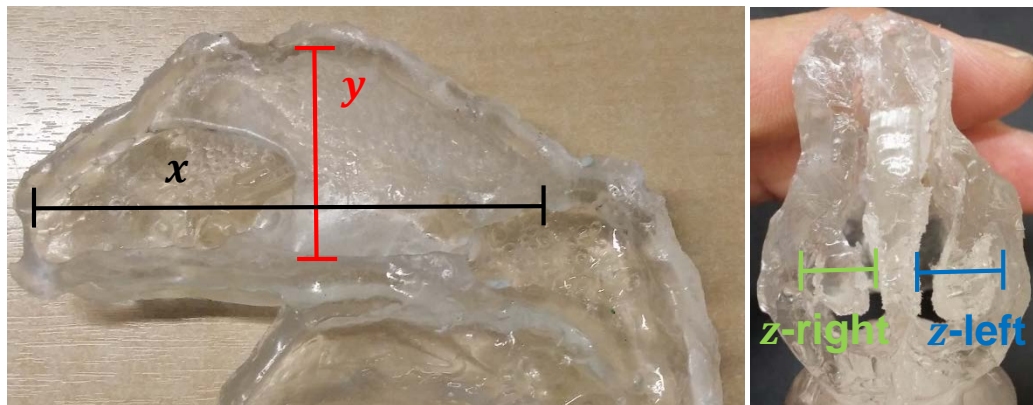


*Figure 5-5 Coronal cross-sectional view (left) and cut-out (right) of the nasal cavity area in the final model. The different depressions within the outer walls (i.e. the conchae) can clearly be seen from this view*

The dimensions for the nasal cavity area of the final model are the following (*figure 5-6*):

- Horizontal length from anterior edge to choana (x): ~ 68 mm

- Vertical height from hard palate to upper ridge ( $y$ ): ~ 35 mm
- Width from outer walls at inferior concha to septum ( $z$ -right): ~ 9 mm  
( $z$ -left): ~ 10 mm

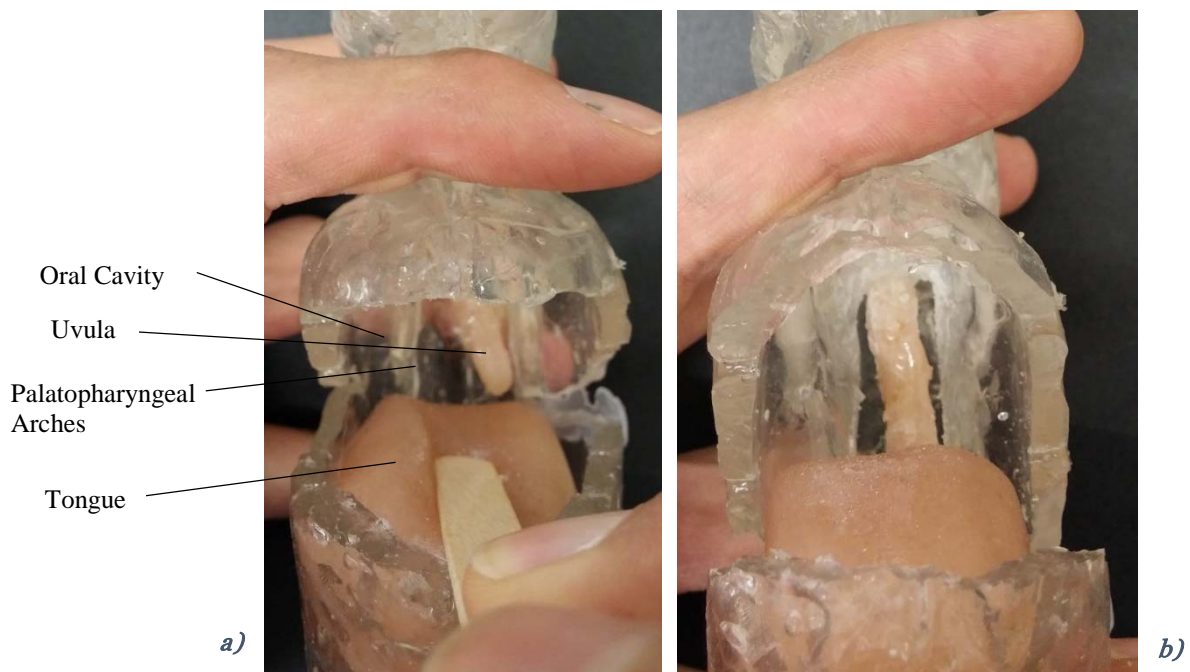


*Figure 5-6 Nasal Cavity of final model outlining the sections used during measurement*

#### **5.2.1.2. Oral Cavity**

When making the model representing the air within the upper respiratory tract, the air in the upper half of the oral cavity is merged with the shape of the tongue used for the lower half of the oral cavity (*figure 5-1 a*). In addition to this, small gaps are present in the lateral walls just under the area where the uvula would be (*figure 5-1 e*), which would partly form the palatopharyngeal arches in the final model. This feature in the final model can be seen as a pair of small ridges on either side of the lateral walls at the posterior end of the oral cavity (*figure 5-7 a*), where the tongue can also be seen to fill the space of the bottom half of the oral cavity. The uvula can be seen to hang down to almost the level of the tongues' surface. *Figure 5-7 b* shows the interface at which the soft palate is connected with the hard palate at the roof of the oral cavity.

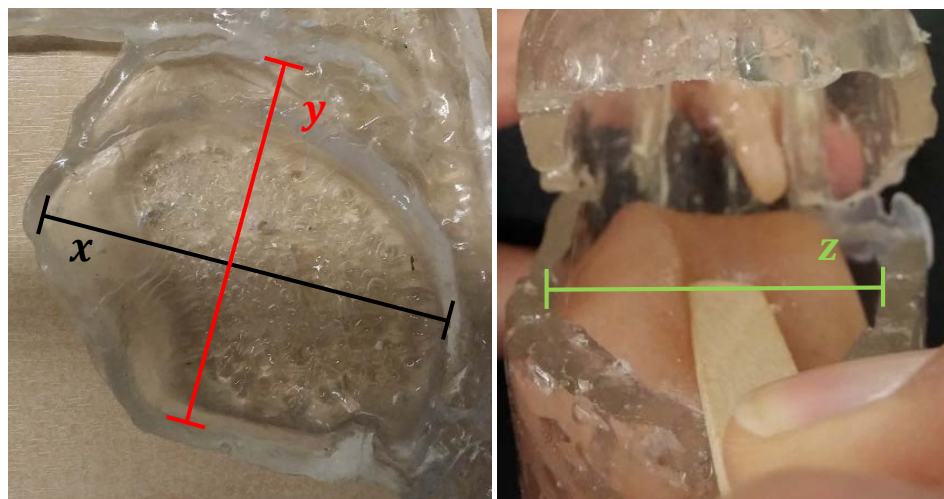




*Figure 5-7 Doctor's check-up: a look into the oral cavity through the opening of the mouth to reveal the tongue and the uvula (left) as well as the point at which the uvula is attached (right)*

The dimensions for the oral cavity area of the final model are the following (figure 5-8):

- Horizontal length from anterior end (lips) to oropharynx ( $x$ ): ~ 64 mm
- Vertical height from roof of oral cavity to hard palate ( $y$ ): ~ 62 mm
- Width of oral cavity at centre ( $z$ -right): ~ 31 mm

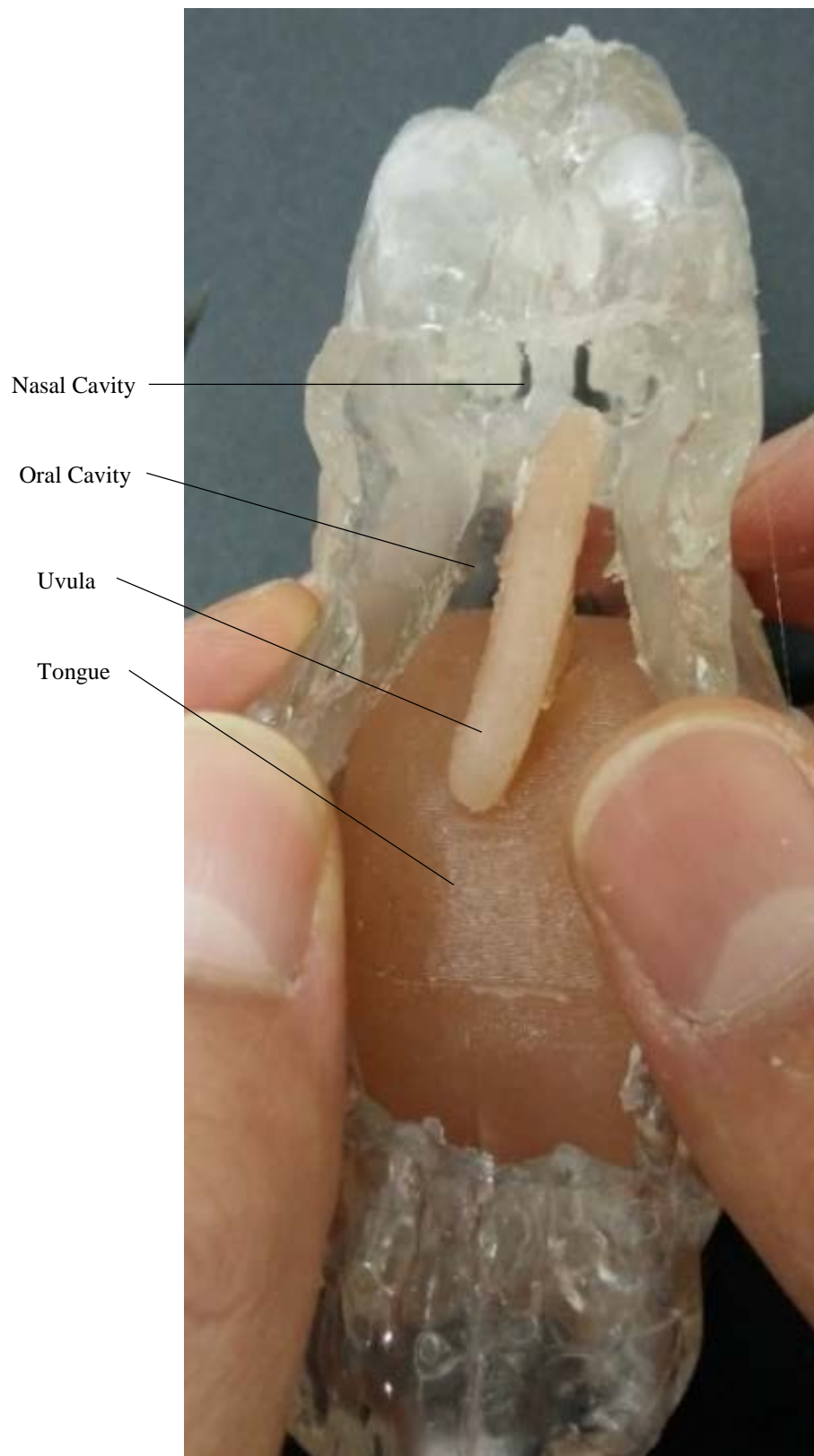


*Figure 5-8 Oral Cavity of final model outlining the sections used during measurement*

### 5.2.1.3. Pharynx

The pharynx can be seen to extend along the entire upper airway, from the nasal cavity at the superior end all the way down to the larynx at the inferior end. *Figure 5-9* shows a posterior view of the final model opened at the pharynx. From this view the distinct features of the other

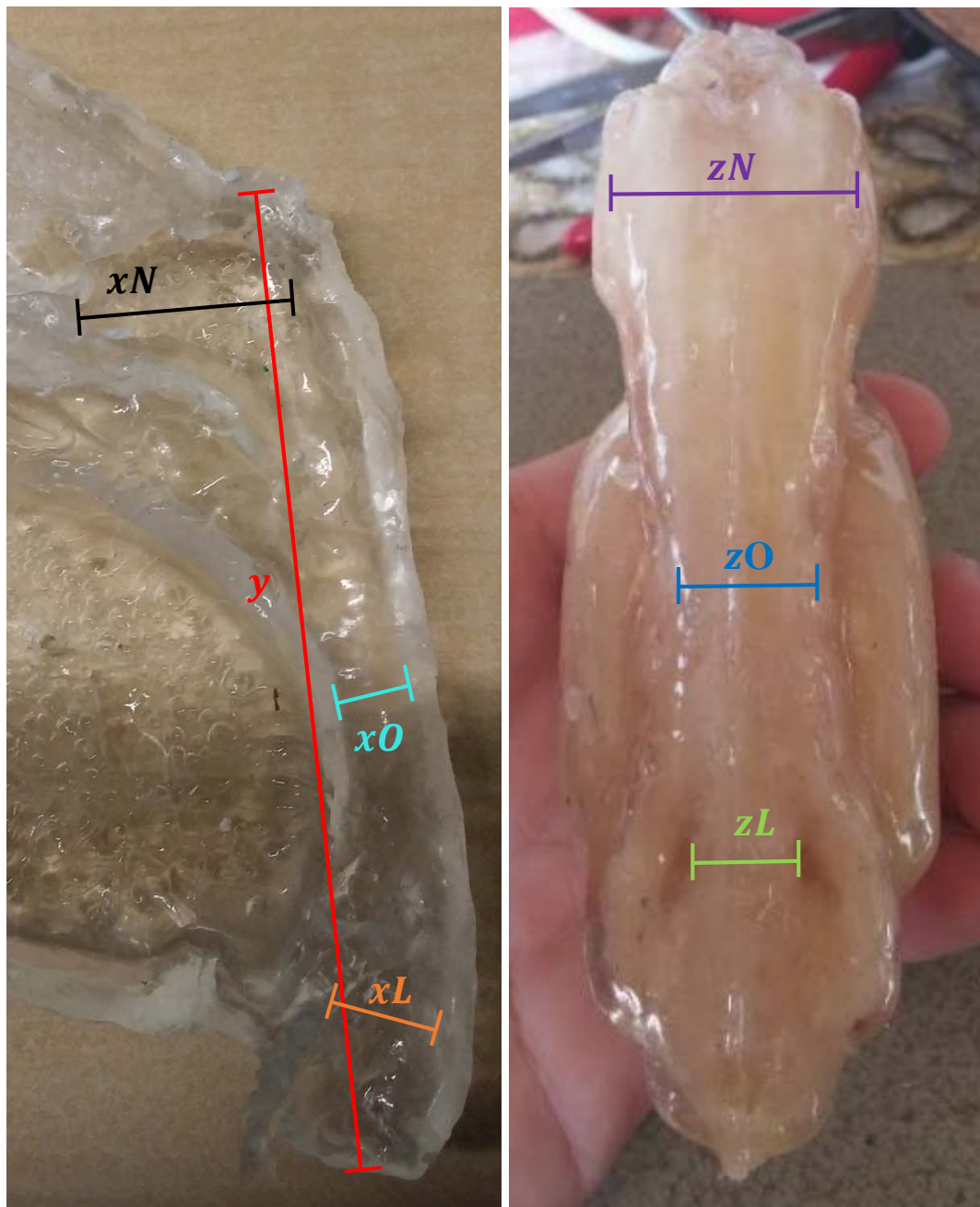
cavities, including the conchae and septum in the nasal cavity, the tongue, uvula, and palatopharyngeal arches in the oral cavity, and the recesses of the larynx, can be clearly seen.



*Figure 5-9 Posterior view of the pharynx of the final model opened posteriorly. The upper airway organs (tongue and uvula) can be clearly seen from their posterior end*

The dimensions for the area of the pharynx in the final model are the following (*figure 5-10*):

- Length at longest portion of Nasopharynx ( $xN$ ): ~ 23 mm
- Width at Nasopharynx ( $zN$ ): ~ 14 mm
- Length at Oropharynx ( $xO$ ): ~ 10 mm
- Width at Oropharynx ( $zO$ ): ~ 10 mm
- Length at Laryngopharynx ( $xL$ ): ~ 12 mm
- Width at narrowest portion of Laryngopharynx ( $zL$ ): ~ 6 mm
- Vertical height of entire pharynx ( $y$ ): ~ 104 mm



*Figure 5-10 The region of the pharynx in the final model outlining the sections used during measurement*

#### 5.2.1.4. Larynx

The printed model representing the space within the upper respiratory tract shows two distinct “holes” at the area of the larynx, which would represent the piriform recesses at the larynx (*figure 5-1 g*). In the final model, these recesses can be seen more obviously by looking superiorly from the inferior end of the airway (*figure 5-11*). *Figure 5-2 g* also highlights the location of these recesses with respect to the pharynx of the final model.



*Figure 5-11 A look at the recesses at the inferior end of the pharynx of the final model*

### 5.2.2. Upper Airway Organ Models

The different colours of the tongue and uvula allowed them to be clearly viewed through the transparent walls of the final upper respiratory tract model. Given their weight and composition, the tongue and uvula react very differently within the upper airway depending on the position and state of the subject. Note that when presenting the following results associated with the organs of the upper airway, given that the purpose was to analyse the accuracy of the model functionally and in terms of the effects of the upper airway organs on proper performance of the upper airway, the latex model for the tongue was used as this provided the most characteristically realistic and *behaviourally* accurate model when resembling a real tongue.

#### 5.2.2.1. Tongue

The model tongue is highly elastic when pulled and stretched (*figure 5-12*), and slightly motile when the upper airway model is shaken.





*Figure 5-12 A look at the final latex model of the tongue (left) and its property to stretch (right)*

In the upright position and at rest, it can be seen to almost take the shape of the entire lower half of the oral cavity (*figure 5-16 a*). Not a lot of difference is seen with respect to the change in its overall shape. However, it can be seen to slightly bulge at the anterior end and fold over onto itself, as the weight of the material within the tongue pulls it downwards to fill the gaps between the tongue and the outer walls. This leaves a considerably large gap between the dorsal surface of the tongue and the roof of the mouth.

In the supine position however, the tongue can be seen to fall back slightly towards the pharynx, taking up more of the empty space at the area of the oropharyngeal isthmus, which can also be seen by the increase in the gap between the tongue and the anterior end of the oral cavity. This shows the effects the tongue may have on the patency of the upper airways, particularly around the region of the fauces, as it collects at the posterior end of the oral cavity (*figure 5-16 b*).

When upright, the distance between the vertical surface of the tongue at its posterior end and the posterior wall of the pharynx at the retrolingual region was measured to be approximately 12mm. However, when supine, the distance was only 8 mm, indicating that patency at the retrolingual region was reduced by a third when supine.

The dimensions for the final tongue model are the following (*figure 5-13*):

- Horizontal length from anterior tip of tongue ( $x$ ): ~ 56 mm
- Vertical height from base of tongue ( $y$ ): ~ 46 mm
- Width of tongue ( $z$ ): 26mm





Figure 5-13 The final tongue model outlining the sections used during measurement

#### 5.2.2.2. Uvula

When looked at through the opening at the anterior end of the oral cavity, the uvula approximately extends downwards to the level of the tongue (*figure 5-7 a*), and is surrounded by a gap on either side at its superior end (*figure 5-7 b*). It is less elastic than the tongue but still remains highly flexible (*figure 5-14*), and is easily moveable and affected by the position of the model.



Figure 5-14 A look at the final gelatine model of the uvula (left) and its property to stretch (right)

The influence of posture on the uvula is very obvious when the model is placed at different angles. A lateral view of the uvula within the final model when placed in the upright position shows how the uvula hangs almost directly inferiorly to reach the level of the tongue surface (*figure 5-16 a*). However, when placed in the supine position, the uvula within the model hangs posteriorly into the lumen of the pharynx, partially blocking the path between the nasopharynx and the oropharynx (*figure 5-16 b*). This shows the obvious affect the uvula has on upper airway patency in the supine position. While upright, the inferior end of the uvula hung approximately 5 mm from the dorsal surface of the tongue, and 28 mm from the posterior end of the oropharyngeal region. However, when supine, the inferior end of the uvula was only approximately 10 mm from the posterior end of the pharyngeal wall.

The dimensions for the final uvula model are the following (*figure 5-15*):

- Length from superior edge to inferior tip ( $x$ ): ~ 34 mm

- Height at edge of attachment to boundaries model ( $y$ ): ~ 13 mm
- Width of uvula ( $z$ ): 5 mm



Figure 5-15 The final uvula model outlining the sections used during measurement

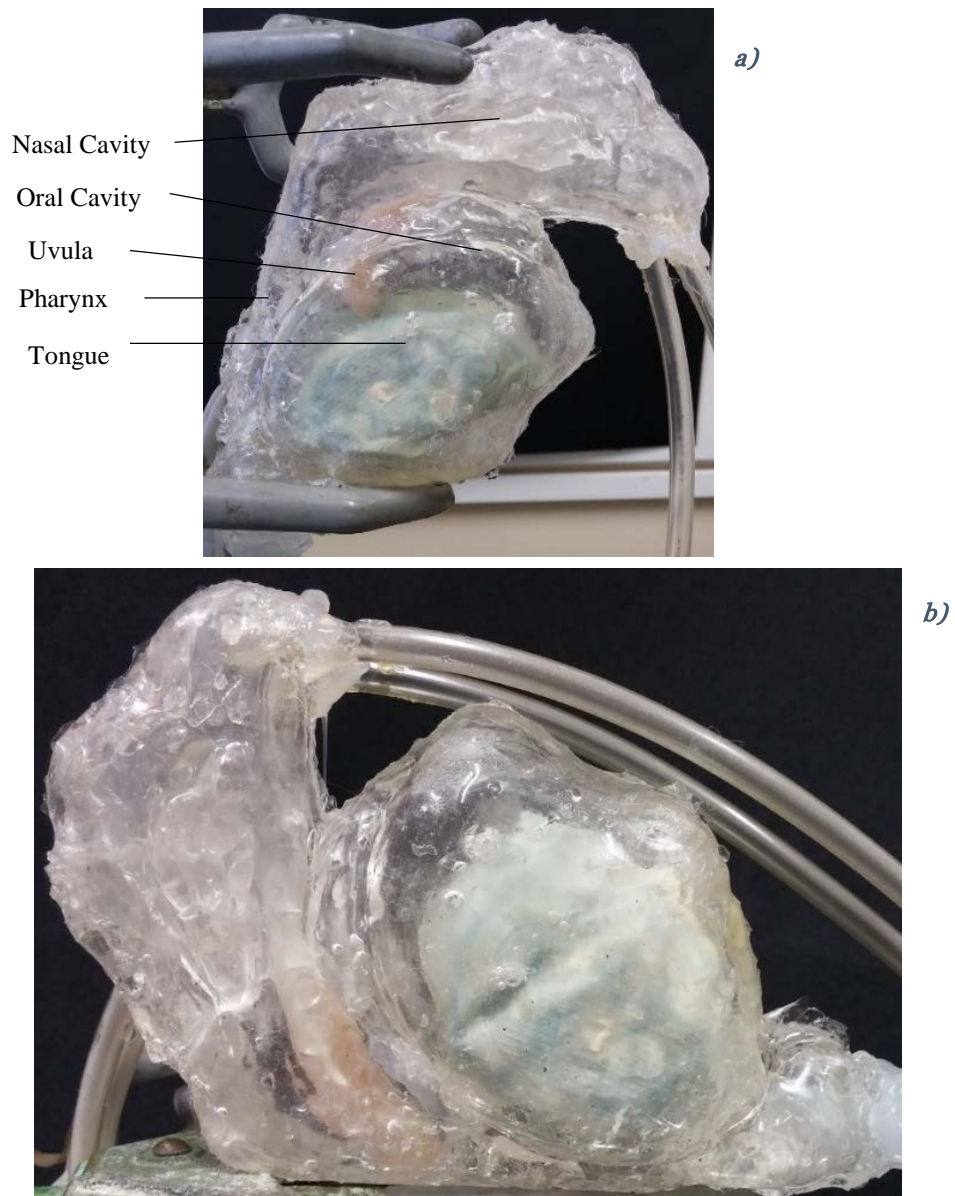





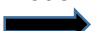
Figure 5-16 A lateral view of the final model with associated organs and their response in the upright (a) and supine (b) positions

## 5.3. Transparency: Visualising Air Flow within the Upper Airway Model

### 5.3.1. Standard Closed-Mouth Respiration

The final developed model was ideal to use in testing air flow within the upper airway. By observing the flow of air through an accurate representation of the upper respiratory tract, the actual flow of air, and the effects of the upper airway organs on that flow, could be physically seen to simulate that which would occur in a living-being.

This was done both in an upright and in a supine position, given that the upper airway organs react differently depending on the position of the subject, which can consequently affect fluid flow. Note that the following figures of the obtained results have been sharpened to allow for easier viewing of air flow within the model, since the high-speed camera only provided black and white images.

- |   |   |  |                                  |
|---|---|--|----------------------------------|
|    | - Entry of air into final model           |    | - Exit of air out of final model |
|  | - Location of smoke flowing through model |  | - Location showing lack of smoke |

#### 5.3.1.1. Upright Position

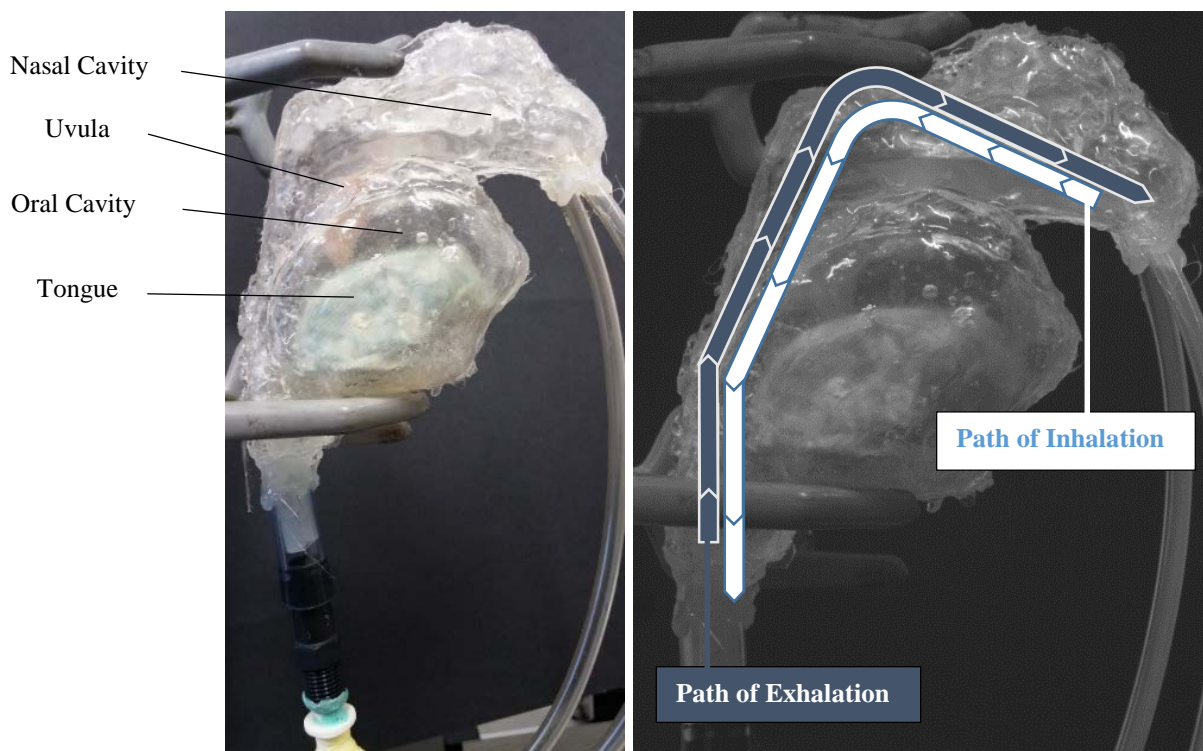


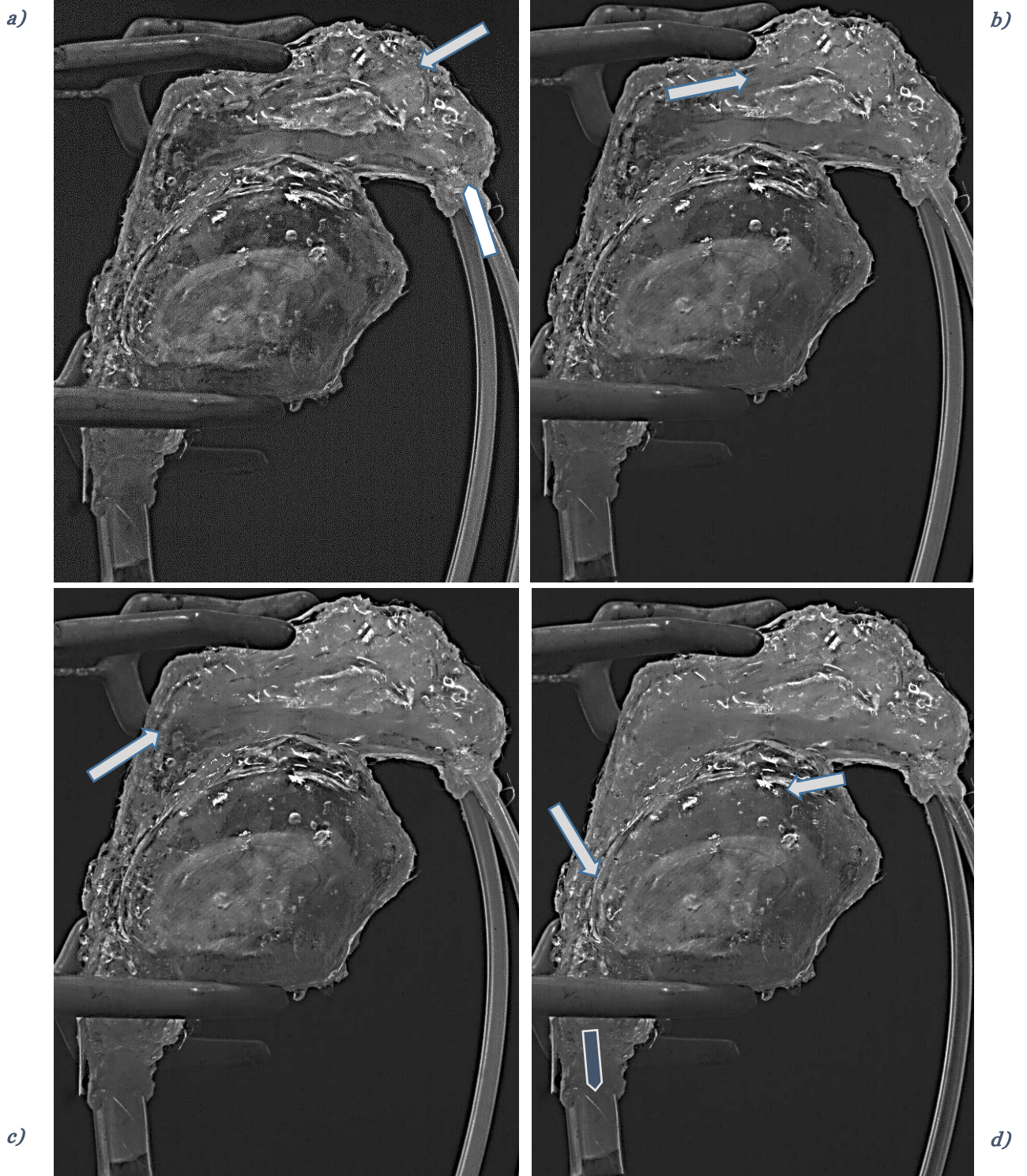
Figure 5-17 Final model ready for nasal breathing visualisation experimentation in the upright position (left) along with snapshot of the experiment taken by high speed camera highlighting the expected path of air (right)

During inhalation in the upright position:

- The air can be seen to travel superiorly to the upper ridge of the nasal cavity with laminar flow in both sides of the nasal cavity (*figure 5-18 a*).
- The nasal structure is angled upwards at its anterior end, allowing it to lead the air posteriorly towards the back of the nasal cavity. The air can be seen to maintain laminar flow for the most part throughout the nasal cavity, except as the angle changes at the upper-most ridge, upon which the air is seen to exhibit turbulent properties (*figure 5-18 b*).
- The air then continues to travel posteriorly and along the nasal conchae towards the posterior nares, and it continues to flow through into the nasopharynx, wherein the air appears to transition to turbulent (*figure 5-18 c*).
- As the air continues to travel down the pharynx, it accelerates while passing through the oropharynx and into the laryngopharynx (*figure 5-18 d*).
- At this point, some air can also be seen to flow anteriorly and cross through the isthmus of the Fauces and across the surface of the tongue into the oral cavity, although the amount of air entering this cavity is very minimal and much slower compared to that which filled the other spaces.
- Even as the inner cavities of the model became saturated with air, the air in the oral cavity can be seen to only travel forward approximately three-quarters of the way up to the tip of the tongue (*figure 5-18 d*).
- The rest of the air exited through the tube connected at the location of the larynx at the end of the laryngopharynx.

The most informative points resulting from this experiment were three. The first being the nature and behaviour of air flow while travelling through the nasal cavity. The second being the flow rate throughout the pharynx. And thirdly, the general behaviour of air in the oral cavity: its reluctance to flow into the oral cavity except after filling all other spaces, and the difference in the extent to which the air filled the oral cavity in the presence and absence of the other open nostril.





*Figure 5-18 Sequence of images showing flow of air in the final model during nasal-only inhalation in the upright position*

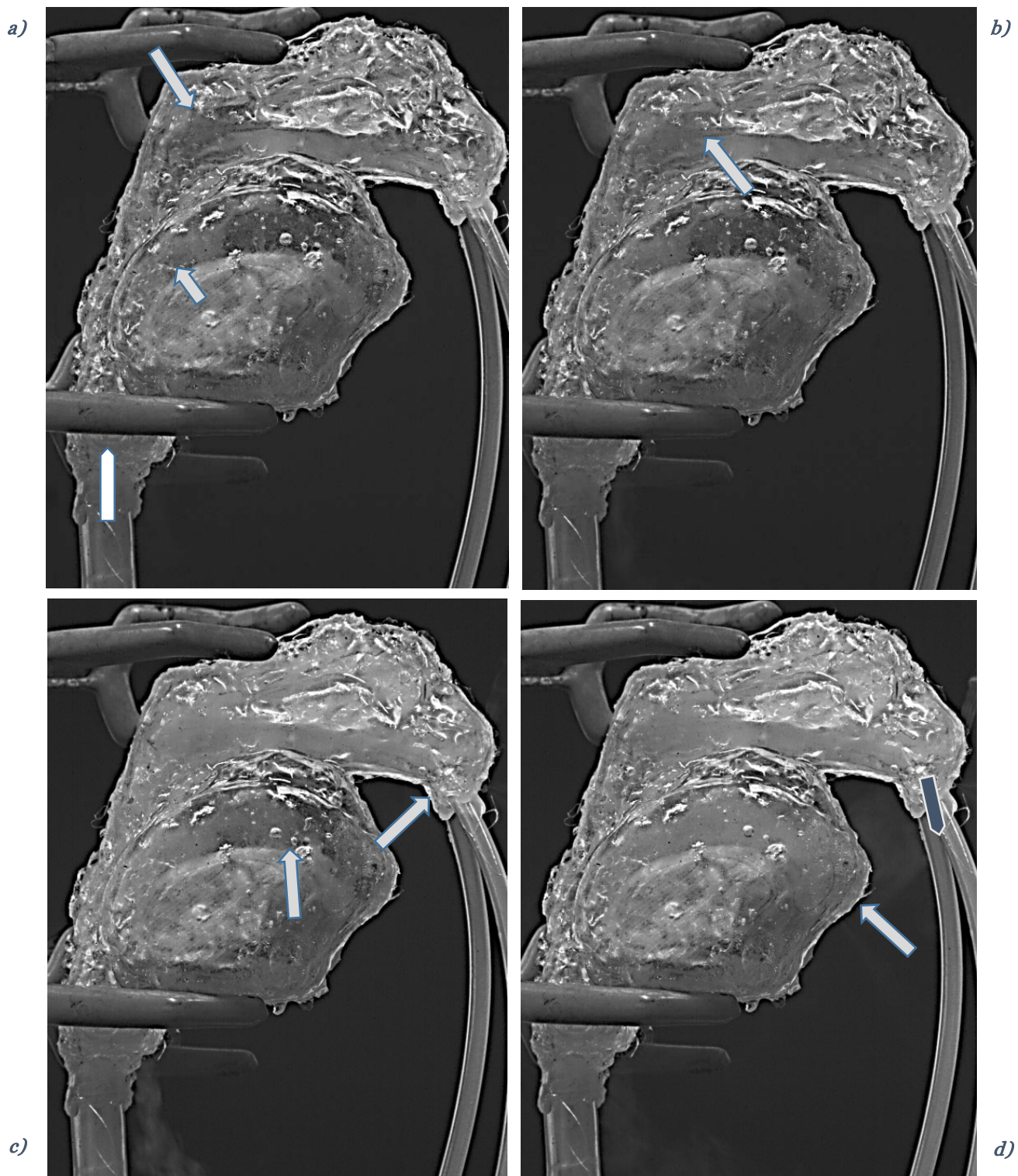
As for exhalation in the upright position:

- As the air can be seen to pass through the upper boundary of the larynx and into the Laryngopharynx, some air can be seen to spread across to the boundary of the uvula in the fauces region (*figure 5-19 a*), but the majority of it travels very rapidly through

the pharynx into the nasal cavity with the bulk of air flowing superiorly towards the region of the sphenoidal sinuses (*figure 5-19 a*).

- There doesn't seem to be any additional resistance along this path of the pharynx, and air appears to remain laminar up until the posterior nares where the nasopharynx opens into the nasal cavities, after which the air seems to transition to turbulent (*figure 5-19 b*).
- It is interesting to note that even as the air saturated the nasopharyngeal region and continued anteriorly through the nasal cavity, the air at the oropharyngeal region still did not proceed anteriorly into the oral cavity, and was somewhat stagnating at the uvula (*figure 5-19 b*).
- The air then spreads within the nasal cavity as the upwards angle of the nasal cavity leads the air towards the anterior end of the cavity where it eventually reaches the nostrils, and can be seen to exit through both nostrils (*figure 5-19 c*).
- Once the air reaches this exit, the air can also be seen to flow more rapidly through the oropharyngeal isthmus into the oral cavity (*figure 5-19 c*), where eventually, the air fills the entire oral cavity space to reach the tip of the tongue (*figure 5-19 d*).

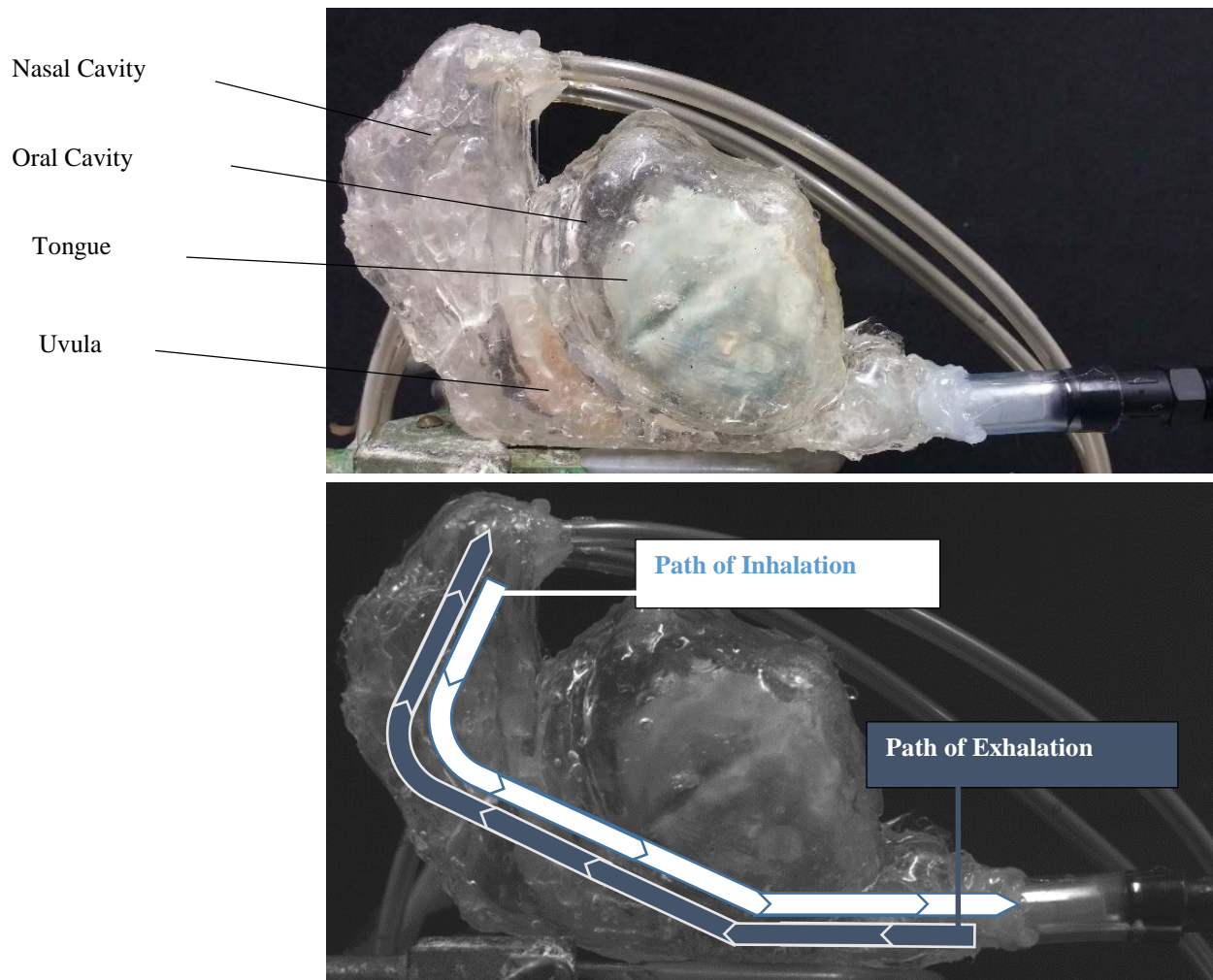
Thus three main observations resulting from this experiment are worth reiterating. One, the lack of resistance and ease of flow of air through the pharynx into the nasal cavity. Two, the transition of air flow from laminar to turbulent upon entry into the nasal cavity. And three, the reluctance of air flow into the oral cavity until the air reaches the nostrils, and the extent to which air flowed in the oral cavity.



*Figure 5-19 Sequence of images showing flow of air in the final model during nasal-only exhalation in the upright position*



### 5.3.1.2. Supine Position



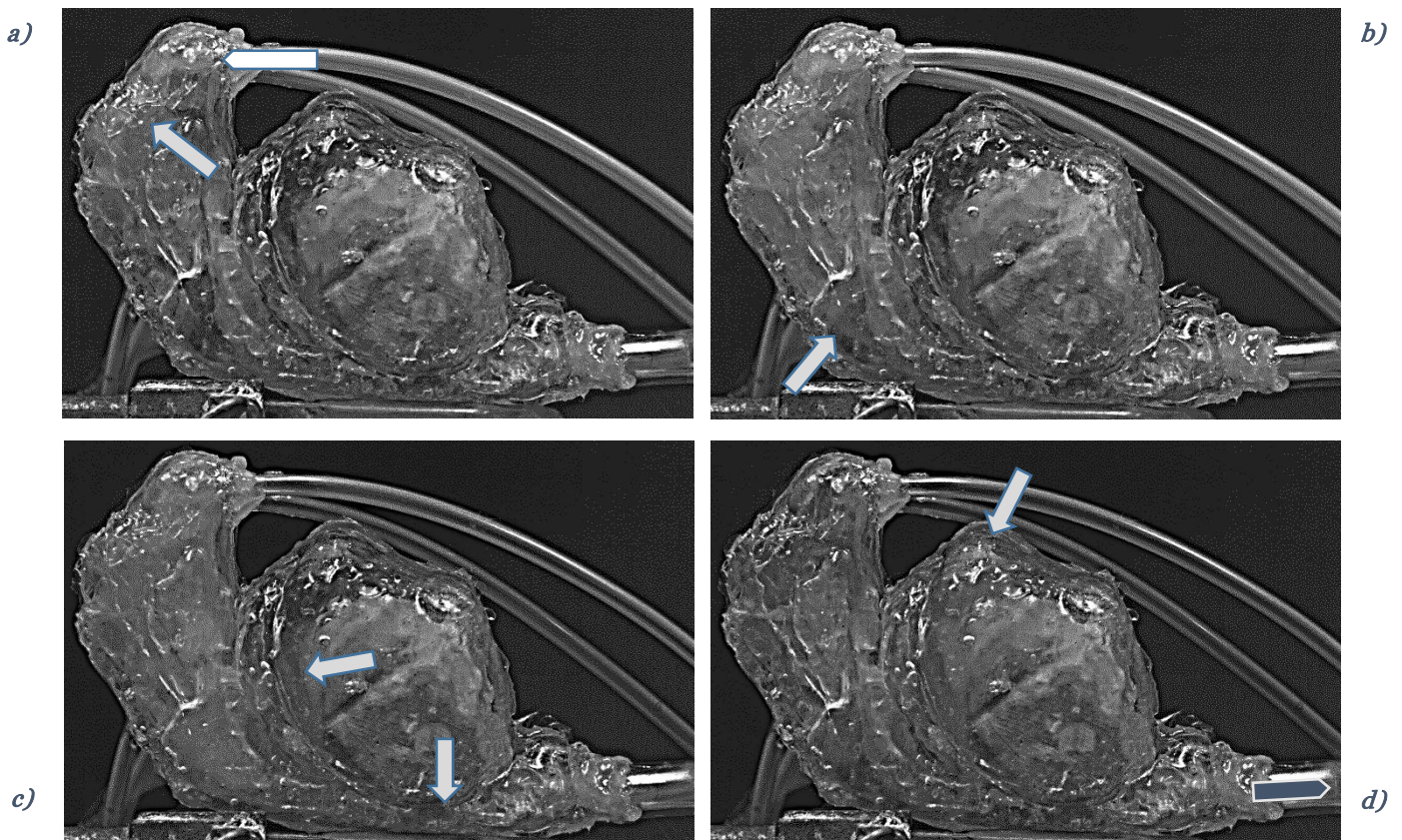
*Figure 5-20 Final model ready for nasal breathing visualisation experimentation in the supine position (top) along with snapshot of the experiment taken by high speed camera highlighting the expected path of air (bottom)*

Once more, during inhalation in the supine position:

- The air upon entry can be seen to travel directly up to the upper ridge of the nasal cavity with laminar flow (*figure 5-21 a*). The air then cycled and spread to fill the entire nasal cavity before reaching the nasopharynx (*figure 5-21 b*).
- The air then eventually, and it seems with difficulty, proceeded downwards through the retropalatal region and into the oropharynx, where it split to fill the retrolingual space and the oral cavity (*figure 5-21 c*). The reluctance of air to enter the oropharynx past the retropalatal region is in stark contrast to the ease with which air entered the pharynx when in the upright position.

- The air entering the oral cavity, in contrast to its behaviour during inhalation in the upright position, flowed along the surface of the tongue up to the tip of the tongue (*figure 5-21 d*).
- Meanwhile, the air which travelled inferiorly past the retrolingual space proceeded towards the direction of the Larynx.
- The path of flow of the air in the oral cavity and retrolingual space in the supine position is comparable to its flow when upright, given that in the supine position the air split almost equally into the oral cavity and the laryngopharynx, while when upright, there was more resistance preventing the air from flowing into the oral cavity.

The important observations worth emphasising for experimentation in this position were, firstly, the contrasting rate of air flow through the pharynx when compared to when upright (at the retropalatal region in particular). Secondly, the ease of air flow into the oral cavity when the air passed the region of the pharyngeal isthmus, indicated by the even flow of air into both the oral cavity and the laryngopharynx. And finally, the extent to which air flowed in the oral cavity compared to its flow when upright.



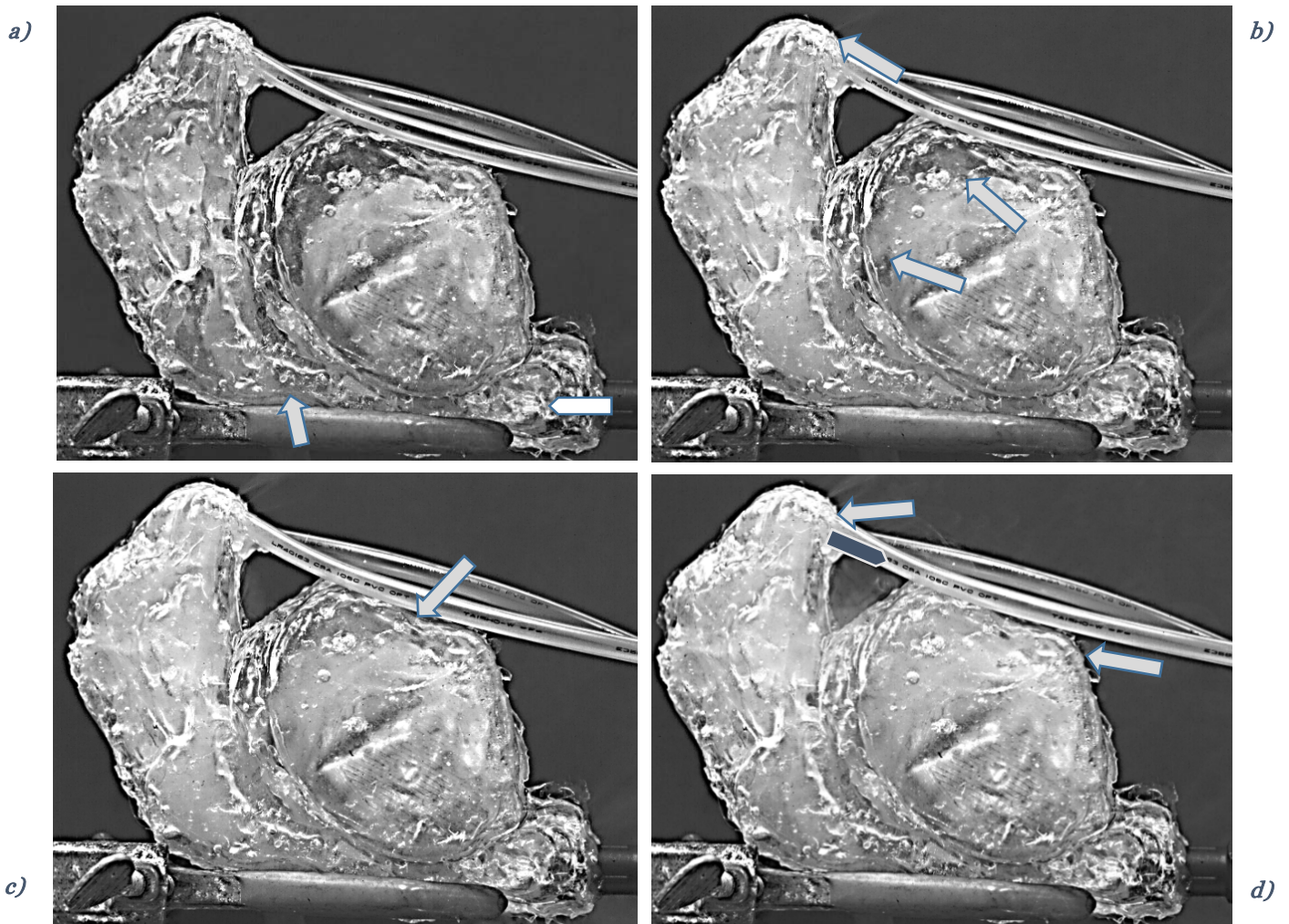
*Figure 5-21 Sequence of images showing flow of air in the final model during nasal-only inhalation in the supine position*

Exhalation was once more induced by supplying positive pressure at the inferior opening of the laryngopharynx. In the supine position:

- The air flowed seamlessly up to the retropalatal region, where it seemed to be met with some resistance at the area of the soft palate (*figure 5-22 a*).
- After passing this area, the air flowed mostly along the upper ridge of the nasal cavity before spreading within the nasal cavity quite smoothly and eventually reaching the nostrils (*figure 5-22 b*).
- Meanwhile, air flowed quite rapidly across the surface of the tongue (*figure 5-22 b*), extending even further than when upright, and past the tip of the tongue, filling the space along the anterior surface of the tongue to almost reach the tongue base where the tongue was attached to the model (*figure 5-22 c and d*).
- An important point to note is that this rapid flow of air in the oral cavity did not occur until the nasal cavity became saturated inside with air, upon which the entire oral cavity was also filled with the air (*figure 5-22 d*). Previous to this there was still a lot more air in the nasal cavity than could be found in the oral cavity by the stage at which a small amount of air seen to reach the anterior end of the oral cavity (*figure 5-22 c*).

The first main difference worth noting with regards to exhalation in the supine position was that the flow of air was met with substantial resistance at the retropalatal region. The second notable difference was the lack of air flow in the oral cavity until the nasal cavity was saturated. And the third difference was how far and fast the air travelled into the oral cavity when compared to all other situations.





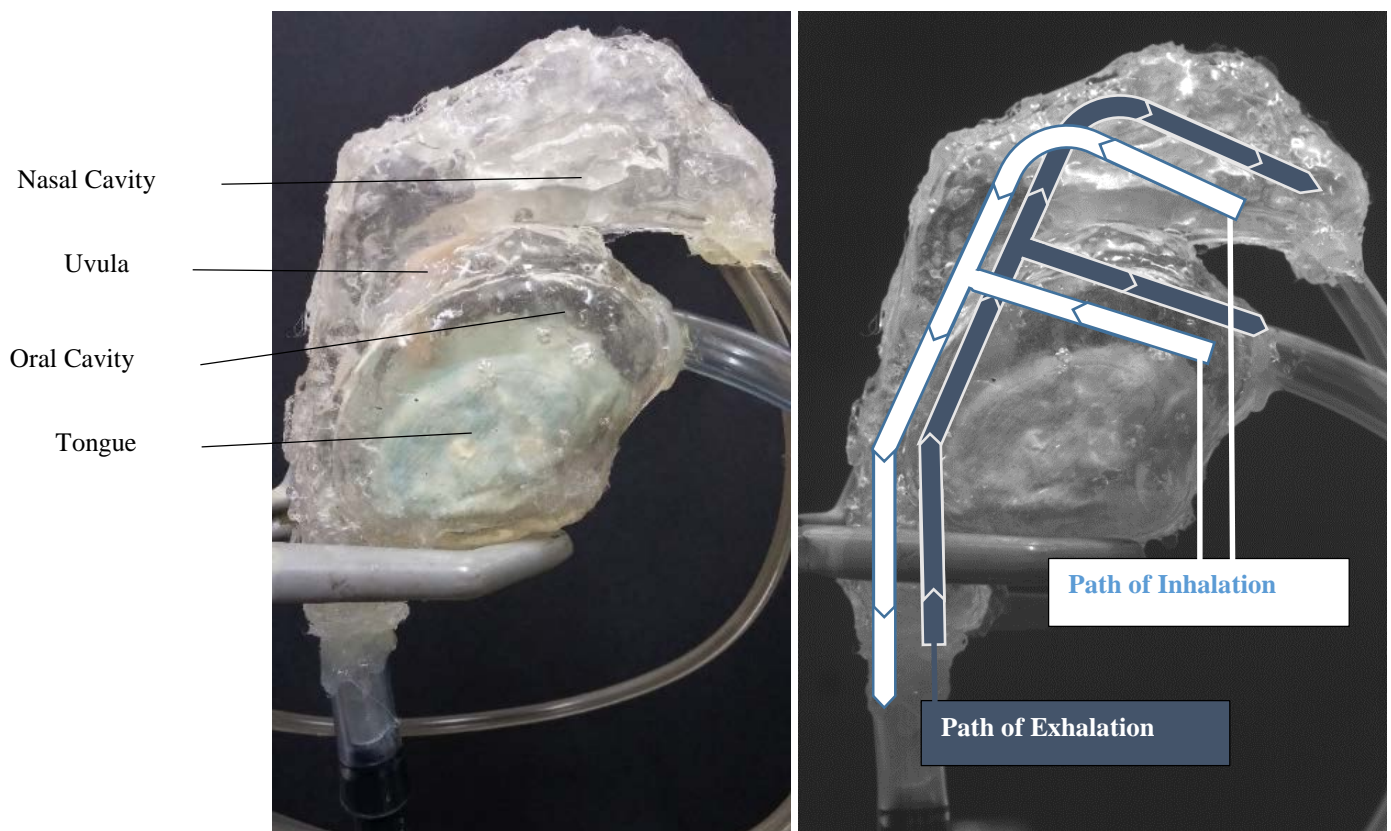
*Figure 5-22 Sequence of images showing flow of air in the final model during nasal-only exhalation in the supine position*

### **5.3.2. Further Experimentation - Open Mouth**

Analysis of air flow in the upper respiratory tract often omits the presence of another point of entry for air other than at the nasal cavity. In fact, very little research has included air flow in the presence of an oral cavity and the possibility of another interface through which the outside air can enter the respiratory system (see 2.5). However, in real-life, OSA and snoring can occur regardless of whether or not the subject has their mouth open, and thus, capturing both scenarios is important as it can provide further insight as to the exact causes of these conditions, and may lead to the possibility of discovering ways in which these issues could be treated. Considering this notion, experimentation with fluid flow under the influence of organ response was once again performed, but in the presence of an open mouth, which was simulated by attaching a tube, larger in diameter than those attached at the nostrils, to the anterior end of the oral cavity in the model. This meant that the larger aperture at the oral cavity through which air could flow better represented the wider opening of the mouth.

As was the case in the previous section of air flow analysis, the upright position was used as the normal by which other observations were compared. This is because, aside from the fact that there should be no loss in muscle tone when a subject is in the upright position, as it is very unlikely that they are asleep, the upright position also negates the effects the tongue and uvula have on airway obstruction during breathing and the ensuing presence of snoring and sleep apnea. Once again, the images depicting the results have been sharpened to better show the flow of air within the model.

### 5.3.2.1. Upright Position



*Figure 5-23 Final model ready for nasal and oral breathing visualisation experimentation in the upright position (left) along with snapshot of the experiment taken by high speed camera highlighting the expected path of air (right)*

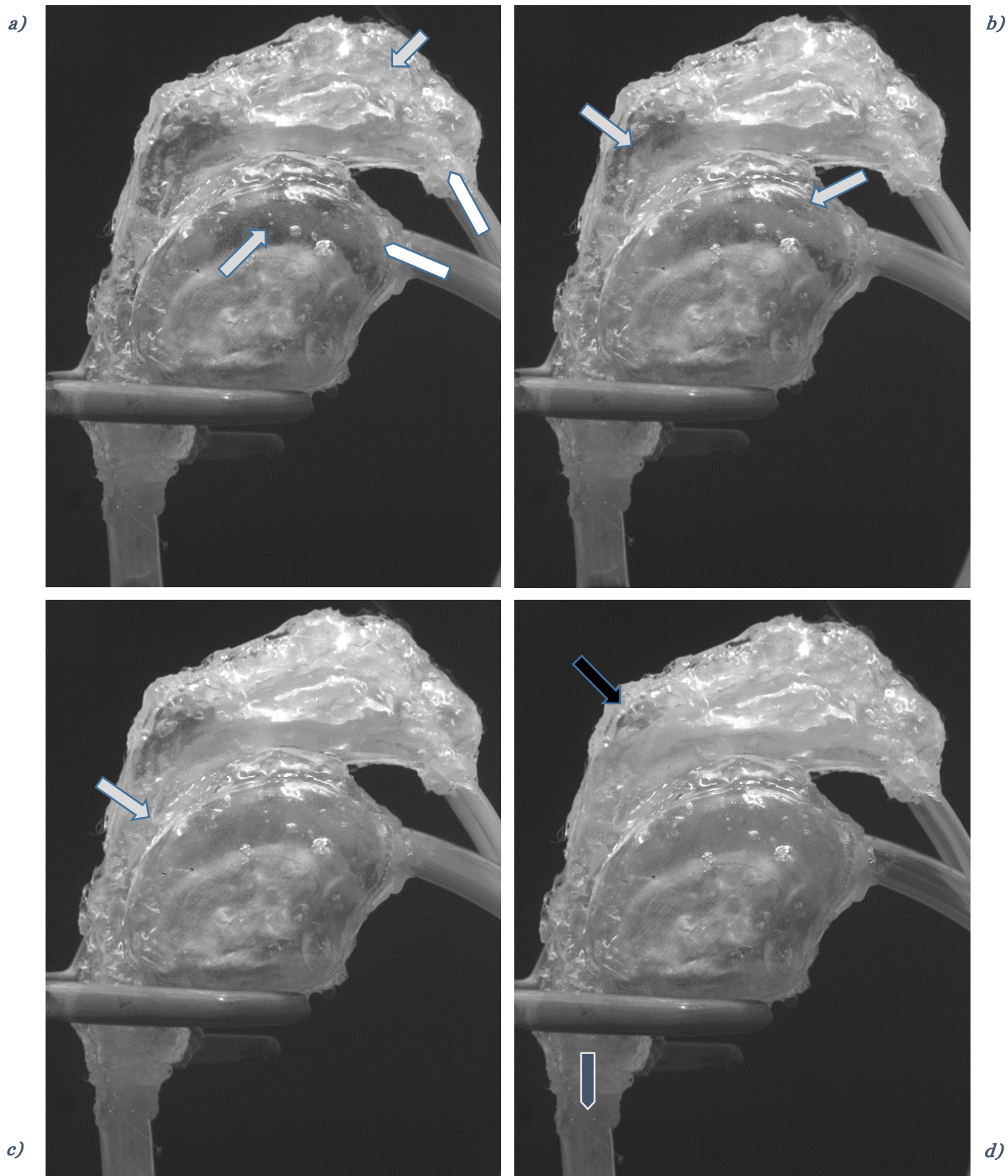
Fluid flow in the presence of an open mouth varied greatly than when air was seen to only exit through the nasal cavity. During inhalation in the upright position:

- The air can be seen to travel both superiorly into the nasal cavity through the nostrils, and into the oral cavity through the gap at the mouth. It is interesting to note that air entered the two cavities rather laminarly, and only transitioned to turbulent at the interface where it met the inner walls of the respiratory tract (*figure 5-24 a*).

- The behaviour of fluid flow in the nasal cavity was very similar to that observed during closed-mouth testing, with the way in which air travelled steadily towards the nasopharynx (see 5.3.1.1). One big difference, however, lies in the fact that, at the posterior end of the nasal cavity, the air flowed along the floor of the nasal cavity (*figure 5-24 b*), and throughout the entire inhalation process, barely any air reached the upper-most ridge of the nasopharynx where the sphenoidal sinuses would be located (*figure 5-24 d*).
- The air entering through the oral cavity flowed along the surface of the tongue right into the oropharyngeal region, and it can be seen that more air overall entered the upper airway through the mouth than the nasal cavity.
- Interestingly enough, some air can be seen to cycle back towards the anterior end of the oral cavity (*figure 5-24 b*).
- The two different paths of air then combine at the oropharyngeal region (*figure 5-24 c*) before the air accelerates once again through the oropharynx into the laryngopharynx.

The four important observations worth summarising from this experiment are the nature of air flow as it entered the model from both entrances, the behaviour of air flow in the nasal cavity and at the nasopharynx, the ratio of air which entered through the mouth when compared to that which entered through the nose, and the behaviour of air flow in the oral cavity.





*Figure 5-24 Sequence of images showing flow of air in the final model during nasal and oral inhalation in the upright position*

During open-mouth exhalation in the upright position:

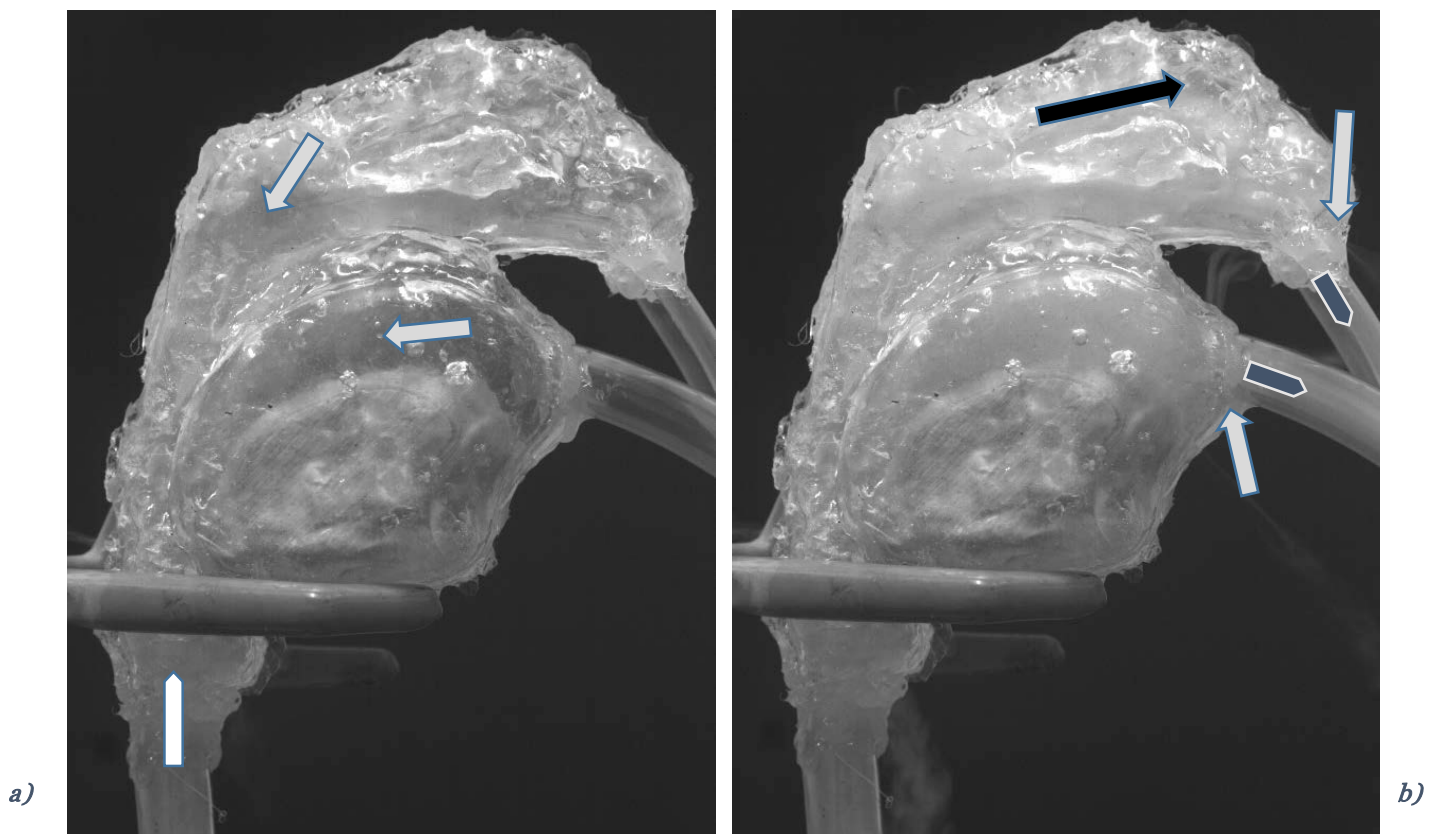
- As the air passes through the upper boundary of the larynx and into the Laryngopharynx, it can once again be seen to travel seamlessly through the pharynx



into the nasal and oral cavities. There seems to be no significant resistance along this path, and air remains laminar up until the oropharynx, where the air splits almost equally to enter the nasal cavity and oral cavities (*figure 5-25 a*).

- Air is also seen to exit the upper airway model through both exits at approximately the same time (*figure 5-25 b*), with the air exiting through the oral cavity turning turbulent once it enters the empty space and flows across the surface of the tongue to exit the upper airway.
- Air travelling superiorly into the nasal cavity spread to fill the nasopharynx before continuing to behave in a fashion very similar to that observed during exhalation in closed-mouth analysis, with one exception in that, once again, even as air saturated the upper airway model, air did not seem to fill the most superior portion of the upper ridge behind the nostrils (*figure 5-25 b*).

Only two points are worth reiterating for this experiment: the rate of air flow when entering the oral and nasal cavities, and, once again, the behaviour of air flow in the nasal cavity and at the nasopharynx.



*Figure 5-25 Sequence of images showing flow of air in the final model during nasal and oral exhalation in the upright position*

### 5.3.2.2. Supine Position

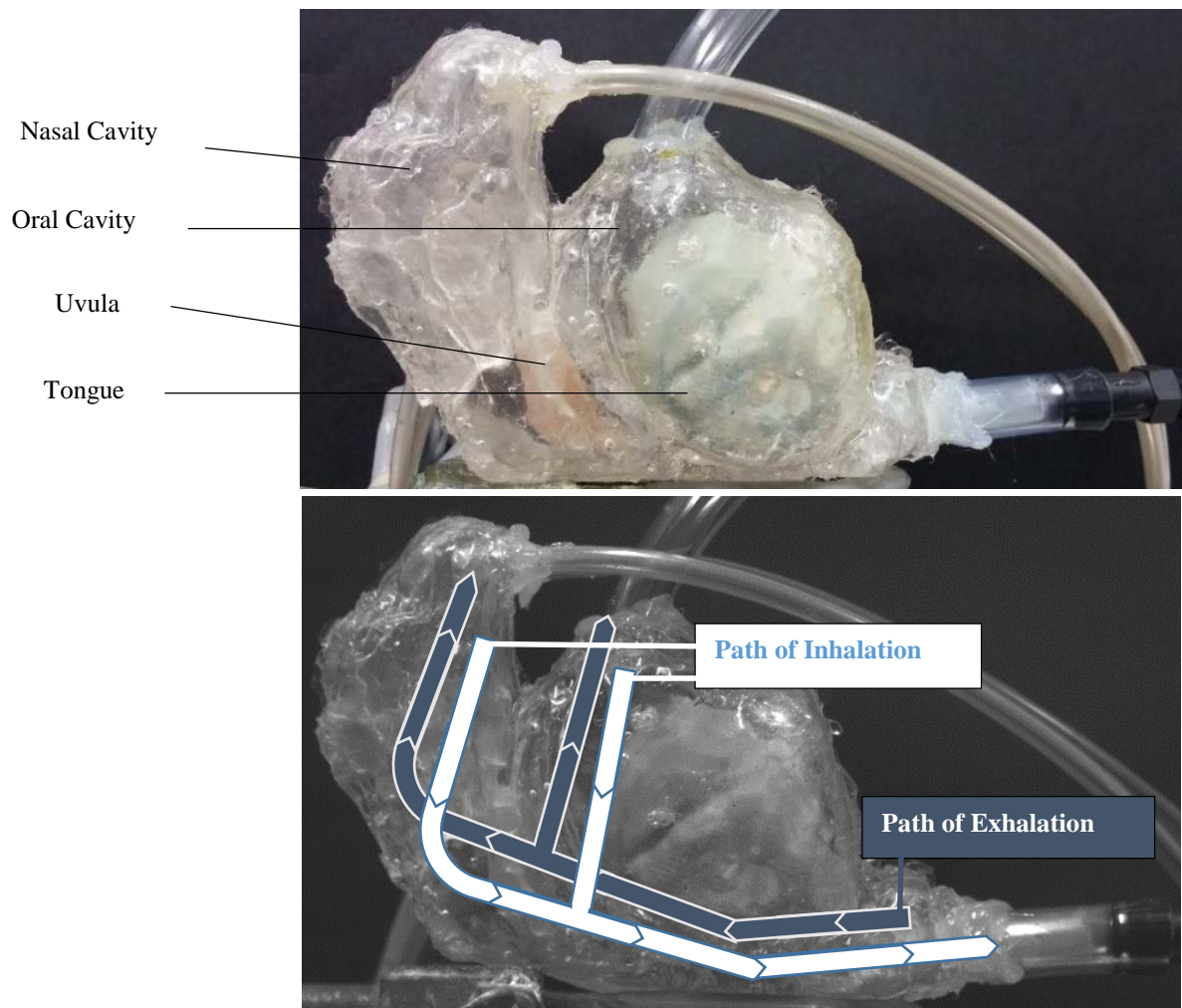


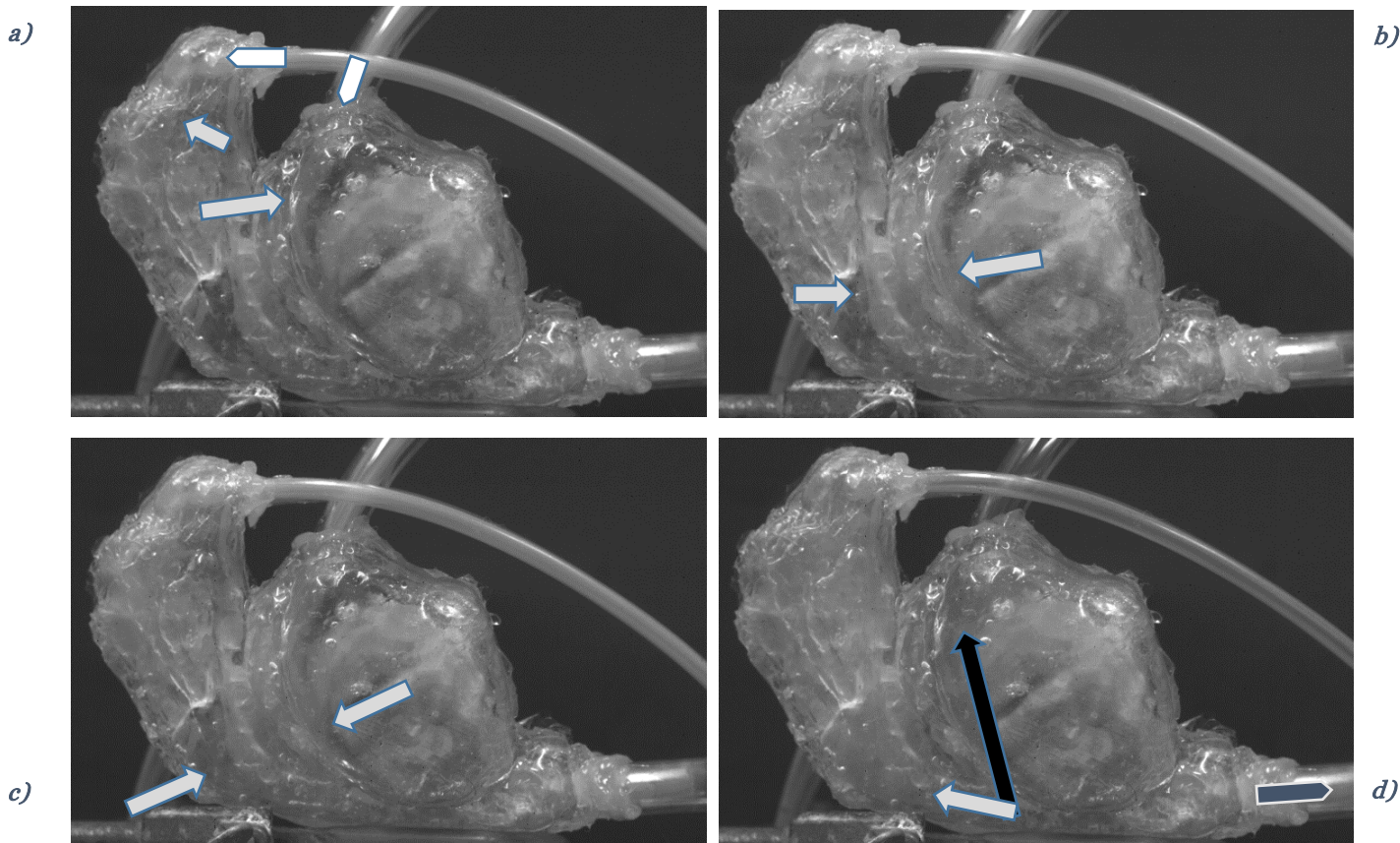
Figure 5-26 Final model ready for nasal and oral breathing visualisation experimentation in the supine position (top) along with snapshot of the experiment taken by high speed camera highlighting the expected path of air (bottom)

Fluid flow in the upper airway model in the supine position during open mouth testing yielded interesting results. During inhalation:

- Air travels ordinarily along the upper ridge of the nasal cavity with laminar flow (figure 5-27 a), and once again cycles and spreads to fill the whole nasal cavity (figure 5-27 c) before entering the nasopharynx.
- In this region, the air once more proceeds through to the retropalatal region with slightly more difficulty to combine with the air entering from the oral cavity.
- A lot more air can also be seen to enter through the oral cavity in the supine position (figure 5-27 a) than even that observed entering through the oral cavity in the upright position with an open mouth.

- Another interesting observation is that the air entering the airway model through the oral opening can be seen to reach all the way to the level of the soft palate before the air which entered through the nasal opening (*figure 5-27 b*), and some of the air can be seen to pass through the isthmus of the fauces superiorly and past the point of attachment of the uvula to enter the nasal cavity directly at the region of the posterior nares (*figure 5-27 b*).
- Once the air flowing through the oral cavity met with the air entering through the nasal cavity, it proceeded inferiorly towards the larynx, but another observation worth noting is that a lot more air collected at the oropharyngeal region where the two pathways met before proceeding with greater difficulty through the retrolingual region into the laryngopharynx (*figure 5-27 c*).
- Finally, the air can be seen to stagnate at the nasopharyngeal area for a longer duration of time than the air which was inhaled through the oral cavity (*figure 5-27 d*), indicating just how fast inhalation through the oral cavity occurred in contrast to that through the nasal cavity.

There are four main points worth reiterating for the results of supine open-mouth inhalation testing. The first being the resistance met by the air when passing the retropalatal and retrolingual regions. The second being the increased rate of air flow in the oral cavity than when compared to upright open-mouth inhalation. The third being the behaviour of air flow at the level of the palate and in particular at the posterior end of the oral cavity. And finally, the difference in air flow between the air in the oral and nasal cavities.



*Figure 5-27 Sequence of images showing flow of air in the final model during nasal and oral inhalation in the supine position*

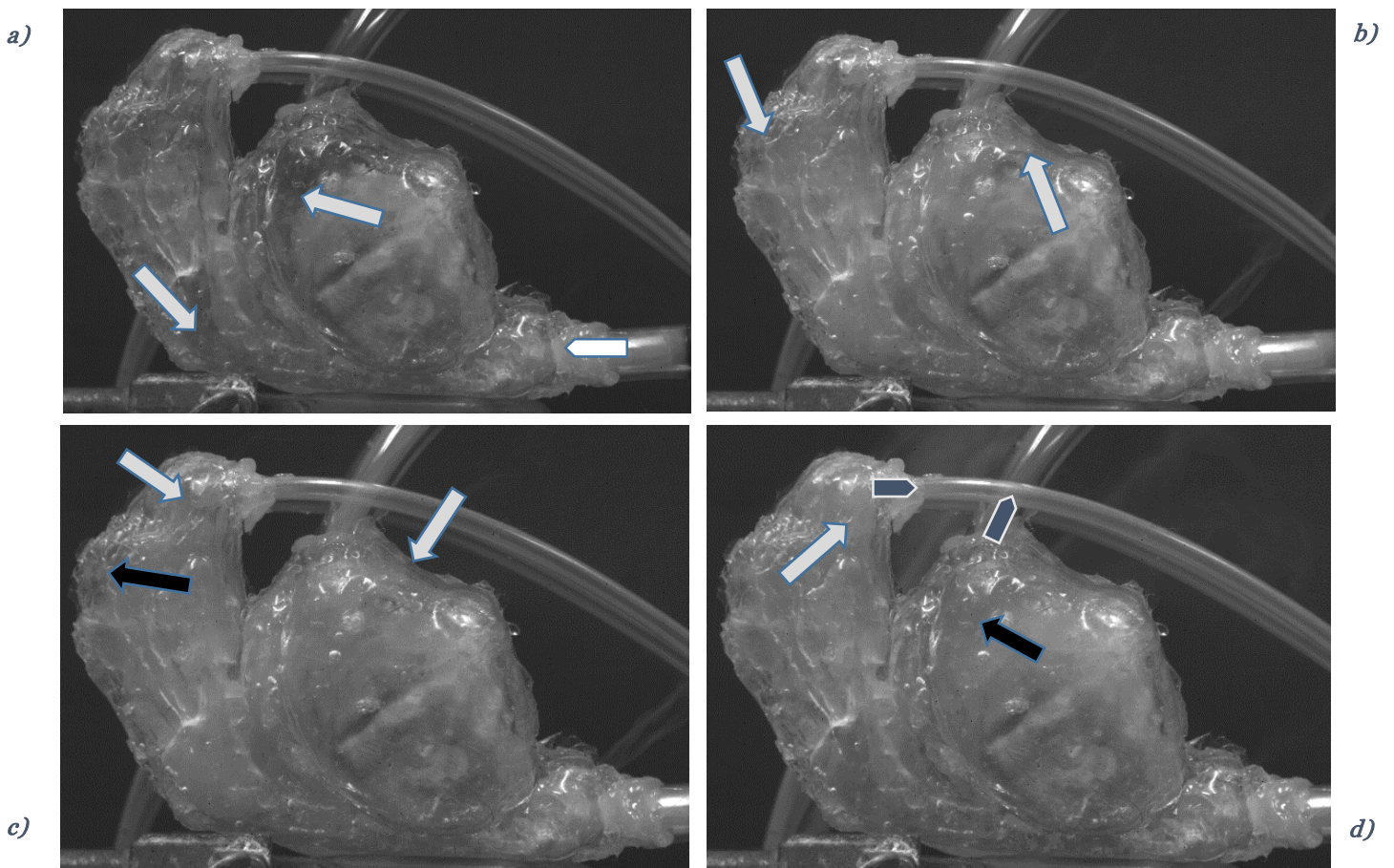
During open-mouth exhalation in the supine position:

- Air flowed rather smoothly past the retrolingual region and into the oropharynx, where the air travelling through the retropalatal region into the nasal cavity was met with some resistance, forcing more air to be expelled through the oral cavity (although initially, air can be seen to flow both superiorly past the pharyngeal isthmus into the nasopharynx and anteriorly into the oral cavity (*figure 5-28 a*)).
- Upon entering the oral cavity, the air can be seen to travel past the tip of the tongue and into the space between the anterior end of the tongue and the anterior end of the oral cavity (*figure 5-28 b*).
- This large bulk of air is also found in this region even before any major mass of air is seen to reach the nostrils (*figure 5-28 b*). Consequently, a large majority of the air leaves through the oral cavity before it exits the nasal cavity.
- By the stage at which air reaches the nostrils, air at the oral cavity already extends past the tip of the tongue and towards the base of the tongue (*figure 5-28 c*).



- Once more, as was seen during open-mouth, supine inhalation, the marked air can be seen to leave the oral cavity before it is all released from the nasal cavity (*figure 5-28 d*).
- Finally, a decrease in air flow can once again be observed at the superior ridge of the nasal cavity behind the nostrils (*figure 5-28 c*), just as that which was observed during open-mouth, upright exhalation.

The first main observation worth noting is the resistance met by the air at the retropalatal region, and the resulting difference in air distribution in the oral and nasal cavities. Secondly, it is worth reiterating the extent to which air flowed in the oral cavity, and especially when compared to its flow in the nasal cavity. This brings about the third point, which is the subsequent expulsion of marked air in the oral cavity before the nasal cavity. Finally, the last point remains, once again, the lack of air flow at the upper ridge of the nasal cavity.



*Figure 5-28 Sequence of images showing flow of air in the final model during nasal and oral exhalation in the supine position*

## 5.4. Flexibility: Measuring Changes in the Upper Airway model

Because the entire model was flexible, it is easy to see how the different effects of the positive and the negative pressures induced by exhalation and inhalation, respectively, affect the size and dimensions of the different areas of the upper airway. The following tables show the effects respiration has on the areas of the cavities within the upper respiratory tract by measuring the changes in width of each section of the upper airway model during both inhalation and exhalation, and while upright and supine:

*Table 5-1 Overview of the measured boundary width displacements in the final upper airway model during respiration in the Upright position. The table shows the measured distances of the various areas at rest, at maximum displacement during inhalation and exhalation, the total distance displaced at the various areas during inhalation and exhalation, and the percentage change in width of the various areas during inhalation and exhalation*

	Upright					
	Nasoph.	Retropal.	Oroph.	Oral Cav.	Retroling.	Laryng.
At Rest (mm)	14	12	10	31	12	6
Inhalation (mm)	14	11.7	9.1	30.5	11.5	6
Exhalation (mm)	14.9	12.5	11.3	31.5	12.4	6.3
Distance decrease (mm)	0.0	0.0	0.9	0.5	0.5	0.0
% decrease	0.0	0.0	9.0	1.6	4.2	0.0
Distance increase (mm)	0.9	0.5	1.3	0.5	0.4	0.5
% increase	6.4	7.5	13	1.6	3.3	5.0

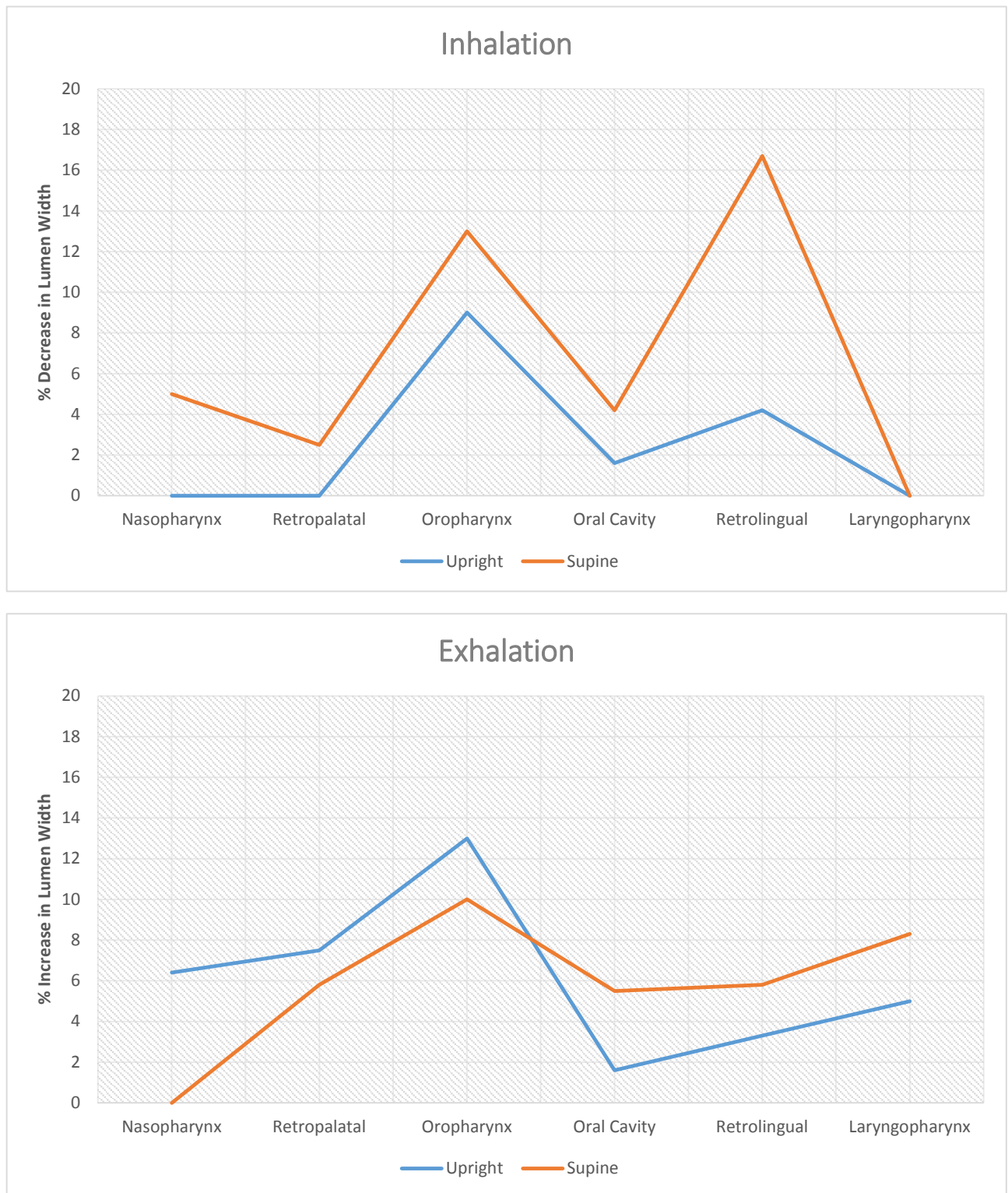
*Table 5-2 Overview of the measured boundary width displacements in the final upper airway model during respiration in the Supine position. The table shows the measured distances of the various areas at rest, at maximum displacement during inhalation and exhalation, the total distance displaced at the various areas during inhalation and exhalation, and the percentage change in width of the various areas during inhalation and exhalation*

	Supine					
	Nasoph.	Retropal.	Oroph.	Oral Cav.	Retroling.	Laryng.
At Rest (mm)	14	12	10	31	12	6
Inhalation (mm)	13.3	11.7	8.7	29.7	10	6
Exhalation (mm)	14	12.7	11	32.7	12.7	6.5
Distance decrease (mm)	0.7	0.3	1.3	1.3	2	0
% decrease	5.0	2.5	13.0	4.2	16.7	0.0
Distance increase (mm)	0	0.7	1	1.7	0.7	0.5
% increase	0.0	5.8	10.0	5.5	5.8	8.3

The changes observed in the width of the boundaries of the final upper airway model can best be seen and interpreted by plotting the extent of change against the distance along the upper airway. A plot of the percentage change in overall width of the lumen at the various regions shows how each region was affected with respect to its own size. This provides a consistent indication of the effects of respiration at each region, recalling that the thickness of material surrounding the boundary shape remained constant.

The following graph compares the effects of the position of the final model at the different stages of the breath cycle:



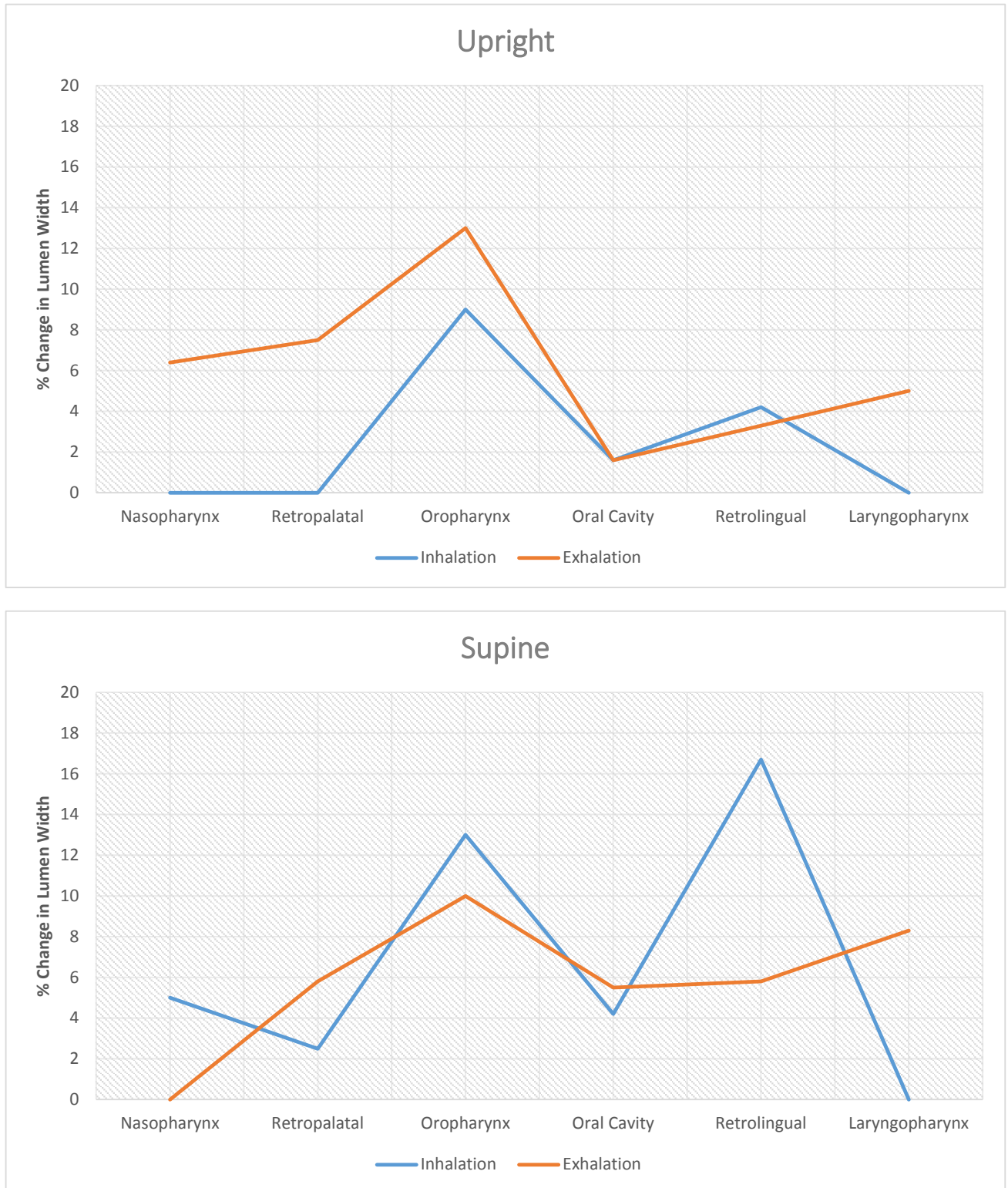


*Figure 5-29 A comparison of the effects of posture on the overall measured displacements of the upper airway boundary width during inhalation (above) and exhalation (below)*

It is evident that the same general trend can be seen for the changes in upper airway width during both upright and supine inhalation, whereas this trend varies greatly during exhalation. Overall, larger deformations can be seen in the supine position in all regions during inhalation, and at the regions inferior to the oropharynx during exhalation. With the exception of supine

inhalation, where the retrolingual space was affected the most, the oropharynx is the region where the largest deformations can be observed.

In comparing the effects of inhalation and exhalation on the width of the lumen at the various areas for the different positions of the final model, the following results were obtained:



*Figure 5-30 A comparison of the effects of the breath cycle (inhalation and exhalation) on the overall measured displacements of the upper airway boundary width while upright (above) and supine (below)*

Once again, the same general trend is observed in the first graph in the upright position during both inhalation and exhalation. However, the measured displacements while supine vary greatly depending on whether or not air flow through the upper airway model was induced by inhalation or exhalation. While supine, the effects of inhalation on the changes in lumen width varied greatly along the length of the airway model, indicating the dynamic response of the upper airway during inhalation when a subject sleeps in the supine position.

## 5.5. Summary

This chapter served to, both numerically and descriptively, provide the results of developing a realistic, transparent model of a complete upper respiratory tract, as well as present the results observed when respiration was simulated using the model. These results included looking at the details of the final model, the feasibility of using its transparency property to analyse fluid behaviour within the model, and looking at the response of the final model to respiration subject to different positions of the model given its flexibility property.

The next chapter will compare these obtained results with the expected results according to that which was revised in *Chapter 2* and other previous research.

## Chapter 6 - DISCUSSION

### 6.1. Introduction

Having presented the details of the overall geometry, dimensions, properties, and response of the final model subject to specific situations in the previous chapter, this chapter will aim to relate the observed results to that which is expected of the upper respiratory tract by looking at previous research and scientific literature, which will be done by presenting the following:

- An investigation into the accuracy of the final model with regards to its geometry and dimensions
- An evaluation of the suitability of using the final model for accurate air flow visualisation within a realistic upper airway by using its property of transparency
- An analysis of the realistic nature of the final developed model by examining its response to respiration using its property of flexibility

Finally, this chapter will examine the final model in terms of limitations and the possibility of improving the final model, as well look into possible uses of the model for future research in the same field.

### 6.2. Analysing the Accuracy of the Developed Model

The aim of the developed model was to serve as a transparent representation for a real upper respiratory tract, and thus in order to be used to characterise the upper airway, it must be modelled accurately.

The developed model of the upper airway was highly accurate in terms of the general details of the upper airway. Given that it was built around a virtual model based on MRI scans of the air passages within a real upper airway, and no subsequent changes were made to affect the overall geometry of the 3D printed part, the final model was a replica of the inner boundaries of the upper respiratory tract, thus successfully serving its purpose.

Furthermore, while certain intricate parts of the various areas of the upper airway were not included which may have also affected the flow of air, such as the pillars of the fauces, their overall structure was at least captured during MRI imaging, and thus their general shape was maintained. For example, while both the palatoglossal and palatopharyngeal arches were

absent, a prominent single arch can still be seen at the posterior end of the oral cavity (*figure 5-7*).

The presence of these details, and thus accuracy of the model, can be examined by looking at each major area individually.

### **6.2.1. Nasal Cavity**

The most important feature of the nasal cavity which needed to be maintained when producing the model was its specific shape, due to the complex geometry associated with the nasal cavity and the presence of the nasal conchae.

First, a general look at the model from the outside reveals the similarity in the overall shape of the nasal cavity with that seen in academic and scientific literature (*figure 5-2 a*). Viewed laterally, the leaf-like shape of the nasal cavity in the anterior two-thirds of the nose is consistent with that seen in diagrams of the nasal cavity in literature and educational models, and the sudden decrease in space before the nasopharynx, and the subsequent bulge at the pharynx is the exact shape found in a real nasal cavity according to scientific literature.

Viewed from the top, the two separate cavities are obvious within the material, separated by the nasal septum. A coronal (frontal) view of the nasal cavity clearly shows the triangular shape separated by the nasal septum into two right-angled triangular halves, as is described in scientific literature (*see 2.2.1.1.1*) (*figure 5-5*).

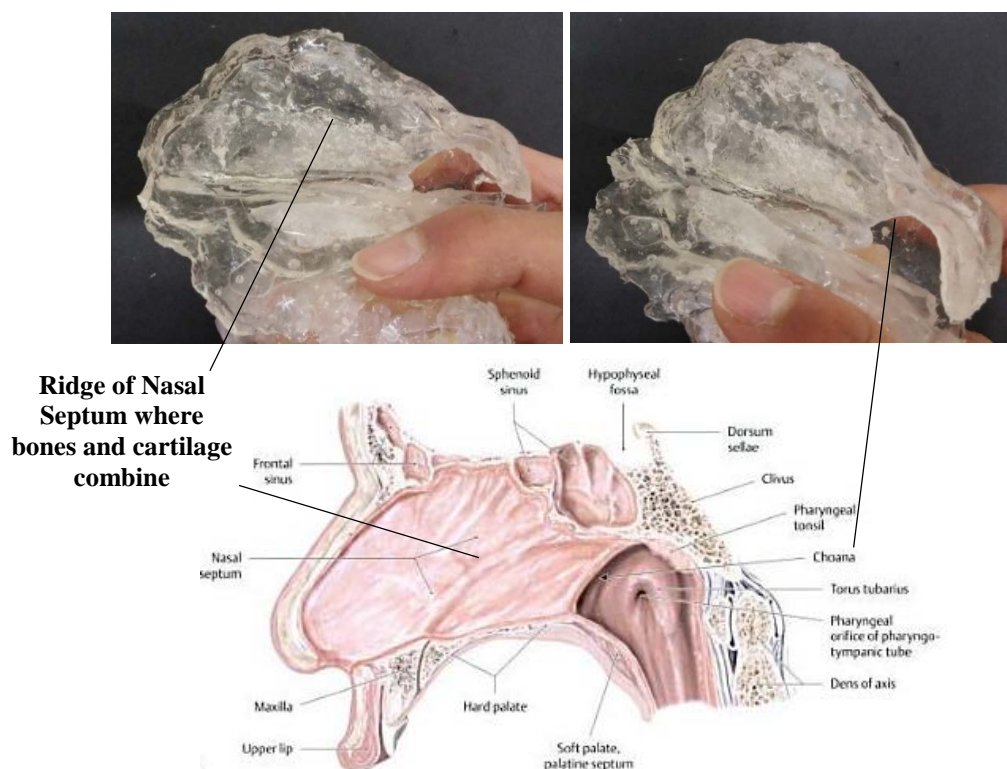
A closer look at the nasal cavity of the model from within reveals the level of detail observed by the model and its likeliness to a real upper airway.

*Figure 5-3* shows the sagittal cross-sectional view of the nasal septum within the model. The nasal septum is very similar in shape to what would be expected to be seen in the human nasal cavity, according to the figures found in other literature. A side-by-side view of the model and one such example from literature (*figure 6-1*) reveals a number of identical features. Firstly, the nasal septum extends exactly up to the posterior boundary of the hard palate. Secondly, at the edge of the hard palate, the posterior boundary of the nasal septum, along with the superior boundaries of the pharynx, create a bulb-like shape where the air from the two different cavities of the nose merge. Thirdly, the shape of the nasal septum is accurate at the choana: the ridge at the apertures through which air enter the two different sides of the nasal cavity at its posterior end. Finally, the ridges running along the nasal septum, which are present at the boundaries where the different bones and cartilages of the

nasal septum combine, are consistent with that found in other literature, and are highlighted in *figure 6-1*.

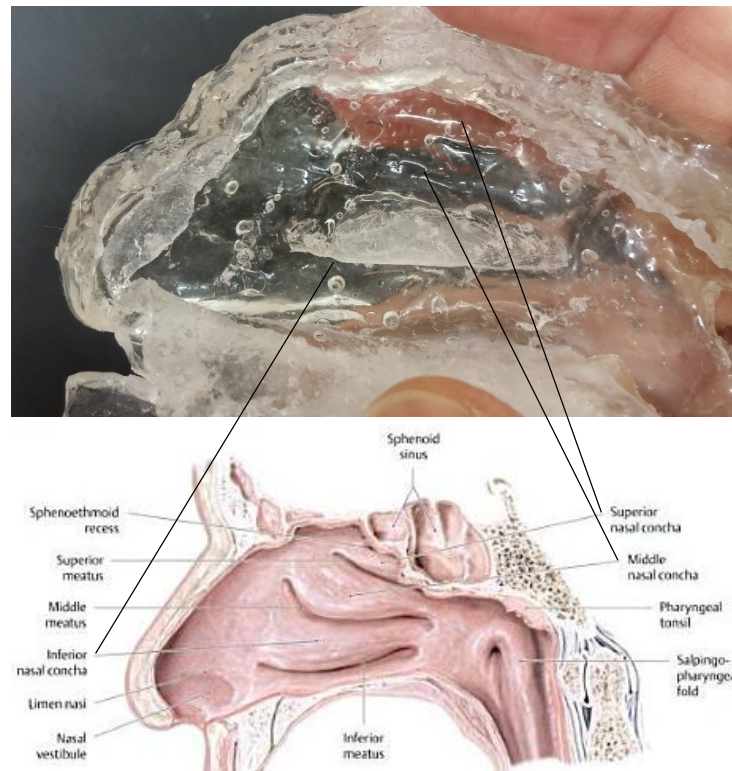
Looking past the nasal septum at the inner surface of the lateral walls, *figure 5-4* shows the presence of the 3 nasal conchae, which is comparable to that seen in other literature (*figure 2-1*). Once again, a look at the details within the model alongside one example of the same area found in literature (*figure 6-2*) affirms that the geometry matches what would be expected in a real nasal cavity. While these “scroll-like” extensions making up the nasal conchae are not as obvious in the model as they are in the accompanying diagram, the three conchae can still be distinguished by looking at the separate depressions within the outer wall, which are highlighted in *figure 6-2*.

Likewise, the coronal cross-sectional view of the nasal cavity of the model (*figure 5-5*) can be seen to match that seen in educational literature (*figure 2-1*). This is more obvious when a coronal section of the nasal cavity of the model is removed and viewed separately. It can be seen from *figure 5-5* that the most obvious feature extending out of the lateral walls of the nasal cavity is the inferior concha, which extends downwards to fill the space at the bottom. Above this, the middle concha can be seen as a slight bulge in the lateral wall, which causes a slight depression just above the inferior conchae, representing the middle meatus. Although, unlike in the diagram of *figure 2-1*, this does not continue laterally to open up into the sinuses.



*Figure 6-1 Sagittal cross-sectional view of developed models nasal cavity septum alongside diagram from scientific literature [16] for comparison*





*Figure 6-2 Sagittal cross-sectional view of outer walls of developed models nasal cavity alongside diagram from scientific literature [16] for comparison*

### 6.2.2. Oral Cavity

The oral cavity shape is quite basic, as it does not necessarily contain any complex irregular geometry, however, the placement and positioning of the related upper airway organs within the oral cavity is crucial for accurate upper airway representation.

When making the air model, which would be the core used in making the final model, the air in the upper half of the oral cavity is merged with the shape of the tongue used for the lower half of the oral cavity. This can be seen in *figure 5-1 d*. In addition to this, small gaps are present in the lateral walls just under the area where the uvula would be, which would form the palatopharyngeal arches in the final model. This feature can be seen as a pair of small ridges on either side of the lateral walls at the posterior end of the oral cavity space in the final model (*figure 5-1 a*). More importantly, the presence of the uvula and the tongue can clearly be seen situated in their respective areas within the oral cavity (*figure 5-7*).

A look at the oral cavity from outside the final model (*figure 5-16*) shows the situation of the tongue on the lower half of the oral cavity. The ratio of empty space above the tongue to the space occupied by the tongue is also a good representation of the overall space occupied by the tongue when compared to the diagrams found in external literature (*figure 2-2*).

Looking into the oral cavity in more detail, *figure 5-7* provides a first-person view of a mouth examination of the model. While it is relatively simple in shape, it is worth noting a few points in the model, which are more easily observed when alongside a scientific illustration of the oral cavity (*figure 6-3*).

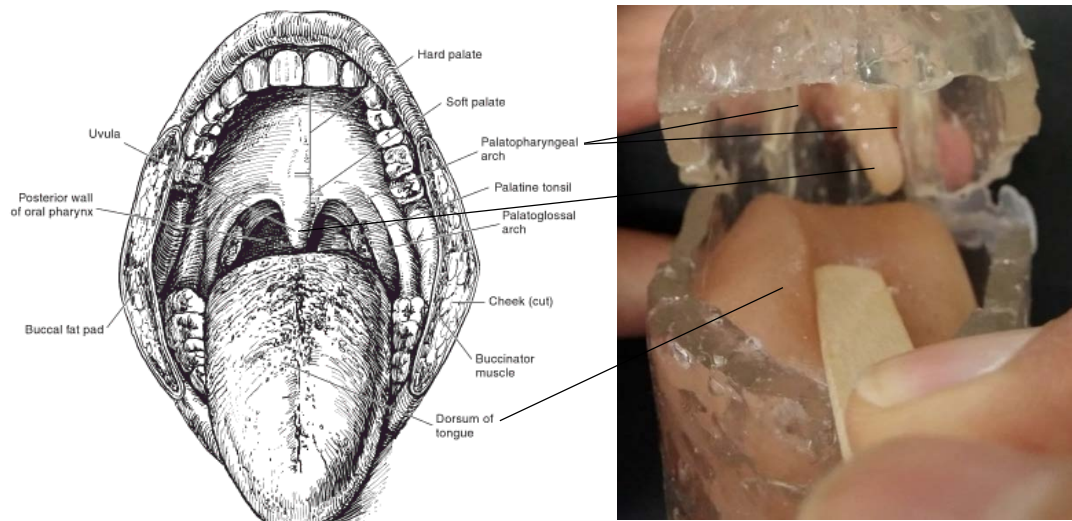
Firstly, the uvula at the posterior end of the oral cavity can be seen to hang down to approximately the same level as the upper surface of the tongue. While the length of the uvula can range from person to person, its distance from the tongue in the final model is accurate in that it does not extend past the level of the surface of the tongue, representing a regular healthy uvula.

Furthermore, the second important point lies at the attachment of the uvula to the model. *Figure 5-7 b* shows part of the roof of the oral cavity where the hard palate meets the soft palate. It is evident that there is a considerable gap on either side of the uvula between the uvula and the lateral walls of the oral cavity. This presents a lack of continuity between the upper edges of the uvula and the laterally-located pillars of the fauces, which is in contrast to what can be seen in scientific illustrations, where the soft palate merges with the lateral walls to form a completely enclosed surrounding, and the uvula emerges out of this surface (*figure 2-2*). One possible way to improve the final model is to ensure the gelatine-model of the uvula is wide at its superior end, and to merge it with the walls of the oral cavity in order to maintain realism and accuracy.

The third point worth noting is that when the mouth of the model is open, it is split at the sides as well as the front, given that it was very difficult to widely open just the anterior end of the oral cavity as would be done naturally if a subject was to open their mouths. Applied realistically, this is the equivalent of a split in the cheeks! This means that the movement of the mouth in the model was not very similar to that which would be found in real life. This problem could be addressed by including an elastic film of rubber on the sides so that when the mouth was to open and the sides were to split, the rubber would stretch and cover the sides, and if the mouth was to close the rubber would contract again. This would in effect simulate the insides of the cheeks. However, in providing this solution, it must be said that the rubber would need to also be transparent in order to view the insides of the oral cavity when viewed laterally.

Finally, the accuracy of the insides of the oral cavity may be compromised by the lack of some of the finer features related to the oral cavity, such as the teeth, the ribs on the roof of the mouth, and the two sets of pillars at the region of the fauces. Although, as mentioned before, while the palatoglossal arches may be absent, the shape of the palatopharyngeal arches was

still maintained in the model, and is situated accurately relative to the uvula and with respect to its general position within the oral cavity.



*Figure 6-3 Anterior view of oral cavity of final model alongside diagram from scientific literature [18] for comparison*

### 6.2.3. Pharynx

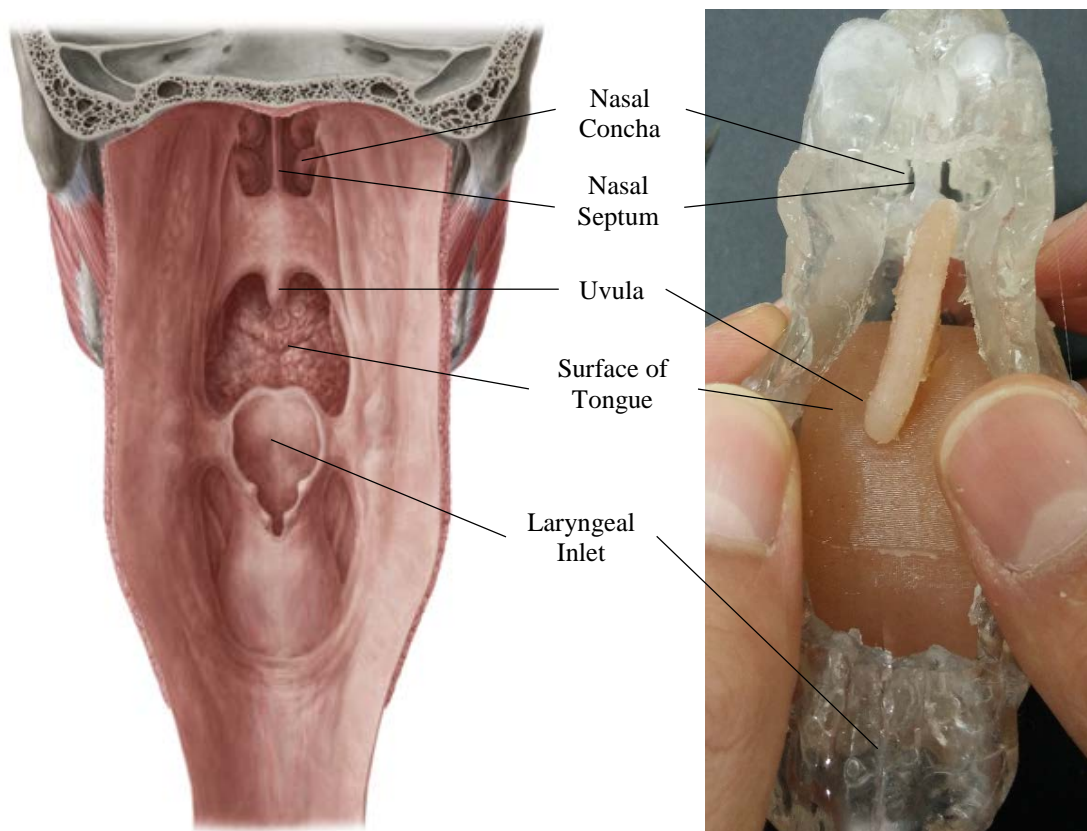
A posterior view of the final model opened at the pharynx (*figure 5-9*) provides the best picture of how the pharynx connects all these separate cavities at their posterior end, and how crucial it is as an intermediary between the separate cavities of the upper respiratory tract.

By comparing the pharynx of the developed model with an illustration of the pharynx found in literature (*figure 6-4*), it can be seen that not only is the developed model accurate in its connection with all the relevant major parts of the upper airway, but from this view all the same main features present in the other areas of the upper respiratory tract can also be identified. These include the conchae and nasal septum of the nasal cavity, the uvula, tongue, and palatopharyngeal arches of the oral cavity, and the inlet of the larynx as well the associated recesses; all of which can be identified by looking through the pharynx in the final model.

Two of the most obvious features not included in the final model, however, which make the model different to diagrams found in scientific literature, and which may also improve model accuracy, are once again the continuity of the soft palate with the lateral walls of the oral cavity, joining the superior end of the uvula with the pillars of the fauces (*see 6.2.2*), and the junction wherein the two different passageways of the gastrointestinal tract and the respiratory tract meet at the larynx, to divide and continue as the oesophagus and trachea, respectively.

Nevertheless, a part of the larynx is included in the final model, and the other passageway associated with the gastrointestinal tract lies outside the scope of this research.

One additional important feature found in the pharynx which also becomes easier to comprehend when seeing and manipulating the pharynx in the final model is its ease to collapse and become obstructed. The lack of thick tissue or support around the majority of the pharynx, combined with its relatively small lumen, makes it highly susceptible to occlusion.



*Figure 6-4 Posterior view of pharynx in final model alongside scientific diagram <sup>3</sup> for comparison*

#### **6.2.4. Larynx**

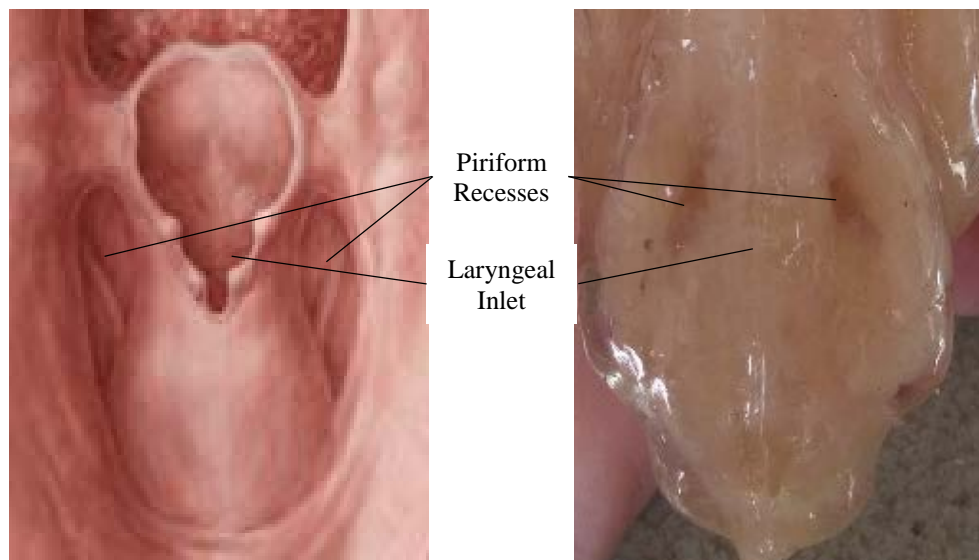
Given that it was not fully considered for the purpose of this research, the larynx itself was not included in the final model. However, the upper boundaries of the larynx at the inferior boundary of the pharynx was included in the final model and the effects of the geometry of that area can be seen in the air model of the upper airway (*figure 5-1 g*).

---

<sup>3</sup> <https://www.kenhub.com/en/library/anatomy/the-pharynx>

The most evident feature is of course the space making up the piriform recesses. Applying this shape as a core to achieve the final model, the two protrusions can be seen to extend across the walls of the lumen; a feature which can be compared with the recesses seen in the earlier diagram of the pharynx (*figure 2-3*). These two protrusions can be better viewed looking superiorly through the model from the bottom end (*figure 5-11*).

While this makes the shape of the inside of the respiratory tract accurate with respect to the obstacles encountered during air flow, two solid protrusions is unrealistic, as these are generally represented by empty space in a real airway, as seen in the following close up image showing this area within the airway (*figure 6-5*).



*Figure 6-5 The laryngeal end of the final model alongside a scientific illustration of the same region <sup>4</sup> for comparison*

### 6.2.5. Upper Airway Organs

The analysis of air flow in both the upright and the supine position showed the effects of the upper airway organs on fluid flow. The first, most obvious and anticipated difference between the airway model in the upright position and in the supine position is the shape of the tongue and uvula. When upright, the tongue seems to fill the inside surface of the inferior half of the oral cavity (*figure 5-16 a*), while when supine, the tongue falls slightly backwards in the posterior direction towards the oropharynx (this can be seen by the gap at the anterior surface of the tongue which becomes present when supine) (*figure 5-16 b*). Likewise, when upright, the uvula hangs downwards and almost rests on the superior surface of the tongue (*figure 5-*

<sup>4</sup> <https://www.kenhub.com/en/library/anatomy/the-pharynx>

16 a), while when supine, the uvula droops posteriorly, blocking the pharynx at the retropalatal region (*figure 5-16 b*).

#### **6.2.5.1. Accuracy and Suitability of Materials Used**

- Gelatine: While the elastic modulus value measured for the gelatine material (see 3.4.1) is considerably larger than the actual values observed for the tongue and uvula, which have been previously measured to be approximately 6,000 Pa and 12,400 Pa, respectively [161-163], it remains a much more realistic value to represent the tongue and uvula with than that observed by silicone rubber, a material used more commonly to represent organs and tissue, which can have a Young's modulus of at least approximately 1,000,000 Pa [164]. Even in comparing the values of properties exhibited by this gelatine material with other materials of similar nature used to model soft tissues, which were found to yield a Young's Modulus of up to 98,000 Pa [165], the gelatine material used in this research was a more fitting material to represent the tongue and uvula with, thus validating this material for use in this research.

- Latex: The latex material used to enclose the silly-putty was ideal as it was largely elastic, and given that only a thin film of latex was used, it was entirely deformable. Furthermore, even though the layer of latex was thin, this boundary was very tough and non-porous, making it ideal to hold the silly-putty inside while maintaining the overall shape of the tongue. Easier deformation can be established by coating with less layers of liquid latex, or more layers can be added if there is a desire to maintain the same shape more rigidly (this would be ideal in representing the human tongue when the subject is awake, given that the lack of loss in muscle tone would cause the tongue to be stiffer).

- Silly-putty: The use of the silly-putty served its purpose in allowing the thin film of latex to deform subject to the effects of gravity, providing a good representation of muscle when relaxed.

#### **6.2.5.2. The Tongue**

The property of the tongue, which is comprised of muscle allowing it to easily change shape, to be elastic yet tough in the final model (*figure 5-12*) is the same property exhibited by the tongue in living beings. At rest when upright, the tongue rests on the floor of the oral cavity, and so assumes its general shape. However, when placed supine, given that the attachment point of the tongue is at the base of the oral cavity, the tongue falls posteriorly towards the pharynx, partially blocking off the lumen at the retrolingual region.



When a person is asleep in the supine position, the loss of muscle tone in the tongue resulting from sleep means that the tongue essentially becomes just a ball of loose muscle, which is then weighed down by gravity to invade into the lumen of the pharynx.

The tongue was measured to be 56mm in length and 46mm in width. This is very similar in length but considerably different in height to the values measured by Malhotra, Huang [163], where the tongue is measured to be 60.6mm in length and 67.4mm in height for the average male, the demographic upon which the final model was based. The closeness in length makes the final tongue model an accurate representation, particularly when considering that the length of the tongue affects the degree of obstruction in the airway. However, with regards to the tongue width, a wider tongue should be considered for the purpose of accuracy, and as it would prevent air from travelling between the tongue and the lateral walls of the oral cavity.

### **6.2.5.3. The Uvula**

Unfortunately, while the model of the uvula itself may be accurate to a real uvula (which is merely composed of tissue), the surrounding muscles, which elevate the uvula and control its position in the oral cavity, can change its dimensions relative to the surrounding organs. And given that the model has no muscle to elevate the model uvula, it would not accurately represent that which would be seen when physically looking at a real uvula when upright. This is because it would be unlikely that the uvula would hang that low given that there would be no loss in muscle tone when upright, and thus the uvula would be slightly elevated. It is due to this reason that the accuracy of the model uvula in the upright position is difficult to gauge given that it is based on an uvula imaged during rest, and when a subject is in the upright position, it is unlikely that there is any loss in muscle tone as the subject would most likely be awake.

The uvulas' response in the supine position, however (when a subject is likely to be asleep), is somewhat accurate in how an uvula would hang posteriorly, partially blocking the pharynx at the retropalatal region.

The uvula part of the final model was measured to be 34mm in length and 5mm in width. Previous research by Reda, Sims [166] has had the average length of the entire soft palate measured at 24mm with the width of the uvula measured at 6.4mm for a healthy subject. In contrast to the comparison between the dimensions of the model tongue and the average tongue, the model of the uvula is similar in width, but not length, to the average uvula. The fact that the model uvula was considerably longer than the average uvula can lead to inaccurate results, given that it would hang closer to the dorsal surface of the tongue when upright, and closer to the posterior wall of the pharynx when supine. In increasing the

accuracy of the final model, it would be worth shortening the uvula in order to represent this organ more realistically. Furthermore, the length of this organ in previous research related to the length of the entire soft palate, which at its superior end encloses the superior border of the fauces region, and merges along the boundaries of the pillars of the fauces. However, once again, in the final model, this width wasn't extended across the entire fauces region, and the width of the uvula itself was considered standard across the entire length of the uvula, even though the average length indicated to in previous research was that of the entire soft palate, and the uvula itself was only measured at 10.2mm in length [166]. This can lead to large inaccuracies when observing the path of air flow during breathing, and in particular at a crucial area like the retropalatal space. The effects of this inaccuracy will later be observed when visualising air flow within the final model.

### **6.3. Validating Accuracy by Using Transparency**

Regarding transparency, the material itself used to make the final model was highly transparent, and thus provided the property necessary in viewing that which occurred within the upper airway model. However, certain areas were difficult to see into, such as the posterior third of the nasal cavity, as the uneven shape of the coating created irregularities on the surface of the core model before the final material had cured, which prevented absolute transparency. This problem can be fixed by ensuring an even coat around the entire model, which would lead to a smooth, clear appearance.

Nevertheless, the general behaviour of fluid flow within the upper airway could still be identified. Therefore, validating the accuracy of the developed model could be done by using its transparency property to physically observe air flow within the final model.

#### **6.3.1. Observed Behaviour of Air Flow during Closed-Mouth Testing**

The general behaviour of air flow within the model was interpreted and compared to the expected behaviour of fluid flow within the airways in order to validate accuracy (see 2.4.3.3).

##### **6.3.1.1. Inhalation**

Inhalation, encouraged by exerting a negative pressure at the laryngeal end of the pharynx, shows precisely how the geometry and associated structures at each different region play an

important role in fluid flow in the upper respiratory tract during respiration. Considering the aforementioned response of the upper airway organs with respect to posture, the effects on fluid flow can be understood by considering the rationale behind the main important points deduced from the previous experiments. During inhalation, these were the following:

- The general behaviour of fluid in the nasal cavity and, in particular, the transition of air flow from laminar to turbulent at the superior conchae
- The resistance to flow of air travelling through the nasopharynx and past the soft palate
- The flow rate of fluid through the nasopharynx and down the pharynx into the laryngopharynx
- The behaviour of air flow within the oral cavity, amount of air flow within the oral cavity, and the lack of flow at the anterior end

In the nasal cavity, the flow of air during inspiration in just this area alone shows how suited the nasal structure is to its' function and as a point of entrance for the body to receive air. The nose is structured in such a way that aids the path of air posteriorly towards the oropharynx, which holds true both while upright (*figure 5-18*) and supine (*figure 5-21*). In the developed model, the air travels through the nostrils and remains laminar throughout most of the nasal cavity, exhibiting properties of turbulence at the uppermost ridges where air collided with the superior boundaries of the nasal cavity (*figure 5-18 b & 5-21 a*), and turning turbulent only upon reaching the nasopharynx (*figure 5-18 c & 5-21 b*). This is similar to the behaviour of air flow seen in previous research [145], wherein air, once more eased towards the nasopharynx by the structure of the nasal cavity, was relatively laminar and streamlined throughout the nasal cavity, transitioning to turbulent at the nasopharyngeal region. One difference, however, is seen between that which was observed using the model and that which was observed in the research conducted by Subramaniam, Richardson [145]. This difference lies mainly in the laminar nature of air flow at the region of the nostrils in the final model (*figure 5-18 a & 5-21 a*), which could be due to the fact that tubes were connected at the nostrils during testing with the final model in order to transfer the visible smoke during inhalation (*see 4.5.2.1*), thus forcing the air travelling into the nasal cavity to remain laminar. This concept can be appreciated by looking at the equation for turbulence (*equation 2.10*). Reynolds number is considered a ratio of the inertial forces to the forces caused by the shear stresses (i.e. inertial forces : viscous forces), thus when air enters the nasal cavity through the tube, it enters with high inertial force, being streamlined straight into the cavity. Had the nostrils been open to the external environment during inhalation, as was the case in the compared research, the inhaled air would not enter the nasal cavity at an already steady flow, and thus a different reaction might have been observed.

Looking at the transition of air flow from laminar to turbulent at the nasopharynx, this behaviour, once again, can best be explained by looking back at the specific equation for Reynolds number (*equation 2.10*) (see 2.4.2.4). As the air entered through the area posterior to the narrow nostrils at a relatively high velocity, the “pipe diameter” value used in the equation for Reynolds number (i.e.  $d$  in the equation) is relatively small with the velocity being steady, thus laminar flow is maintained. Even though the area within which air flows slightly expands as air travels through the nasal cavity, the cavities remain narrow, preventing the air from transitioning to turbulent, except at the upper edge where the surface structure is irregular. However, once the air reaches the nasopharynx, the two cavities combine and open to the much wider nasopharyngeal region, and the value representing the “pipe diameter” in the equation for Reynolds number substantially increases, leading the air to become turbulent and lose its laminar formation. This transition to turbulence was also observed in the results obtained by Subramaniam, Richardson [145], where vortices are seen to form in this same area.

We can start to see some of the effects of posture on fluid flow by analysing the behaviour of the air travelling during inhalation from the nasopharynx into the oropharynx. When upright, air flows through the nasal cavity, past the nasopharynx, and into the oropharynx at a somewhat steady rate, before accelerating through the oropharynx and into the laryngopharynx (*figure 5-18 d*). However, when the model is placed in a supine position, air stagnated at the nasopharynx before proceeding into the oropharynx with what seemed like extra effort (*figure 5-21 b*). This is no doubt a result of the partial occlusion caused by the obstruction which is the uvula as it blocks a large part of the pharyngeal lumen at the retropalatal region. This shows precisely how an abnormally sized or abnormally functioning uvula can affect smooth fluid flow within the upper airway, indicating why the area of the retropalatal space is highly influential in the presence of OSA. This corresponds to the slight fluctuations in pressure forces also observed in this area in previous models analysed using computational fluid dynamics [152, 158].

After exiting the nasopharynx and passing the retropalatal space to enter the oropharynx, the air travelling through the pharynx all the way down to the laryngopharynx was seen to accelerate through this region (*figure 5-18 d & 5-21 c*) when compared to its rate of flow in the preceding regions. The acceleration through the oropharynx and into the laryngopharynx is similar to the spike in velocity observed in previous research at the area posterior to the oral cavity [152, 154], which is to be expected when considering the equation for volumetric flow rate (*equation 2.1*) (see 2.4.2.1.1), and recognising that, in applying the law of continuity (see 2.4.2.2), the flow would need to accelerate when passing from a tube of certain radius into a

tube of smaller radius. This illustrates the narrowness of the pharynx when compared to the other cavities of the respiratory tract. Considering Bernoulli's principle and the accompanying equation (*equation 2.9*) (*see 2.4.2.3*), and given that the fluid which is being considered is air and thus the  $gz$  term can be ignored, and after removing the constant in the equation, it can be rearranged to become  $\frac{v^2}{2} = -\frac{p}{\rho}$ , indicating that the pressure at a particular area is directly proportional to the velocity (i.e.  $p \propto v$ ). Thus given the increase in velocity observed at the oropharyngeal and retrolingual regions, if the pressure was to be measured at this area, a spike in pressure would be expected just as that which was observed in previous research [151, 152, 154]. This was in fact the case with regards to the observed results related to the changes in lumen width (*see 5.4*), which provides an indication of the changes in pressure at these regions (*figure 5-29 & 5-30*).

While the effects of the uvula during inhalation show how detrimental the uvula is on natural fluid flow in the respiratory tract, the main effects of posture, and the consequential response of the upper airway organs on air flow, are more prominent during inhalation when observing the effects of the tongue and the behaviour of fluid flow past the retrolingual space, from the oropharynx into the laryngopharynx. This is the same which can be seen in previous research, where the main fluctuations in pressure and largest velocity profiles are observed at the oropharynx-laryngopharynx region [151, 152, 154, 155, 158].

While upright, the air accelerates through the oropharyngeal region into the laryngopharynx with little resistance, with only some air spreading anteriorly into the oral cavity after the majority of air reaches the larynx. Moreover, air entering the oral cavity only extended approximately three-quarters of the distance across the surface of the tongue (*figure 5-18 d*). However, when placed in the supine position, the air entering the oropharynx split almost equally to fill both the retrolingual space and the oral cavity (*figure 5-21 c*). The air entering the oral cavity also continued to the area around the tip of the tongue (*figure 5-21 d*), in contrast to the shorter distance which the air travelled during inhalation when upright. This indicates more resistance found at the retrolingual space which would force air to circulate and travel anteriorly into the oral cavity. The source of this resistance without a doubt is the tongue, which blocked part of the lumen at the retrolingual space when supine. Furthermore, another important feature which would have aided in this observed result is the fact that the uvula hung posteriorly into the lumen of the pharynx instead of hanging across the oropharyngeal isthmus and blocking the air travelling through into the oral cavity as it might have done when upright. In comparing this with previous research, it is interesting to note that there is, in fact, no flow rate through the oral cavity [155]. While it is difficult to determine why this is the case, it is worth noting that in their research, Yu, Zhang [155] used CFD to obtain

their desired results, and so the oral cavity area might have been *virtually* subjected to the condition of no flow, negating the possibility of any flow within this area. This provides a clear indication of the importance of physical testing when analyzing the realistic behaviour of air flow within a system such as the respiratory system.

The fact that the tongue was more influential than the uvula in affecting fluid flow during inhalation can possibly be attributed to the shape of the upper airway organs, as well as their location with respect to the end at which the positive and negative pressures were induced. In the model, the uvula is seen to be slightly curved anteriorly when upright, and inferiorly when supine. This curve and the resultant space caused by such a shape could cause air travelling through the airway during inhalation to be met with less resistance than air travelling past the uvula during exhalation for example. Furthermore, the tongue is much closer than the uvula to the end of the airway at which negative pressure was induced, forcing the tongue to be pulled back further into the airways during inhalation due to the effects of the negative pressure, thus further decreasing the size of the lumen at the retrolingual region and inhibiting flow.

#### **6.3.1.2. Exhalation**

By exerting positive pressure at the laryngeal end of the pharynx, exhalation through the developed model of the upper respiratory tract not only shows the impact of posture on fluid flow, but it also highlights the difference between the effects during inhalation and exhalation of the upper airway organs. This further aids to validate the model by considering the important points resulting from the observations noted during the experiments involving exhalation in the final model, which were the following:

- The reluctance, or lack thereof, of air flow into the oral cavity
- The behaviour of fluid flow within the oral cavity itself
- The behaviour of air flow as it entered the nasopharynx from the oropharynx, and the behaviour of air within the nasal cavity

After passing through the laryngopharynx and up into the oropharynx, air can be seen to accelerate once again through the oropharynx (*figure 5-19 a & 5-22 a*), the reason behind which was described earlier. Almost instantly, the difference between inhalation and exhalation can be observed when looking at fluid flow behaviour. While during inhalation, the main obstruction was seen at the retrolingual space as air travelled inferiorly, during exhalation, the main effects on air flow can be seen at the retropalatal space, as air travelled superiorly into the nasopharynx.



While upright, air flowed quite rapidly throughout the pharynx with laminar flow to reach the nasopharynx (*figure 5-19 b*). Some of the air also crossed into the fauces region (*figure 5-19 a*), although the majority of air travelled into the oral cavity only once the air had reached the nostrils (*figure 5-19 c*), indicating a more resistant path which is no doubt not only influenced by the fact that the path from the laryngopharynx to the nostrils is clear during exhalation while upright, but it is also influenced by the uvula hanging across the isthmus of the fauces. The air can also be seen to travel further anteriorly when compared to its flow during upright inhalation (*figure 5-19 d*), but this is to be expected given that exhalation involved exerting a positive pressure and forcing the air into the upper respiratory tract, thus filling the empty cavities.

However, when supine, the air was seen to meet a lot of resistance at the area of the soft palate (*figure 5-22 a*), where the uvula partially hangs into the lumen of the pharynx. Air once again split to fill both the oral cavity and the nasopharynx (*figure 5-22 b*), just as that which was seen during supine inhalation. Furthermore, the air travelling into the oral cavity can be seen to extend further anteriorly into the oral cavity, past the tip of the tongue and further down towards the base of the tongue (*figure 5-22 d*). This can be attributed to the fact that there was a wider gap between the anterior tip of the tongue and the anterior wall of the oral cavity. However, the air travelled at a much faster pace as well, suggesting that this path of flow through the oral cavity now became the path of less resistance, indicating just how much resistance the uvula places at the retropalatal region, preventing air from travelling up into the nasopharynx during expiration. The additional force of air at the anterior end of the oral cavity may also explain why air sometimes leaks out of the mouth during exhalation when people snore! Comparing this to that which was observed in previous research once more [155], no air flow is measured in the oral cavity area due to the virtual application of a 0 flow condition at the oral outlet, once again demonstrating the importance of developing a realistic system wherein unexpected behaviour can be observed in order to better understand the nature of flow.

An investigation into the shape of the upper airway and its associated organs, as well as their relative positions along the airway, can once again be causes for why the uvula seems to have more of an effect on fluid flow during exhalation, and why the tongue still affects the flow of air in the airways even though it's effects are reduced when compared to its effects during inhalation. As mentioned previously, the shape of the uvula can lead to more resistance at the retropalatal space during exhalation. Moreover, with regards to the position of the upper airway organs along the respiratory tract, exhalation involves a positive pressure initiated at the laryngeal end of the upper airway, which, in contrast to what happens during inhalation,

would force the tongue to be pushed forward into the oral cavity, giving the uvula a larger role in affecting fluid flow in the upper airway.

An interesting point to note was the saturation of the nasal cavity with air before the oral cavity both while upright (*figure 5-19 c*) and supine (*figure 5-22 b*), even though the air had travelled more freely into the oral cavity. The reason behind this behaviour is undetermined. However, it may be due to the fact that the main path of air flow involved exiting through the nose, and as such the lack of an opening at the oral cavity prevented free air flow through that region.

### **6.3.2. Observed Behaviour of Air Flow during Open-Mouth Testing**

By introducing another point of entry and exit in the upper respiratory tract, the factors which influence fluid flow behavior during respiration can be better understood.

#### **6.3.2.1. Inhalation**

Inducing inhalation at the laryngeal end of the upper airway in the presence of another open path into the model served to provide a better understanding of the general flow of air within the upper airway. This was outlined by considering the following main points:

- The nature of air flow through the oral and nasal cavities
- The behaviour of air flow in the nasal cavity and oral cavity
- The behaviour of air flow throughout the rest of the model
- A comparison of air flow in the nasal and oral cavities at the same time

The first most obvious difference observed during inhalation in the presence of an open mouth is the entry of air through both the nose and the mouth (*figure 5-24 a & 5-27 a*). It is interesting to note that air entered the model through both entrances laminarly during both upright (*figure 5-24 a*) and supine (*figure 5-27 a*) inhalation, although it was suspected that air would become turbulent once entering the oral cavity in particular, due to the large expansion of space (this is once again related to the “pipe diameter” value in the turbulence equation (*equation 2.10*)). The reluctance of air to transition to turbulent upon entry into the oral cavity might be due to the fact that the air travelled through a tube in order to enter the oral cavity. Given that Reynolds number is a function of inertial force, the air would have entered the oral cavity with enough momentum to remain laminar. This same concept was observed earlier when viewing the air entering through the nostrils during closed-mouth inhalation (see 6.3.1.1). If the behaviour of air was captured entering the oral cavity past the lips through an

open mouth without a tube, turbulent behaviour might have been observed. This, however, is difficult to determine certainly without testing. The larger area of the oral cavity also meant that, overall, more air flowed through the oral cavity than through the nasal cavity; an observation which was especially true when supine (*figure 5-27 b*). This response when supine is no doubt the result of the occlusion of air at the retropalatal region due to the effects of the uvula, causing the negative pressure induced during inhalation to draw more air from the path of least resistance: through the oral cavity. This larger flow of air through the oral cavity is the same as that observed in previous research during nasal and oral inhalation [155].

What is of greater interest is the actual behaviour of air flow after entering the separate cavities. The biggest difference observed between closed-mouth and open-mouth inhalation at the nasal cavity region is the distribution of air within the empty spaces. During open-mouth inhalation, air only flowed throughout the inferior half of the nasal cavity at its posterior end (*figure 5-24 b & 5-27 c*), and the superior area of the nasopharynx didn't fill with air throughout the entire inhalation process when upright (*figure 5-24 d*). This indicates just how much negative pressure is lost at the nasal end in the presence of an open mouth, showing how the oral entry dominates the majority of air drawn due to, once again, the much larger space within this area (it is worth recalling that air filled the entire nasopharyngeal area during closed-mouth upright inhalation testing (see 5.3.1.1)). This lack of air flow in some parts of the nasal cavity during upright open-mouth inhalation was not seen during supine open-mouth inhalation, wherein the air, upon entering the nasal cavity, was drawn posteriorly not only due to the effects of the negative pressure of inhalation, but also due to the effects of gravity (*figure 5-27 d*). The observed filling of the entire nasal cavity with air while supine can also be a result of the partially blocked pharyngeal lumen at the retropalatal region, since air flowed through this region with greater difficulty, and so it would slightly build up at the nasopharynx. In fact, this concept is reinforced by the fact that some air still remained at the nasopharynx even as all the marked air in the tube attached to the oral cavity had been drawn (*figure 5-27 d*), showing the differences in pulling pressure between these two cavities. In saying this however, it is difficult to use this particular observation to validate the ratio of air drawn in the nasal and oral cavities, given that the *amount* of marked air during inhalation depended on the amount which was stored within the tubes prior to inducing inhalation, which might have differed due to the sizes of the tubes.

Looking at the oral cavity during inhalation in the upright position, the only point worth noting is the behaviour of the flow of air to cycle back towards the anterior end of the oral cavity (*figure 5-24 b*). This behaviour was not observed in the supine position (*figure 5-27 b*), and

thus it can be deduced that this effect was brought about by the blockage of air by the uvula hanging down towards the tongue and partially blocking the opening to the oropharynx, illustrating once again the effects the uvula can have on air flow.

The general behaviour of air flowing through the nasal and oral cavities is difficult to validate by looking at previous research, given that there is a lack of performed experimentation which indicate the specific air behaviour in all these areas at the same time, and the results obtained in previous research are largely based on numerical outcomes and general flow and velocity profiles. This idea provides further cause for using physical realistic models in order to observe behaviour which may not be accurate when simulated in a virtual environment. Nevertheless, in terms of comparing the overall flow of air, the results obtained by Yu, Zhang [155] show a clear reduction in air flow in the nasal cavity during nasal and oral breathing when compared to during nasal only breathing, and that the majority of air flow occurs through the mouth, further supporting that which was observed using the final model.

In the supine position, the drawing force of air in the oral cavity was, once again, much larger than that at the nasal cavity. The air entering through the oral cavity can be seen to reach the level of the uvula before it does so by the air entering through the nasal cavity (*figure 5-27 a*). At this point, some air can be seen to “leak” superiorly into the nasal cavity alongside the site at which the uvula was attached to the hard palate (*figure 5-27 b*). This design fault meant that the model uvula was so thin at the area where it was attached to the walls of the boundaries model that there existed unrealistic gaps on either side (*figure 5-7 b*), allowing air to transition between the two cavities at the level of the uvula without passing into any region of the pharynx.

While supine, even though it was the path of less resistance, air flowing through the oral cavity was still ultimately met with resistance due to the obstruction caused by the tongue, which fell posteriorly into the pharynx partly occluding the lumen at the retrolingual space. This led to the build-up of air observed in the oropharynx (*figure 5-27 d*) as less air was allowed through the retrolingual space. These results are similar to those which were obtained by Kleinstreuer and Zhang [153] when observing the deposition of particles in the upper airway, and they also correspond to the large velocity distributions captured in this area by Wang, Liu [152] and Yu, Zhang [155].

### **6.3.2.2. Exhalation**

The effects of positively forcing air through the model respiratory tract in the presence of an open mouth highlighted the main effects of constrictions at the retropalatal region even further. These can be seen by considering the following main points:

- The distribution of air into the nasal and oral cavities from the oropharynx
- The difference in flow rates in the oral and nasal cavities
- The behaviour of air flow in the oral and nasal cavities

During exhalation, it was interesting to note that there was no major resistance to air flow at the retrolingual region when subjected to both the upright (*figure 5-25 a*) and the supine (*figure 5-28 a*) positions. Previous research conducted by Yu, Zhang [155] in observing nasal and oral exhalation has also indicated high flow rates in the entire region of the pharynx with no specific area of exception. The retropalatal region, however, once again showed its detrimental effects on fluid flow.

During exhalation in both positions, air flowing through the oropharynx was seen to split almost evenly and begin to flow both superiorly into the nasopharynx as well as anteriorly into the oral cavity (*figure 5-25 a & 5-28 a*). However, in the upright position, air filled both cavities at approximately the same rate and exited at the same time (*figure 5-25 b*), whereas in the supine position, it could be seen that the air was met with resistance at the retropalatal region (*figure 5-28 a*), forcing much more air to flow at a faster rate through the oral cavity, an observation similar to that achieved by Yu, Zhang [155] during open mouth exhalation even without the effects of the obstruction of the uvula. The air flowing through the mouth extended past the tip of the tongue and towards the base of the tongue, even in the presence of an opening at the anterior end of the oral cavity (*figure 5-28 c*). The flow in this region can be contrasted to the flow in the nasal cavity where, when supine, the air can be seen to reach the tongue's anterior end before any real mass of air is seen to reach the nostrils of the nasal cavity (*figure 5-28 b*). The transfer of this large bulk of air through the oral cavity in particular is the result of two factors: one, the forced flow of air throughout the upper airway model due to the positive pressure induced at its inferior end, and two, the effects the uvula has on restricting the air from entering the nasopharyngeal region. This is also the reason the majority of the marked air is seen to exit the oral cavity while some still remained within the nasal cavity (*figure 5-28 d*).

Finally, the difference in the distribution of driving pressure throughout the oral and nasal cavities is once more reinforced by acknowledging that air barely saturated the nasal cavity, which can be recognised by a lack of air flow at the upper-ridge of the nasal cavity posterior to the nostrils while upright (*figure 5-25 b*), and the delayed filling of this region when supine (*figure 5-28 c*). This indicates a path of less resistance through the oral cavity. However, in evaluating this same concept, the obstruction at the retropalatal region when supine should have provided further cause to prevent air from filling the entire nasal cavity, and yet what was observed was that the marked air eventually saturated the nasal cavity when supine (*figure 5-*

28 d) but not when upright. This exceptional case might be explained by considering the same effects which were highlighted earlier during open-mouth inhalation: the effects of gravity on distributing the marked air within the cavities.

## **6.4. Investigating Effects of Respiration on Upper Airway Response**

Given that the amount of previous research conducted which involved measuring changes in the upper airway shape during respiration is very limited, it is very difficult to gauge the accuracy of the responses observed of the developed model walls during respiration. However, while it still wouldn't provide a definite indication of the accuracy of the chosen material with regards to representing the tissue of the upper respiratory tract, by measuring the changes in dimension of the different areas of the upper airway during respiration, and comparing them with the expected response of the upper airway walls, an indication of the distribution of pressure at the various areas can be achieved, and the flexibility of the material comprising the boundaries of the final upper airway model can be tested to confirm its suitability for accurate representation.

In presenting the results of the changes in lumen width of the upper airway model, the percentage increase and decrease in width with respect to the initial width was plotted in order to provide an indication of the extent to which each separate area was affected, and thus provide an idea of the response of the upper airway walls at each part of the upper airway when comparing respiration while upright and supine, and during inhalation and exhalation.

### **6.4.1. Response of Upper Airway Subject to Breath Cycle**

#### **6.4.1.1. During Inhalation**

*Figure 5-29* provides the most obvious indication of the effects of posture on airflow, and the resulting distribution of pressure in the upper respiratory tract.

As an overview, the general trend of upper airway wall displacement during inhalation in the supine position is almost identical to that which can be seen in the upright position. This indicates the consistent effects of the differences in lumen area on flow velocity and pressure, with the obvious difference being that more displacement can be seen by the walls in the supine position, which is to be expected given that the obstructions caused by maintaining the supine position would force a greater exerted effort induced by the negative pressure



gradient, leading to higher values of velocity and greater values in pressure (recall from the Law of Continuity equation (*equation 2.6*) that changes in upper airway lumen will lead to changes in velocity, and from Bernoulli's equation (*equation 2.9*) that velocity is proportional to pressure (*see also 2.4.3.3 for expected fluid behaviour in airways*)). This same concept is also likely to be the reason that the relative displacements measured at the oropharyngeal region are some of the largest given the narrow width of the lumen in this area. A deviation in the general trend can be observed, however, in the recorded wall displacements at the nasopharynx and at the retrolingual region.

When upright, the uvula hangs across the fauces region of the oral cavity, providing a somewhat obstruction-free path of air flow at the retropalatal region just past the nasopharynx and preventing restriction during inhalation. As such, no displacement is measured by the upper airway walls in either the nasopharynx or the retropalatal space posterior to the uvula. When supine, however, a large displacement in the airway walls can be seen at the nasopharynx (with respect to the initial size of this area), and a relatively smaller displacement can be seen at the retropalatal region (once again with respect to this regions' initial size). This indicates that, when supine, the uvula indeed plays a role in affecting airway patency, which can lead to variations in pressure during respiration at the areas surrounding the uvula. However, while the effects of the uvula remain significant, the biggest difference during inhalation can indeed be seen at the retrolingual area.

While upright, not a lot of change can be seen by the pharyngeal walls at the retrolingual region, and the largest percentage reduction in width can be seen at the oropharyngeal region. During supine inhalation, however, this observed trend is very different, and relative wall displacement is substantially larger in the retrolingual region not only when compared to relative wall displacement while upright, but also when compared to the relative displacements along the entire airway. This further expresses the negative effects of the tongue (and thus its potential for obstruction) on fluid flow in the upper airway in the supine position, and in particular during inhalation.

#### **6.4.1.2. During Exhalation**

A similarity in the general trend between upright and supine exhalation was once again seen with regards to the relative displacements of the upper airway walls from the laryngopharynx up to the oral cavity and oropharynx (*figure 5-29*). The results, however, differ largely as the relative displacements of the airway walls are measured superior to the oropharyngeal area. Unlike that which was observed during inhalation, the larger displacements are measured while upright and not when supine at the section of the nasopharynx down to the oropharynx.

In order to interpret this, it is worth considering what was discussed earlier with regards to the behaviour of air flow during closed-mouth breathing (see 6.3.1.2). It was discovered earlier that the obstruction at the retropalatal space appears to have a larger influence during exhalation in general than the obstruction at the retrolingual space (although the obstruction at the retrolingual region was still present during both inhalation and exhalation). With that in mind, if exhalation is brought about by applying a positive pressure at the laryngeal end (just as that which occurs during breathing in living beings), and the retropalatal space is a site of occlusion (which is the case when supine), then it would stand to reason that larger displacements would be observed when supine than those which would be observed while upright from the section of the laryngopharynx to the area of the retropalatal space. With the exception of the displacements recorded at the oropharynx, this expected trend is precisely what was observed (*figure 5-29*). On the other hand, when no obstruction is present between the oropharynx and the nasopharynx, air flows freely up to the nasopharynx and out through the nostrils, causing larger values to be measured for the percentage increase in lumen width at the superior end of the upper airway when upright. Moreover, the highest relative displacements can once again be seen at the area of the oropharynx. However, given the aforementioned behaviour, a larger displacement should have been observed at the oropharynx in the supine position than that which was measured when upright. Because there is no clear explanation for why this was not the case, this could possibly be due to errors in measurement at this area.

In considering the observed trend for exhalation and given that, as seen earlier, obstructions at the retrolingual end play a larger role during inhalation, the same trend would be expected (*figure 5-29*) in that larger displacements should be observed at one end of the graph during inhalation when comparing the values measured when upright with the values measured when supine. While the reason why this was not the case remains unclear, it is important to consider that, just as in the case with exhalation, inhalation is also induced at the end of the larynx, and the main contributor to airway obstruction during inhalation is the tongue, with the most influential area of obstruction being the retrolingual space. Thus the fact that this area was much closer to the source of the negative pressure in the model could have had a crucial effect on the dynamic response of the upper airway to breathing when comparing inhalation and exhalation.

## 6.4.2. Response of Upper Airway Subject to Posture

### 6.4.2.1. While Upright

The results observed in *figure 5-30* for respiration when upright are relatively ordinary. Given that there were no obstructions present in the pharyngeal lumen, the general trend is the same during both inhalation and exhalation, with the peaks and troughs providing an indication to the differences in pressure at the separate areas of the upper airway. Nevertheless, it is important to recall that the values plotted for wall displacements are relative to original size, and so provide an indication of the degree to which each area was affected by the flow of air during respiration.

The measured changes in displacement at the walls of the oral cavity, which were relatively small, were consistent during both inhalation and exhalation given that an obstruction-free path of air was present while upright, which allowed air to enter and exit the airway through the nose without the need for the majority of air to travel anteriorly into the oral cavity. Moreover, the uvula extending across the oropharyngeal isthmus led to the possibility of a greater path of resistance being established at the fauces region, further supporting the behaviour of air which was observed previously during closed-mouth breathing (see 6.3.1).

The greater relative displacements of the airway walls observed during exhalation can be attributed to the same reason which was mentioned in the previous sub-chapter (see 6.3.1.2), wherein air was seen to flow anteriorly to the tip of the oral cavity during exhalation in contrast to only flowing approximately three-quarters of the way anteriorly during inhalation (see 5.3.1.1). This was the result of the forced exertion of air through the airways compared to the induced negative pressure causing air to be pulled from the atmosphere. It is also important to recall that the measured flow rate during inhalation was less than the flow rate measured during exhalation (see 4.5.3), which is also likely to be the reason why displacements were seen at the laryngopharynx during exhalation.

### 6.4.2.2. While Supine

The graph from *figure 5-30* really shows the effects of the upper airway organs on airflow, and in particular contrasts the different effects of the uvula and the tongue during exhalation and inhalation. The response of the upper airway model walls to respiration at the oropharyngeal and oral cavity regions were relatively similar, while the main differences can be noted at the retropalatal and retrolingual regions. As such, only the response of the model at these two regions will be evaluated.

During exhalation, it can be seen that a larger proportion of overall wall displacement was measured at the retropalatal region when compared to that which was measured during inhalation, although the difference is not very large (a difference of 3.3% in the change of lumen width). This further validates the fact that, while both the uvula and the tongue play a role in obstructing the upper airway, the uvula plays a larger role during exhalation in particular. This could also be the reason why a larger relative wall displacement value was measured at the nasopharynx during inhalation, since the uvula blocked air flow during exhalation thus preventing large pressures from impacting the area of the nasopharynx.

Evaluating the observed results for the changes in lumen width measured at the retrolingual area makes the effects of the tongue on inhalation in particular very obvious. Not only does the tongue play a more important role in obstruction during inhalation, which agrees with the same results obtained in previous research [151, 152, 154, 155, 158], but the difference in the percentage change in lumen width between inhalation and exhalation is relatively large (a difference of 10.9% in the change of lumen width) when compared to the difference observed between inhalation and exhalation at the retropalatal region. Furthermore, the largest relative wall displacements can be seen at the retrolingual space during inhalation, and not at the narrower oropharynx, as observed previously with all other results.

The large and varied changes of relative lumen size during inhalation while supine, in contrast to the more steady changes observed during exhalation, also provides a better understanding as to why more prominent and distinct snoring sounds can more often be heard during the inhalation component of the breath cycle when a sleeping subject snores.

## **6.5. Limitations**

This research provides a good indication of how complex and precise the human body is for its function. Even though a lot of steps were undertaken in order to maintain consistent geometry and characteristics, there still remains a lot of limitations with regards to the current developed model, both for use in further research and in its accuracy in representing the upper respiratory tract. The realization that, after all that was considered, only one part of one system in one area of the body is being researched proves just how intricate the human body and its function is!

One large criticism to be made of the final developed model which was mentioned previously is the fact the uvula, or the soft palate in general, did not merge at its sides with the rest of the oral cavity (*figure 6-3*). This meant that air could “leak” from the nasal cavity alongside the

uvula into the oral cavity, and vice versa, without having to enter the pharynx, which was in fact the case when observing air flow during experimentation (see 6.3.2.1). The final model could be made more accurate by reshaping the soft palate to allow it to merge with the roof of the oral cavity.

One of the first and most evident drawbacks of modelling any particular organ is that, in the more specific sense, no two organs are exactly the same in terms of shape and size, and the same organ would slightly differ from person to person. This would mean that any model developed may be applied to a single particular individual (such as is the case in this research), but may not provide the exact same results when applied to another individual. Therefore, all the model can provide is a general indication of what would occur when the organ is subjected to the conditions introduced in this research. The best way in which this issue could be addressed is by using standardized models to represent the average organ shape in humans. Research has already been undertaken which involves obtaining average values for the dimensions of specific organs in order to present a model of the ideally shaped organ. This has been done, for example, to model the nasal cavity [167] and the pharynx [168]. Thus in the future, modelling using the same process as that presented in this research can involve adapting the final model to use such standardized models in order to model the “ideal” organ which would better act as a standard representation for any given healthy individual. This would mean that the results obtained by conducting experiments on this model would be more relevant in a general sense to any particular given subject. With that mentioned, however, it is important to note that the final model developed in this research was based on a healthy airway, and so although the model could be used to get an idea of generic air flow and organ response in the upper airway, utilising such a model in order to observe the reaction of the upper airway in the presence of diseases such as OSA may not produce the most accurate results, given that the presence of diseases in the upper airway is usually an indication of an unhealthy and irregular airway.

Most of the more obvious limitations in the model were related to its representation of the upper airway. Firstly, in considering the organs modelled which were associated with the upper airway (namely the tongue and the uvula), one obvious limitation in the model is the fact that, with the exception of slight deformations, the shapes of these organs is fixed. This means that the uvula and the tongue hold a specific contour within the upper respiratory tract without the option of changing the shape. This is not the case in reality, where the effects of nerve activity controls the activity of muscles which govern the positions and movements of the soft palate and the tongue during wakefulness and sleep. Having mentioned that, not a lot of muscle movement occurs during sleep, which was the state relevant to this research, and

so accuracy in modelling could still be attained by selecting the right material which would correspond to the composition of these organs subject to different states. The different shapes in which the organs can be found in could then be imitated so that experimentation using these different configurations would yield the results associated with the desired variation in shape. However, nothing short of using the real material would provide the exact desired properties. Thus one way in which modelling could be improved is by in fact using real organs. The tongue, for example, could be obtained by using a real animal tongue laser cut and adapted to the desired realistic shape.

Also related to the tongue shape, one further method which may have an effect on accuracy is the fact that the model tongue was scaled down to 0.9 times the size of the real tongue, so that it may have room to deflect and deform within the model (see 3.4.2). Although it maintained the same geometry, this meant that the model of the tongue used in the final complete model was not a replica of the regular tongue imaged from the subject. In having a real tongue to model the tongue in the final model, scaling down would not be required.

Looking at a related limitation concerning the overall airway, one of the biggest problems in modelling an organ system is the inclusion of all the relevant organs. One such group of organs is crucial in upper airway function and even shape: the muscles. Aside from omitting entire muscle tissue, and thus structures comprised of muscle (such as the hyoid muscle), from the upper airway model, the *support* maintained by the muscles surrounding the upper airway was also omitted from the final model. This contrasts with some mathematical models which were designed to represent the function of the upper airway and have indeed included the support of the surrounding muscle tissue in their research [149].

Furthermore, aside from affecting the accuracy in the *geometry* of the final model, the omission of muscles also meant that their effects were not included in the final complete model, even though the effects of these muscles in upper airway function and patency is one of the most crucial and contributing factors leading to the presence of diseases such as OSA (see 2.3.1.2). Just like the tongue, muscle tone surrounding the upper airway changes depending on the state of a subject, and so while the final model remained flexible, the lack of change in the stiffness of the material meant that the response of the model to the very changes which bring about diseases such as OSA were not entirely measured accurately. This problem may be mitigated by using a material whose stiffness is affected by the application of heat or an electric current. In this way, its property of stiffness could be controlled to represent the changes in muscle tone depending on the subject's state of wakefulness. However, the material would still need to be transparent if visualisation was to be achieved.



Another set of tissues associated with the upper respiratory tract omitted from the final model which may be involved with the presence, or lack thereof, of OSA are the adenoids. The presence of enlarged adenoids has been found to influence the existence of sleep apnea syndromes and particularly in infants [169, 170]. While this research is mainly focused on the upper airway of adults, the presence of such influential organs would only serve to further increase the accuracy of the developed model, and could be considered for future research.

In addition to the omission of muscles and adenoids in the final model, another important feature associated with the upper respiratory tract which was not included in the final model is the nature of the tissue lining the upper respiratory tract. This is important given that some research has found that the surface tension created by the tissue lining the upper airway during negative intraluminal pressures while breathing (see 2.3.1.2) does in fact play a role in the factors which bring about OSA [171, 172]. Therefore, even active simulation of OSA in the final developed model would still not provide a complete representation of all the forces involved in the presence of OSA. With that being said, simulating the actual tissue within the model while maintaining transparency is an almost impossible task with the regular materials which were used to develop the final model, and more research would need to be conducted in order to find either a transparent material which exhibits the same surface properties as that of the upper airway tissue, or a coating which could be used on the insides of the final model which would still keep the model transparent.

## 6.6. Future Research

The development of an accurate, physical, flexible, transparent model of the upper airway can lead to countless research possibilities when measuring air flow in the upper respiratory tract under various circumstances. The inclusion of these properties in the final model means that different situations and conditions can be applied to the model in order to physically view their effects on fluid flow and respiration in real time. Some ideas for these variations in testing include:

- Enveloping the pharynx in a thick, viscous liquid or high air pressure in order to represent the presence of a thicker neck, in effect simulating fat and thus observing the effects of obesity on respiration
- Observing respiration in the model after lodging particles into the lumen of the airway at different areas to observe the effects of obstructions caused by foreign particles, and how this may affect air flow depending on the area at which the obstruction occurs

- Observing respiration in the model while pinching different areas of the upper respiratory tract in order to observe the effects of partial or full occlusions on fluid flow in the airways, and how these effects may vary depending on the area of occlusion
- Subjecting the model to twisting, bending, and other forms of deformations, and subsequently analysing fluid flow in the upper airway in order to observe the effects of awkward sleeping positions and bad posture on efficient respiration
- Using different sized models for the tongue and uvula in order to observe the effects of abnormal upper airway organs on breathing
- Varying the parameters of breathing in order to study the effects these may have on the response of the upper airway and the associated organs
- Running the breathing simulation and dyeing the air in front of the nasal and oral cavities in order to observe the nature inhalation and uptake of air in these regions
- Running similar experiments in the recovery position to measure any changes in upper airway and organ response during respiration

In addition to undergoing testing using only the upper respiratory tract, this model can be expanded by combining it with other models to simulate the entire respiratory system. For example, the breathing simulator can include a casted model of the branches and features of the lung in order to accurately represent the lower respiratory tract, which would then be connected to the inferior end of the model of the upper respiratory tract. This would produce an entire system accurately representing the respiratory system, no doubt increasing experimentation accuracy, as well as widening the range of possibilities in including influential factors which could bring about a larger variety of diseases and disorders.

Finally, in the case where the purpose of research is to analyse fluid flow, it is recommended that a more obvious methodology be used in order to visualise air flow within the model. The use of a coloured dye in a stream of air running throughout the model would provide a good visualisation of the streamlines associated with fluid flow in the airway during respiration. Even dyed liquid could be used and forced throughout the airway to measure fluid flow within the specific geometry of the upper respiratory tract. However, in doing so, a different material would be needed for the uvula, given that the gelatine material used was water-soluble!

## 6.7. Summary

By evaluating the final developed model of the upper respiratory tract, and comparing the results attained through its use with those which were expected by looking at known physical

laws and the results of previous research, the efficacy of using the developed model as a transparent representation of the upper airway was validated, and the limitations of this model, as well as its possible uses for future research, were outlined.

## Chapter 7 - CONCLUSION

The purpose of this research was to develop an accurate, transparent, flexible model of the upper airway along with the related organs and associated respiration system so that it may be used for future research in order to physically observe the flow of air within the upper respiratory tract under desired, controllable conditions, while providing the freedom of altering the upper airway in order to represent a variety of real-life scenarios, in effect measuring their effects on air flow, and using the obtained results to better understand conditions such as obstructive sleep apnea in order to find better methods of treatment.

A final model of the upper airway was developed, along with the associated organs, which is almost entirely transparent, and holds the precise accurate shape of an upper respiratory tract in each part of the organ. It is flexible enough to be manipulated so that it may both represent the flexible properties of the surrounding tissue of the upper airway, as well as provide the freedom of being altered for further research. Furthermore, a breath cycle characteristic of that belonging to normal, steady human breathing was successfully simulated and combined with the model in order to establish a complete system of respiration involving the upper respiratory tract.

The system was then validated by analysing fluid flow within this system and comparing the results to those derived through previous research and in other literature. It was found that air flow within the developed model, and the response of the model wall to the air flow, behaved just as it would have been expected to in a normal respiratory tract, according to other literature and by analysing the flow of fluids in the context of their governing laws. Furthermore, the effects of posture and obstructions on fluid flow within the airways as a result of the response of the associated organs to different postures yielded similar results to those discovered previously. More specifically, in the supine position, the tongue had a large influence on air flow during inhalation as the air was forced through the partially occluded lumen at the retrolingual region, while during exhalation, even though the tongue still played an important role in occluding the airway, the uvula presented the biggest problem by partially occluding the pharyngeal lumen at the retropalatal region.

## REFERENCES

1. Olsen, B.D., *Understanding Human Anatomy Through Evolution - Second Edition*. 2009: Bruce D. Olsen. 232.
2. Wood, A.W., *Physiology, Biophysics, and Biomedical Engineering*. 2012: Taylor & Francis Group.
3. Rogers, K., *The Respiratory System*. 2010: Britannica Educational Pub.
4. Lepore, M., R. Anolik, and M. Glick, *Diseases of the respiratory tract*. Burket's Oral Medicine, Diagnosis and Treatment, 10th ed. Hamilton, BC Decker Inc, 2003: p. 341-348.
5. Karci, E., Y.S. Dogrusoz, and T. Ciloglu. *Detection of post apnea sounds and apnea periods from sleep sounds*. in *Engineering in Medicine and Biology Society, EMBC, 2011 Annual International Conference of the IEEE*. 2011.
6. Munson, B.R., et al., *Fundamentals of fluid mechanics*. 2009: Wiley.
7. Pierce, R.J. and C.J. Worsnop, *Upper Airway Function and Dysfunction in Respiration*. Clinical and Experimental Pharmacology and Physiology, 1999. **26**(1): p. 1-10.
8. Sahin-Yilmaz, A. and R.M. Naclerio, *Anatomy and Physiology of the Upper Airway*. Proceedings of the American Thoracic Society, 2011. **8**(1): p. 31-39.
9. Sériès, F., *Upper airway muscles awake and asleep*. Sleep Medicine Reviews, 2002. **6**(3): p. 229-242.
10. Whittemore, S., *The Respiratory System*. 2009: Chelsea House. 110.
11. Weaker, F., *Structures of the Head and Neck*. 2013: F. A. Davis Company.
12. Rosdahl, C.B. and M.T. Kowalski, *Textbook of Basic Nursing*. 2008: Lippincott Williams & Wilkins.
13. Schlossberg, L. and G.D. Zuidema, *The Johns Hopkins Atlas of Human Functional Anatomy*. 1997: John Hopkins University Press.
14. Netter, F.H., *Atlas of Human Anatomy*. 2014: Elsevier Health Sciences. 66.
15. Finucane, B.T., B.C.H. Tsui, and A.H. Santora, *Principles of Airway Management*. 2011: Springer New York. 742.
16. Schünke, M., et al., *Thieme Atlas of Anatomy: Head and Neuroanatomy*. 2007: Thieme.
17. Waugh, A. and A. Grant, *Ross & Wilson Anatomy and Physiology in Health and Illness*. 2014: Elsevier Health Sciences UK.
18. Clemente, C.D., *Clemente's Anatomy Dissector: Guides to Individual Dissections in Human Anatomy with Brief Relevant Clinical Notes*. 2010: Wolters Kluwer/Lippincott Williams & Wilkins Health.
19. Kumar, A.M., *Anand's Human Anatomy for Dental Students*. 2012: Jaypee Brothers, Medical Publishers.
20. Fritsch, H. and W. Kuehnel, *Color Atlas of Human Anatomy*. 2011: Thieme. 456.
21. Van De Water, T.R. and H. Staecker, *Otolaryngology: Basic Science and Clinical Review*. 2011: Thieme.
22. McMinn, R.M.H., *Last's Anatomy: Regional and Applied*. 2003: Elsevier Australia.
23. Schünke, M., et al., *Atlas of Anatomy: Neck and Internal Organs*. 2006: Thieme.
24. Gaga, M., A. Vignola, and P. Chanez, *Upper and lower airways: similarities and differences*. European Respiratory Monograph, 2001. **6**: p. 1-15.
25. Michael, J. and S. Sircar, *Fundamentals of Medical Physiology*. 2010: Thieme New York.
26. Katz, I.M., B.M. Davis, and T.B. Martonen, *A numerical study of particle motion within the human larynx and trachea*. Journal of Aerosol Science, 1999. **30**(2): p. 173-183.
27. Martonen, T.B., Z. Zhang, and R.C. Lessmann, *Fluid Dynamics of the Human Larynx and Upper Tracheobronchial Airways*. Aerosol Science and Technology, 1993. **19**(2): p. 133-156.
28. Lee, C.H., et al., *An investigation of upper airway changes associated with mandibular advancement device using sleep videofluoroscopy in patients with obstructive sleep apnea*. Archives of Otolaryngology–Head & Neck Surgery, 2009. **135**(9): p. 910-914.
29. Sher, A.E., *Upper airway surgery for obstructive sleep apnea*. Sleep Medicine Reviews, 2002. **6**(3): p. 195-212.
30. Wilkins, L.W., *Anatomy and Physiology Made Incredibly Easy!* 2009: Wolters Kluwer Health/Lippincott Williams & Wilkins.
31. Fujimura, Y., *Evidence of M cells as portals of entry for antigens in the nasopharyngeal lymphoid tissue of humans*. Virchows Archiv, 2000. **436**(6): p. 560-566.

32. Holgate, S.T., *The airway epithelium is central to the pathogenesis of asthma*. Allergology International, 2008. **57**(1): p. 1-10.
33. Kim, D.Y., et al., *The airway antigen sampling system: Respiratory M cells as an alternative gateway for inhaled antigens*. Journal of Immunology, 2011. **186**(7): p. 4253-4262.
34. Kojima, T., et al., *Regulation of Tight Junctions in Upper Airway Epithelium*. BioMed Research International, 2012. **2013**: p. 11.
35. Nawijn, M.C., et al., *E-cadherin: Gatekeeper of airway mucosa and allergic sensitization*. Trends in Immunology, 2011. **32**(6): p. 248-255.
36. Takano, K.I., et al., *Expression of tight junction proteins in epithelium including Ck20-positive M-like cells of human adenoids in vivo and in vitro*. Journal of Molecular Histology, 2008. **39**(3): p. 265-273.
37. Holgate, S.T., *Epithelium dysfunction in asthma*. Journal of Allergy and Clinical Immunology, 2007. **120**(6): p. 1233-1244.
38. Schleimer, R.P., et al., *Epithelium: At the interface of innate and adaptive immune responses*. Journal of Allergy and Clinical Immunology, 2007. **120**(6): p. 1279-1284.
39. Verin, E., et al., *Comparison between anatomy and resistance of upper airway in normal subjects, snorers and OSAS patients*. Respiration Physiology, 2002. **129**(3): p. 335-343.
40. Ayappa, I. and D.M. Rapoport, *The upper airway in sleep: physiology of the pharynx*. Sleep Medicine Reviews, 2003. **7**(1): p. 9-33.
41. Fouke, J.M., J.P. Teeter, and K.P. Strohl, *Pressure-volume behavior of the upper airway*. Journal of Applied Physiology, 1986. **61**(3): p. 912-918.
42. Strohl, K.P. and J.M. Fouke, *Dilating forces on the upper airway of anesthetized dogs*. Journal of Applied Physiology, 1985. **58**(2): p. 452-458.
43. Schwab, R.J., et al., *Upper airway and soft tissue anatomy in normal subjects and patients with sleep-disordered breathing. Significance of the lateral pharyngeal walls*. American Journal of Respiratory and Critical Care Medicine, 1995. **152**(5): p. 1673-1689.
44. Fritsch, H., et al., *Color Atlas and Textbook of Human Anatomy*. 2008: Thieme.
45. Sieck, G.C. and H.M. Gransee, *Respiratory Muscles: Structure, Function, and Regulation*. 2012: Morgan & Claypool.
46. Gea, J., et al., *Respiratory diseases and muscle dysfunction*. Expert Review of Respiratory Medicine, 2012. **6**(1): p. 75-90.
47. Sanders, M.H., R.J. Givelber, and T. Lee-Chiong, *Overview of obstructive sleep apnea in adults*. Sleep: A comprehensive handbook, 2006: p. 231-240.
48. Torpy, J.M., C. Lynn, and R.M. Golub, *Sleep Apnea*. JAMA, 2011. **305**(9): p. 956-956.
49. Heatley, E.M., et al., *Obstructive sleep apnoea in adults: A common chronic condition in need of a comprehensive chronic condition management approach*. Sleep Medicine Reviews, 2012(0).
50. Young, T., P.E. Peppard, and D.J. Gottlieb, *Epidemiology of Obstructive Sleep Apnea: A Population Health Perspective*. American Journal of Respiratory and Critical Care Medicine, 2002. **165**(9): p. 1217-1239.
51. Beck, R., et al., *The Acoustic Properties of Snores*. European Respiratory Journal, 1995. **8**(12): p. 2120-2128.
52. Stoohs, R. and C. Guilleminault, *Snoring during NREM sleep: respiratory timing, esophageal pressure and EEG arousal*. Respiration physiology, 1991. **85**(2): p. 151-167.
53. Skatrud, J.B. and J.A. Dempsey, *Airway resistance and respiratory muscle function in snorers during NREM sleep*. Journal of Applied Physiology, 1985. **59**(2): p. 328-335.
54. Gleadhill, I.C., et al., *Upper airway collapsibility in snorers and in patients with obstructive hypopnea and apnea*. American Review of Respiratory Disease, 1991. **143**(6): p. 1300-1303.
55. Liistro, G., et al., *Pattern of snoring in obstructive sleep apnea patients and in heavy snorers*. Sleep, 1991. **14**(6): p. 517-525.
56. Gottlieb, D.J., et al., *Does Snoring Predict Sleepiness Independently of Apnea and Hypopnea Frequency?* American Journal of Respiratory and Critical Care Medicine, 2000. **162**(4): p. 1512-1517.
57. Vries, N.d., M. Ravesloot, and J.P.V. Maanen, *Positional Therapy in Obstructive Sleep Apnea*. 2015: Springer International Publishing.
58. Mannino, D.M., et al., *Chronic obstructive pulmonary disease surveillance---United States, 1971--2000*. Respiratory care, 2002. **76**(10): p. 1184-1199.
59. Lindberg, A., et al., *Prevalence of Chronic Obstructive Pulmonary Disease according to BTS, ERS, GOLD and ATS Criteria in Relation to Doctor's Diagnosis, Symptoms, Age, Gender, and Smoking Habits*. Respiration, 2005. **72**(5): p. 471-479.
60. Von Mutius, E., et al., *Prevalence of asthma and atopy in two areas of West and East Germany*. American Journal of Respiratory and Critical Care Medicine, 1994. **149**(2): p. 358-364.



61. Huang, R., et al., *Respiration Simulation of Human Upper Airway for Analysis of Obstructive Sleep Apnea Syndrome*, in *Life System Modeling and Intelligent Computing*. 2010, Springer Berlin Heidelberg. p. 588-596.
62. Verwimp, J., L. Ameye, and M. Bruyneel, *Correlation between sleep parameters, physical activity and quality of life in somnolent moderate to severe obstructive sleep apnea adult patients*. *Sleep and Breathing*, 2013: p. 1-8.
63. Gay, P.C. and P.A. Selecky, *Are Sleep Studies Appropriately Done in the Home?* *Respiratory Care*, 2010. **55**(1): p. 66-75.
64. Kryger, M.H., T. Roth, and W.C. Dement, *Principles and Practice of Sleep Medicine: Expert Consult Premium Edition - Enhanced Online Features*. 2010: Elsevier Health Sciences.
65. Jafari, B. and V. Mohsenin, *Polysomnography*. *Clinics in chest medicine*, 2010. **31**(2): p. 287-297.
66. Berry, R.B., et al., *Portable monitoring and autotitration versus polysomnography for the diagnosis and treatment of sleep apnea*. *Sleep*, 2008. **31**(10): p. 1423.
67. Mulgrew, A.T., et al., *Diagnosis and Initial Management of Obstructive Sleep Apnea without Polysomnography A Randomized Validation Study*. *Annals of Internal Medicine*, 2007. **146**(3): p. 157-166.
68. Whitelaw, W.A., R.F. Brant, and W.W. Flemons, *Clinical Usefulness of Home Oximetry Compared with Polysomnography for Assessment of Sleep Apnea*. *American Journal of Respiratory and Critical Care Medicine*, 2005. **171**(2): p. 188-193.
69. Collop, N.A., *Portable Monitoring*. *Sleep Medicine Clinics*, 2009. **4**(3): p. 435-442.
70. Remmers, J.E., E.K. Sauerland, and A.M. Anch, *Pathogenesis of upper airway occlusion during sleep*. *Journal of Applied Physiology*, 1978. **44**(6): p. 931-938.
71. Woodson, B.T. and R. Franco, *Physiology of sleep disordered breathing*. *Otolaryngologic Clinics of North America*, 2007. **40**(4): p. 691-711.
72. Mathew, O.P., Y.K. Abu-Osba, and B.T. Thach, *Influence of upper airway pressure changes on genioglossus muscle respiratory activity*. *Journal of Applied Physiology*, 1982. **52**(2): p. 438-444.
73. Trudo, F.J., et al., *State-related Changes in Upper Airway Caliber and Surrounding Soft-Tissue Structures in Normal Subjects*. *American Journal of Respiratory and Critical Care Medicine*, 1998. **158**(4): p. 1259-1270.
74. Susarla, S.M., et al., *Biomechanics of the upper airway: Changing concepts in the pathogenesis of obstructive sleep apnea*. *International Journal of Oral and Maxillofacial Surgery*, 2010. **39**(12): p. 1149-1159.
75. Hudgel, D.W., et al., *Instability of ventilatory control in patients with obstructive sleep apnea*. *American Journal of Respiratory and Critical Care Medicine*, 1998. **158**(4): p. 1142-1149.
76. Jelev, A., et al., *Microdialysis perfusion of 5-HT into hypoglossal motor nucleus differentially modulates genioglossus activity across natural sleep-wake states in rats*. *The Journal of Physiology*, 2001. **532**(2): p. 467-481.
77. Fogel, R.B., et al., *Genioglossal activation in patients with obstructive sleep apnea versus control subjects: mechanisms of muscle control*. *American journal of respiratory and critical care medicine*, 2001. **164**(11): p. 2025-2030.
78. Mezzanotte, W.S., D.J. Tangel, and D.P. White, *Waking genioglossal electromyogram in sleep apnea patients versus normal controls (a neuromuscular compensatory mechanism)*. *Journal of Clinical Investigation*, 1992. **89**(5): p. 1571.
79. De Backer, W., *Upper airway reflexes and obstructive sleep apnoea*. *European Respiratory Journal*, 1993. **6**(1): p. 9-10.
80. Verbraecken, J.A. and W.A. De Backer, *Upper Airway Mechanics*. *Respiration*, 2009. **78**(2): p. 121-33.
81. Kuna, S.T., J.S. Smickley, and C.R. Vanoye, *Respiratory-related pharyngeal constrictor muscle activity in normal human adults*. *American journal of respiratory and critical care medicine*, 1997. **155**(6): p. 1991-1999.
82. Jordan, A.S. and D.P. White, *Pharyngeal motor control and the pathogenesis of obstructive sleep apnea*. *Respiratory Physiology & Neurobiology*, 2008. **160**(1): p. 1-7.
83. Kobayashi, I., et al., *Inspiratory coactivation of the genioglossus enlarges retroglossal space in laryngectomized humans*. *Journal of Applied Physiology*, 1996. **80**(5): p. 1595-1604.
84. Mezzanotte, W.S., D.J. Tangel, and D.P. White, *Influence of sleep onset on upper-airway muscle activity in apnea patients versus normal controls*. *American Journal of Respiratory and Critical Care Medicine*, 1996. **153**(6): p. 1880-1887.
85. Wheatley, J.R., et al., *Influence of sleep on response to negative airway pressure of tensor palatini muscle and retropalatal airway*. *Journal of Applied Physiology*, 1993. **75**(5): p. 2117-2124.

86. Basner, R.C.M.D., *Continuous Positive Airway Pressure for Obstructive Sleep Apnea*. The New England Journal of Medicine, 2007. **356**(17): p. 1751-8.
87. Lee, W., et al., *Epidemiology of Obstructive Sleep Apnea: A Population-Based Perspective*. Expert Review of Respiratory Medicine, 2008. **2**(3): p. 349-364.
88. Abad, V.C. and C. Guilleminault, *Treatment options for obstructive sleep apnea*. Current Treatment Options in Neurology, 2009. **11**(5): p. 358-367.
89. Horner, R.L., et al., *Sites and sizes of fat deposits around the pharynx in obese patients with obstructive sleep apnoea and weight matched controls*. European Respiratory Journal, 1989. **2**(7): p. 613-622.
90. Shelton, K.E., et al., *Mandible enclosure of upper airway and weight in obstructive sleep apnea*. American Review of Respiratory Disease, 1993. **148**: p. 195-195.
91. Shelton, K.E., et al., *Pharyngeal fat in obstructive sleep apnea*. American Review of Respiratory Disease, 1993. **148**(2): p. 462-6.
92. Stauffer, J.L., et al., *Morphology of the Uvula in Obstructive Sleep Apnea*. The American review of respiratory disease, 1989. **140**: p. 724.
93. Foster, G.D., et al., *Resting energy expenditure, body composition, and excess weight in the obese*. Metabolism, 1988. **37**(5): p. 467-472.
94. Hill, J.O., et al., *Effects of exercise and food restriction on body composition and metabolic rate in obese women*. The American journal of clinical nutrition, 1987. **46**(4): p. 622-630.
95. Wadden, T.A., et al., *Long-term effects of dieting on resting metabolic rate in obese outpatients*. Jama, 1990. **264**(6): p. 707-711.
96. Teodorescu, M., et al., *Association between asthma and risk of developing obstructive sleep apnea*. JAMA, 2015. **313**(2): p. 156-164.
97. Oksenberg, A., et al., *Association of body position with severity of apneic events in patients with severe nonpositional obstructive sleep apnea*. CHEST Journal, 2000. **118**(4): p. 1018-1024.
98. Cartwright, R.D., *Effect of sleep position on sleep apnea severity*. Sleep: Journal of Sleep Research & Sleep Medicine, 1984.
99. Walsh, J.H., et al., *Effect of body posture on pharyngeal shape and size in adults with and without obstructive sleep apnea*. Sleep, 2008. **31**(11): p. 1543.
100. Bonnet, M.H., *Effect of sleep disruption on sleep*. Sleep, 1985. **8**(0): p. 1.
101. Gleeson, K., C.W. Zwillich, and D.P. White, *The Influence of Increasing Ventilatory Effort on Arousal from Sleep*. Am Rev Respir Dis, 1990. **142**: p. 295-300.
102. Lal, C., C. Strange, and D. Bachman, *Neurocognitive impairment in obstructive sleep apnea*. Chest, 2012. **141**(6): p. 1601-1610.
103. Owens, J.A., *Neurocognitive and behavioral impact of sleep disordered breathing in children*. Pediatric pulmonology, 2009. **44**(5): p. 417-422.
104. Dinges, D.F., *An overview of sleepiness and accidents*. Journal of Sleep Research, 1995. **4**: p. 4-14.
105. Findley, L., et al., *Vigilance and automobile accidents in patients with sleep apnea or narcolepsy*. Chest, 1995. **108**(3): p. 619-624.
106. Avis, K.T., K.L. Gamble, and D.C. Schwebel, *Obstructive Sleep Apnea Syndrome Increases Pedestrian Injury Risk in Children*. The Journal of Pediatrics, 2015. **166**(1): p. 109-114.
107. Randerath, W.J., B.M. Sanner, and V.K. Somers, *Sleep Apnea: Current Diagnosis and Treatment*. 2006: Karger.
108. Ohayon, M.M., *The effects of breathing-related sleep disorders on mood disturbances in the general population*. The Journal of clinical psychiatry, 2003. **64**(10): p. 1195-200; quiz, 1274-6.
109. Lee, W., et al., *The Relation Between Apnea and Depressive Symptoms in Men with Severe Obstructive Sleep Apnea: Mediation Effects of Sleep Quality*. Lung, 2015: p. 1-7.
110. Macey, P.M., et al., *Brain structural changes in obstructive sleep apnea*. Sleep, 2008. **31**(7): p. 967.
111. Yaouhi, K., et al., *A combined neuropsychological and brain imaging study of obstructive sleep apnea*. Journal of sleep research, 2009. **18**(1): p. 36-48.
112. Friedman, M., *Sleep Apnea and Snoring: Surgical and Non-surgical Therapy*. 2009: Saunders/Elsevier.
113. Caples, S.M., et al., *Surgical Modifications of the Upper Airway for Obstructive Sleep Apnea in Adults: A Systematic Review and Meta-Analysis*. Sleep, 2010. **33**(10): p. 1396-1407.
114. Riley, R.W., N.B. Powell, and C. Guilleminault, *Inferior mandibular osteotomy and hyoid myotomy suspension for obstructive sleep apnea: a review of 55 patients*. Journal of Oral and Maxillofacial Surgery, 1989. **47**(2): p. 159-164.
115. Riley, R.W., N.B. Powell, and C. Guilleminault, *Obstructive sleep apnea and the hyoid: a revised surgical procedure*. Otolaryngology--head and neck surgery: official journal of American Academy of Otolaryngology-Head and Neck Surgery, 1994. **111**(6): p. 717-721.

116. Woodson, B.T. and R.J. Toohill, *Transpalatal advancement pharyngoplasty for obstructive sleep apnea*. The Laryngoscope, 1993. **103**(3): p. 269-276.
117. Weitzman, E.D., E. Kahn, and C.P. Pollak, *Quantitative analysis of sleep and sleep apnea before and after tracheostomy in patients with the hypersomnia-sleep apnea syndrome*. Sleep, 1979. **3**(3-4): p. 407-423.
118. Schmidt-Nowara, W., et al., *Oral appliances for the treatment of snoring and obstructive sleep apnea: a review*. Sleep-Lawrence, 1995. **18**(6): p. 501-510.
119. Ferguson, K.A., et al., *Oral appliances for snoring and obstructive sleep apnea: a review*. SLEEP-NEW YORK THEN WESTCHESTER-, 2006. **29**(2): p. 244.
120. Ono, T., et al., *A tongue retaining device and sleep-state genioglossus muscle activity in patients with obstructive sleep apnea*. Angle Orthodontist, 1996. **66**(4): p. 273-280.
121. Ono, T., et al., *The effect of the tongue retaining device on awake genioglossus muscle activity in patients with obstructive sleep apnea*. American journal of orthodontics and dentofacial orthopedics : official publication of the American Association of Orthodontists, its constituent societies, and the American Board of Orthodontics, 1996. **110**(1): p. 28-35.
122. Yoshida, K., *Effect of a prosthetic appliance for treatment of sleep apnea syndrome on masticatory and tongue muscle activity*. Journal of Prosthetic Dentistry, 1998. **79**(5): p. 537-544.
123. Kribbs, N.B., et al., *Objective measurement of patterns of nasal CPAP use by patients with obstructive sleep apnea*. American Review of Respiratory Disease, 1993. **147**(4): p. 887-895.
124. Sanders, M.H. and N. Kern, *Obstructive sleep apnea treated by independently adjusted inspiratory and expiratory positive airway pressures via nasal mask*. Physiologic and clinical implications. Chest, 1990. **98**(2): p. 317-324.
125. Strohl, K.P. and S. Redline, *Nasal CPAP therapy, upper airway muscle activation, and obstructive sleep apnea*. American Review of Respiratory Disease, 1986. **134**(3): p. 555-558.
126. Sullivan, C.E., et al., *Reversal of Obstructive Sleep Apnoea by Continuous Positive Airway Pressure Applied Through the Nares*. The Lancet, 1981. **317**(8225): p. 862-865.
127. Chai, C.L., A. Pathinathan, and B. Smith, *Continuous positive airway pressure delivery interfaces for obstructive sleep apnoea*. Cochrane database of systematic reviews (Online), 2006(4).
128. Smith, P.L., et al., *Indications and Standards for Use of Nasal Continuous Positive Airway Pressure (CPAP) in Sleep-Apnea Syndromes*. American Journal of Respiratory and Critical Care Medicine, 1994. **150**(6): p. 1738-1745.
129. Sánchez, A.I., et al., *CPAP and behavioral therapies in patients with obstructive sleep apnea: Effects on daytime sleepiness, mood, and cognitive function*. Sleep Medicine Reviews, 2009. **13**(3): p. 223-233.
130. LaNasa, P.J. and E.L. Upp, *Fluid Flow Measurement: A Practical Guide to Accurate Flow Measurement*. 2014: Elsevier Science.
131. Wyka, K., P. Mathews, and J. Rutkowski, *Foundations of Respiratory Care*. 2011: Cengage Learning.
132. Douglas, J.F., et al., *Fluid Mechanics*. Fifth Edition ed. 2005: Pearson/Prentice Hall.
133. Tu, J., K. Inthavong, and G. Ahmadi, *Computational Fluid and Particle Dynamics in the Human Respiratory System*. 2012: Springer Netherlands.
134. Smits, A.J., *A physical introduction to fluid mechanics*. 2000: John Wiley.
135. Beachey, W., *Respiratory Care Anatomy and Physiology: Foundations for Clinical Practice*. 2013: Elsevier Health Sciences.
136. Heinsohn, R.J. and J.M. Cimbala, *Indoor Air Quality Engineering: Environmental Health and Control of Indoor Pollutants*. 2003: Taylor & Francis.
137. Heinzer, R.C., et al., *Lung volume and continuous positive airway pressure requirements in obstructive sleep apnea*. American journal of respiratory and critical care medicine, 2005. **172**(1): p. 114-117.
138. Bijaoui, E.L., et al., *Mechanical properties of the lung and upper airways in patients with sleep-disordered breathing*. American journal of respiratory and critical care medicine, 2002. **165**(8): p. 1055-1061.
139. Clark, S.A., et al., *Assessment of inspiratory flow limitation invasively and noninvasively during sleep*. American journal of respiratory and critical care medicine, 1998. **158**(3): p. 713-722.
140. Tenhunen, M., et al., *Increased respiratory effort during sleep is non-invasively detected with movement sensor*. Sleep and Breathing, 2011. **15**(4): p. 737-746.
141. Lin, C.-L., et al., *Characteristics of the turbulent laryngeal jet and its effect on airflow in the human intra-thoracic airways*. Respiratory Physiology & Neurobiology, 2007. **157**(2-3): p. 295-309.
142. Xi, J., P.W. Longest, and T.B. Martonen, *Effects of the laryngeal jet on nano- and microparticle transport and deposition in an approximate model of the upper tracheobronchial airways*. Journal of Applied Physiology, 2008. **104**(6): p. 1761-1777.

143. Aittokallio, T., A. Virkki, and O. Polo, *Understanding sleep-disordered breathing through mathematical modelling*. Sleep Medicine Reviews, 2009. **13**(5): p. 333-343.
144. Keyhani, K., P.W. Scherer, and M.M. Mozell, *Numerical Simulation of Airflow in the Human Nasal Cavity*. Journal of Biomechanical Engineering, 1995. **117**(4): p. 429-441.
145. Subramaniam, R.P., et al., *Computational Fluid Dynamics Simulations of Inspiratory Airflow in the Human Nose and Nasopharynx*. Inhalation Toxicology, 1998. **10**(2): p. 91-120.
146. Chouly, F., et al., *Modelling the human pharyngeal airway: validation of numerical simulations using in vitro experiments*. Medical & Biological Engineering & Computing, 2009. **47**(1): p. 49-58.
147. Shome, B., et al., *Modeling of Airflow in the Pharynx With Application to Sleep Apnea*. Journal of Biomechanical Engineering, 1998. **120**(3): p. 416-422.
148. Wilquem, F. and G. Degrez, *Numerical modeling of steady inspiratory airflow through a three-generation model of the human central airways*. Transactions -American Society of Mechanical Engineers Journal of Biomedical Engineering, 1997. **119**: p. 59-65.
149. Aittokallio, T., M. Gyllenberg, and O. Polo, *A model of a snorer's upper airway*. Mathematical Biosciences, 2001. **170**(1): p. 79-90.
150. Condos, R., et al., *Flow limitation as a noninvasive assessment of residual upper-airway resistance during continuous positive airway pressure therapy of obstructive sleep apnea*. American journal of respiratory and critical care medicine, 1994. **150**(2): p. 475-480.
151. Nithiarasu, P., et al., *Steady flow through a realistic human upper airway geometry*. International Journal for Numerical Methods in Fluids, 2008. **57**(5): p. 631-651.
152. Wang, Y., et al., *Numerical analysis of respiratory flow patterns within human upper airway*. Acta Mechanica Sinica, 2009. **25**(6): p. 737-746.
153. Kleinstreuer, C. and Z. Zhang, *Airflow and particle transport in the human respiratory system*. Annual Review of Fluid Mechanics, 2010. **42**: p. 301-334.
154. Zhang, Z. and C. Kleinstreuer, *Airflow structures and nano-particle deposition in a human upper airway model*. Journal of computational physics, 2004. **198**(1): p. 178-210.
155. Yu, G., Z. Zhang, and R. Lessmann, *Fluid flow and particle diffusion in the human upper respiratory system*. Aerosol Science and Technology, 1998. **28**(2): p. 146-158.
156. Martonen, T.B., et al., *Three-dimensional computer modeling of the human upper respiratory tract*. Cell biochemistry and biophysics, 2001. **35**(3): p. 255-261.
157. Hahn, I., P.W. Scherer, and M.M. Mozell, *Velocity profiles measured for airflow through a large-scale model of the human nasal cavity*. Journal of Applied Physiology, 1993. **75**(5): p. 2273-2287.
158. Mylavarapu, G., et al., *Validation of computational fluid dynamics methodology used for human upper airway flow simulations*. Journal of Biomechanics, 2009. **42**(10): p. 1553-1559.
159. Cheng, K.H., et al., *Deposition of ultrafine aerosols in the head airways during natural breathing and during simulated breath holding using replicate human upper airway casts*. Aerosol Science and Technology, 1995. **23**(3): p. 465-474.
160. Tennent, R.M., *Science Data Book*. 1976: Oliver & Boyd.
161. Huang, Y., A. Malhotra, and D.P. White, *Computational simulation of human upper airway collapse using a pressure/state-dependent model of genioglossal muscle contraction under laminar flow conditions*. Journal of Applied Physiology, 2005. **99**(3): p. 1138-1148.
162. Huang, Y., D.P. White, and A. Malhotra, *Use of Computational Modeling to Predict Responses to Upper Airway Surgery in Obstructive Sleep Apnea*. The Laryngoscope, 2007. **117**(4): p. 648-653.
163. Malhotra, A., et al., *The Male Predisposition to Pharyngeal Collapse*. American Journal of Respiratory and Critical Care Medicine, 2002. **166**(10): p. 1388-1395.
164. AZO Materials. *Silicone Rubber*. 2015; Available from: <http://www.azom.com/properties.aspx?ArticleID=920>.
165. Markidou, A., W.Y. Shih, and W.-H. Shih, *Soft-materials elastic and shear moduli measurement using piezoelectric cantilevers*. Review of Scientific Instruments, 2005. **76**(6): p. 064302.
166. Reda, M., et al., *Morphological Assessment of the Soft Palate in Habitual Snoring Using Image Analysis*. The Laryngoscope, 1999. **109**(10): p. 1655-1660.
167. Liu, Y., et al., *Creation of a standardized geometry of the human nasal cavity*. Journal of Applied Physiology, 2009. **106**(3): p. 784-795.
168. Daniel, M.M., et al., *Pharyngeal Dimensions in Healthy Men and Women*. Clinics, 2007. **62**(1): p. 5-10.
169. Brouillette, R.T., S.K. Fernbach, and C.E. Hunt, *Obstructive sleep apnea in infants and children*. The Journal of Pediatrics, 1982. **100**(1): p. 31-40.
170. Richardson, M.A., et al., *Evaluation of tonsils and adenoids in sleep apnea syndrome*. The Laryngoscope, 1980. **90**(7): p. 1106-1110.

171. Jokic, R., et al., *Surface Tension Forces in Sleep Apnea: The Role of a Soft Tissue Lubricant*. American Journal of Respiratory and Critical Care Medicine, 1998. **157**(5): p. 1522-1525.
172. Kirkness, J.P., et al., *Relationship between surface tension of upper airway lining liquid and upper airway collapsibility during sleep in obstructive sleep apnea hypopnea syndrome*. Journal of Applied Physiology, 2003. **95**(5): p. 1761-1766.
173. National Institute of Biomedical Imaging and Bioengineering. *Computed Tomography (CT)*. 2013; Available from: <http://www.nibib.nih.gov/science-education/science-topics/computed-tomography-ct>.
174. Berger, A., *Magnetic resonance imaging*. BMJ : British Medical Journal, 2002. **324**(7328): p. 35-35.
175. 3D-Doctor. *3D Surface Rendering*. 2015; Available from: <http://www.ablesw.com/3d-doctor/surface.html>.
176. LiveScience. *What is Selective Laser Sintering*. 2013; Available from: <http://www.livescience.com/38862-selective-laser-sintering.html>.

# APPENDICES

## Appendix I - Understanding the Technology

### Imaging Modalities and Magnetic Resonance Imaging (MRI)

Medical imaging provides the ability to non-invasively view and analyse structures and tissue within the body, making it crucial for clinical analysis, and one of the most useful tools for diagnosing and treating certain diseases. A wide range of imaging modalities exist, such as ultrasound, thermography, radiography, and tomography, which involves imaging single “slices” or planes of an object to yield an image (i.e. a “tomogram”) of the objects’ cross-section at that plane. This is done through the use of penetrating waves, such as x-rays or radio-frequency waves, which penetrate the skin at a particular plane to provide specific information which allows an external computer to reconstruct a representation of the structures beneath the skin.

One of the most common methods of obtaining a tomogram is through the use of “Computed Tomography” (CT), or “Computed Axial Tomography” (CAT), scans. In a CT scan, x-rays are emitted from an x-ray tube which rotates around the patient, projecting narrow beams of x-rays through the body. The x-ray beam travels through the tissue in the body, and as it leaves the outer surface of the body it is picked up by a special digital x-ray detector directly opposite the x-ray source. This data is then transferred to a computer where, using specific mathematical techniques, a two-dimensional image slice of the patient is constructed at the plane of the x-rays [173].

The methods used to obtain images during Magnetic Resonance Imaging (MRI) scans are similar to those used during CT scans, in which single “slices” of the body are imaged in order to provide a picture of the cross-section of the tissues and structures at the specific plane where scanning occurs. However, in contrast to CT, different technologies and concepts are used in MRI to provide the required illustrations of the body. In MRI, the body’s natural magnetic properties are utilised by using the hydrogen nuclei present in the abundant water content of the body. When placed in a strong magnetic field such as that produced by the MRI machine, the hydrogen protons’ axes, which are randomly aligned under normal circumstances, line up with the poles produced by the magnetic field, creating a “magnetic vector” oriented along the axis of the MRI scanner. A radio frequency (RF) pulse is then emitted by the MRI machine at the area of the body which is to be examined. This allows the



magnetic vector to be deflected at that plane. Once the RF source is switched off, the hydrogen protons' axes return to their previous alignment, re-establishing the previously created magnetic vector. The return of the magnetic vector to its resting state causes the emission of a radio wave signal, which is then picked up by receiver coils around the area of the body being scanned. The intensity of the received signal is then plotted on a grey scale to build a cross-sectional image of the tissue under the skin [174]. By repeating this process along the body or along a specific part of the body, a series of grayscale images are obtained which represent the different tissue beneath the skin, and where the different shades in each image show different layers and organs associated with that particular frame.

## **Model Reconstruction**

Through the use of certain modern applications, it is possible to convert a simplistic model of an object into a virtual, solid, three-dimensional representational image or model. This process is referred to as 3D rendering, and one common form of 3D rendering is surface rendering.

Surface rendering with medical-application software 3D Doctor™ is performed by combining 3D raster image and vector boundary technology into complex rendering algorithms. These optimized proprietary algorithms are then used with user-selected object boundaries to create the corresponding virtual 3D models [175]. By highlighting the areas and boundaries concerned with the desired object, an entire 3D model can be made and exported for further analysis or processing.

## **3D printing and Additive Manufacturing**

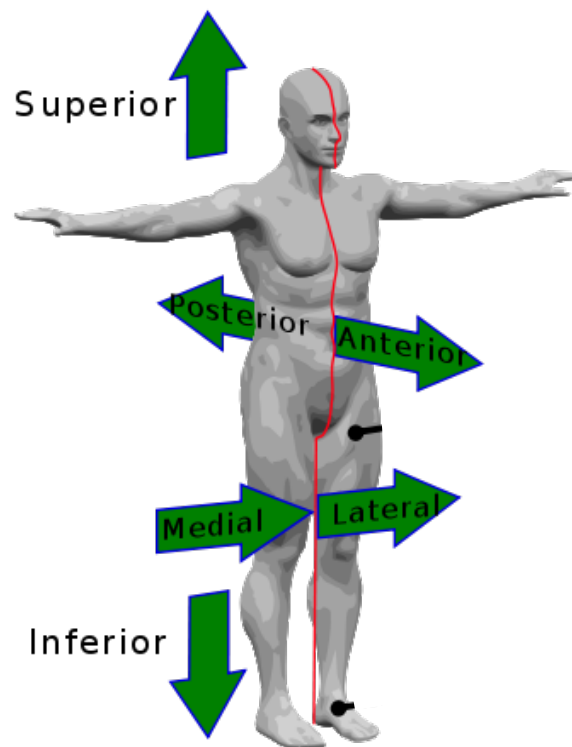
In a general sense, 3D printing refers to the process of creating a physical three-dimensional object out of a virtual model. Initially, the model which needs to be printed is usually designed using CAD (Computer Aided Design) software in order to create a new object. Alternatively, a virtual model of an already existing physical object can be obtained through the use of a 3D scanner in situations where an existing object needs to be copied. Once this is completed, the final virtual model is "sliced" into hundreds of horizontal layers in order to be exported in a format readily recognised by the 3D printer.

The 3D printing itself is most commonly done through the use of additive processes, in which an extruder hangs from a base on a set of rails, and the base is given the freedom to move

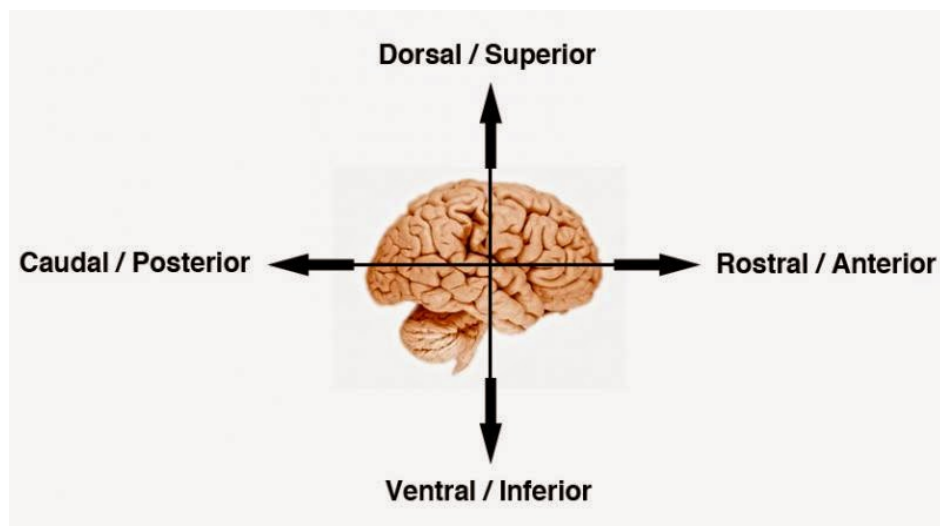
back and forth along the axis of the railing, while the railing itself moves in either direction perpendicular to the direction of the movement of the base. During movement of these two parts, an independently controlled horizontal platform ascends and descends, providing a total of three degrees of motion during printing. The extruder then deposits a layer of the material of the final object on the platform, and the platform is lowered, allowing the extruder to deposit another layer, and so on. Thus the laying down of these successive layers results in the “printing” of the final product. This process is the more common process used when printing with conventional household 3D printers.

While this is the simplest and most common method of 3D printing, more complex methods exist, such as Fused Deposition Modeling (FDM), Stereolithography (SLA) and Selective Laser Sintering (SLS), which also involves slicing of the virtual model into horizontal layers for printing, however the printing process itself differs to that which was mentioned earlier. In SLS, a bed of powder made from the material of the final product is spread on a horizontal platform, and the powder is heated to just under melting point. Subsequently, an infra-red laser selectively heats the cross-section of the final model at that particular layer, tipping the temperature above melting point and fusing the powdered material. The powder bed is then lowered, and a new layer of powder is applied on top, crystalizing the shape outlined by the laser on the layer below, and allowing the process to be repeated once more, until the final model is complete [176].

## Appendix II - Anatomical Terms of Location



5



6

<sup>5</sup> [https://upload.wikimedia.org/wikipedia/commons/7/79/Anatomy\\_Directional\\_terms-ca.svg](https://upload.wikimedia.org/wikipedia/commons/7/79/Anatomy_Directional_terms-ca.svg)

<sup>6</sup> <http://biogeonerd.blogspot.co.nz/2014/09/directional-terms-human.html>

## Appendix III - Technical Information and Data Sheets

### Solaris

<b>TECHNICAL OVERVIEW</b>	
<b>Mix Ratio:</b> 1A : 1B by volume or weight	
<b>Mixed Viscosity, cps:</b> 1,200	(ASTM D-2393)
<b>Specific Gravity, g/cc:</b> 0.99	(ASTM D-1475)
<b>Specific Volume, cu. in./lb.:</b> 28.1	(ASTM D-1475)
<b>Pot Life:</b> 240 minutes (73°F/23°C)	(ASTM D-2471)
<b>Cure time:</b> 24 hrs (73°F/23°C)	
<b>Color:</b> Clear	
<b>Shore A Hardness:</b> 15	(ASTM D-2240)
<b>Tensile Strength, psi:</b> 180	(ASTM D-412)
<b>100% Modulus, psi:</b> 25	(ASTM D-412)
<b>Elongation @ Break:</b> 290%	(ASTM D-412)
<b>Die B Tear Strength, pli:</b> N/A	(ASTM D-624)
<b>Shrinkage, in./in.:</b> < .001	(ASTM D-2566)
<b>Useful Temp. Range:</b> -149°F to 400°F (-100°C to 205° C)	
<b>Dielectric Strength, volts/mil:</b> 366	(ASTM D-149)
<b>Dielectric Constant, 100 Hz:</b> 2.78	(ASTM D-150)
<b>Dissipation Factor, 100 Hz:</b> 0.00	(ASTM D-150)
<b>Volume Resistivity, ohms-cm:</b> 3.16E+15(ASTM D-257)	
<b>Thermal Conductivity:</b> 0.18	(ASTM D-1461)
<b>Refractive Index:</b> 1.41 nm	(ASTM D-1218)
* All values measured after 7 days at 73°F/23°C	

## Dragon Skin

### TECHNICAL OVERVIEW

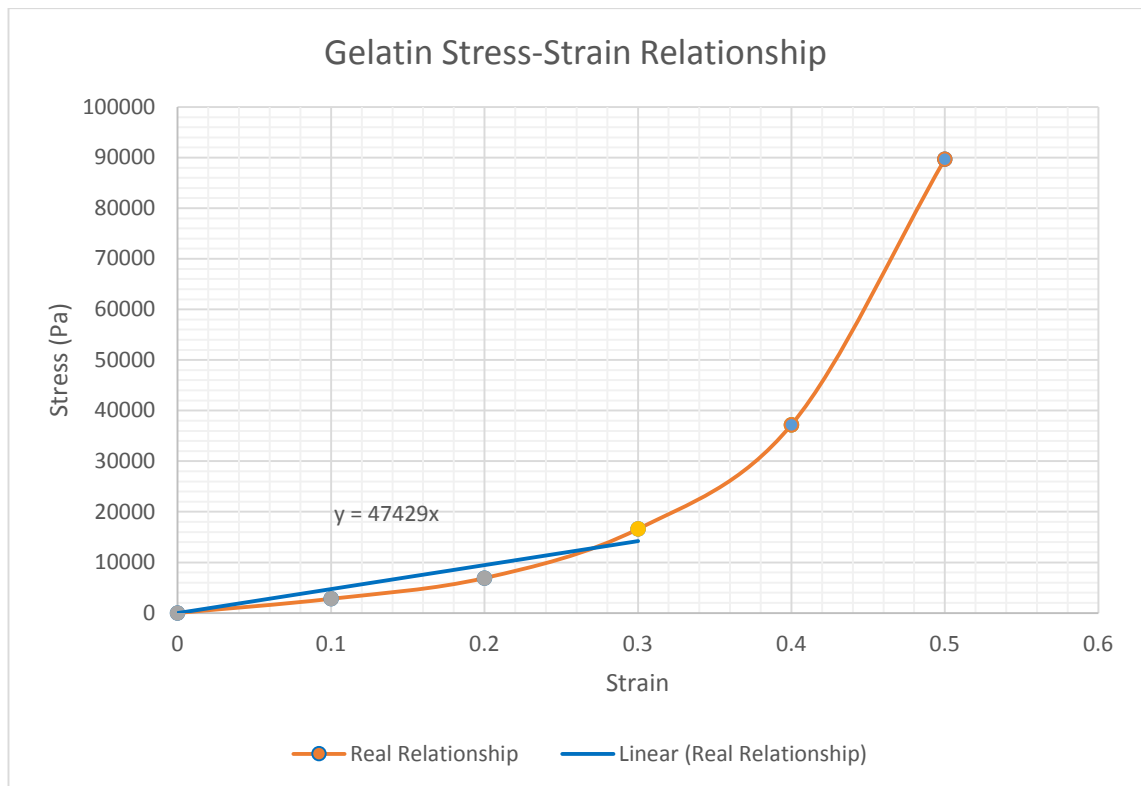
	Mixed Viscosity (ASTM D-2393)	Specific Gravity (g/cc) (ASTM D-1475)	Specific Volume (cu. in./lb.) (ASTM D-1475)	Pot Life (ASTM D-2471)	Cure Time	Shore A Hardness (ASTM D-2240)	Tensile Strength (ASTM D-412)	100% Modulus (ASTM D-412)	Elongation at Break % (ASTM D-412)	Die B Tear Strength (ASTM D-624)	Shrinkage (in./in.) (ASTM D-2566)
Dragon Skin® 10 Very Fast	23,000 cps	1.07	25.8	4 min.	30 min.	10A	475 psi	22 psi	1000%	102 pli	< .001 in./in.
Dragon Skin® 10 Fast	23,000 cps	1.07	25.8	8 min.	75 min.	10A	475 psi	22 psi	1000%	102 pli	< .001 in./in.
Dragon Skin® 10 Medium	23,000 cps	1.07	25.8	20 min.	5 hours	10A	475 psi	22 psi	1000%	102 pli	< .001 in./in.
Dragon Skin® 10 Slow	23,000 cps	1.07	25.8	45 min.	7 hours	10A	475 psi	22 psi	1000%	102 pli	< .001 in./in.
Dragon Skin® 20	20,000 cps	1.08	25.6	25 min.	4 hours	20A	550 psi	49 psi	620%	120 pli	< .001 in./in.
Dragon Skin® 30	30,000 cps	1.08	25.7	45 min.	16 hours	30A	500 psi	86 psi	364%	108 pli	< .001 in./in.

**Mix Ratio:** 1A:1B by volume or weight  
**Color:** Translucent

**Useful Temperature Range:** -65°F to +450°F (-53°C to +232°C)  
**Dielectric Strength** (ASTM D-147-97a): >350 volts/mil

\*All values measured after 7 days at 73°F/23°C

## Special-Effects Gelatine



$\rho = 1150 \text{ kg/m}^3$

$E = 47 \text{ kPa}$

## Commercial 3D Printer

### Product Parameters

Printer:

Printing technology: hot melt stack forming technology

Operating interface: 3.5 inch full color IPS touch screen

Build size: 230×150×150mm

Printing precision:  $\pm 0.2$

Filament diameter: 1.75mm

Extruder diameter: 0.4mm

Software:

Name of software: Flashprint

Support files: stl、obj

Operating systems: Windows

Linux

Mac OS

Appearance dimension:

Machine dimension: 485×400×335mm

Package dimension:

Net weight:

Package weight:

Input voltage: 100-240V, 50-60Hz

Output voltage: 24V

Data transmission: USB, SD card, Wifi

## PVA Filament

DATA SHEET	
Filament Diameter	1.75mm
Print Temperature	180 - 205°C
Brands	FormFutura
Material type	PVA filaments
Weight	± 0.3 Kg ± 2% of filament